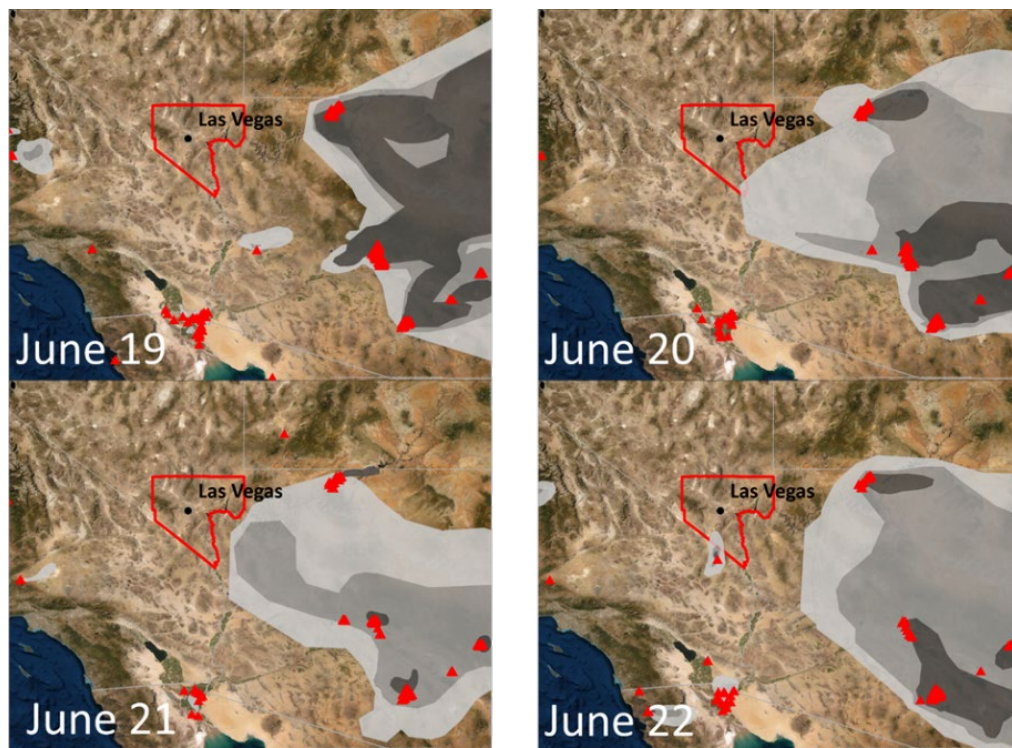# Exceptional Event Demonstration for Ozone Exceedances in Clark County, Nevada – June 22, 2020

Final Report Prepared for

U.S. EPA Region 9
San Francisco, CA

July 2021

STi ⟩ Sonoma Technology

This document contains blank pages to accommodate two-sided printing.

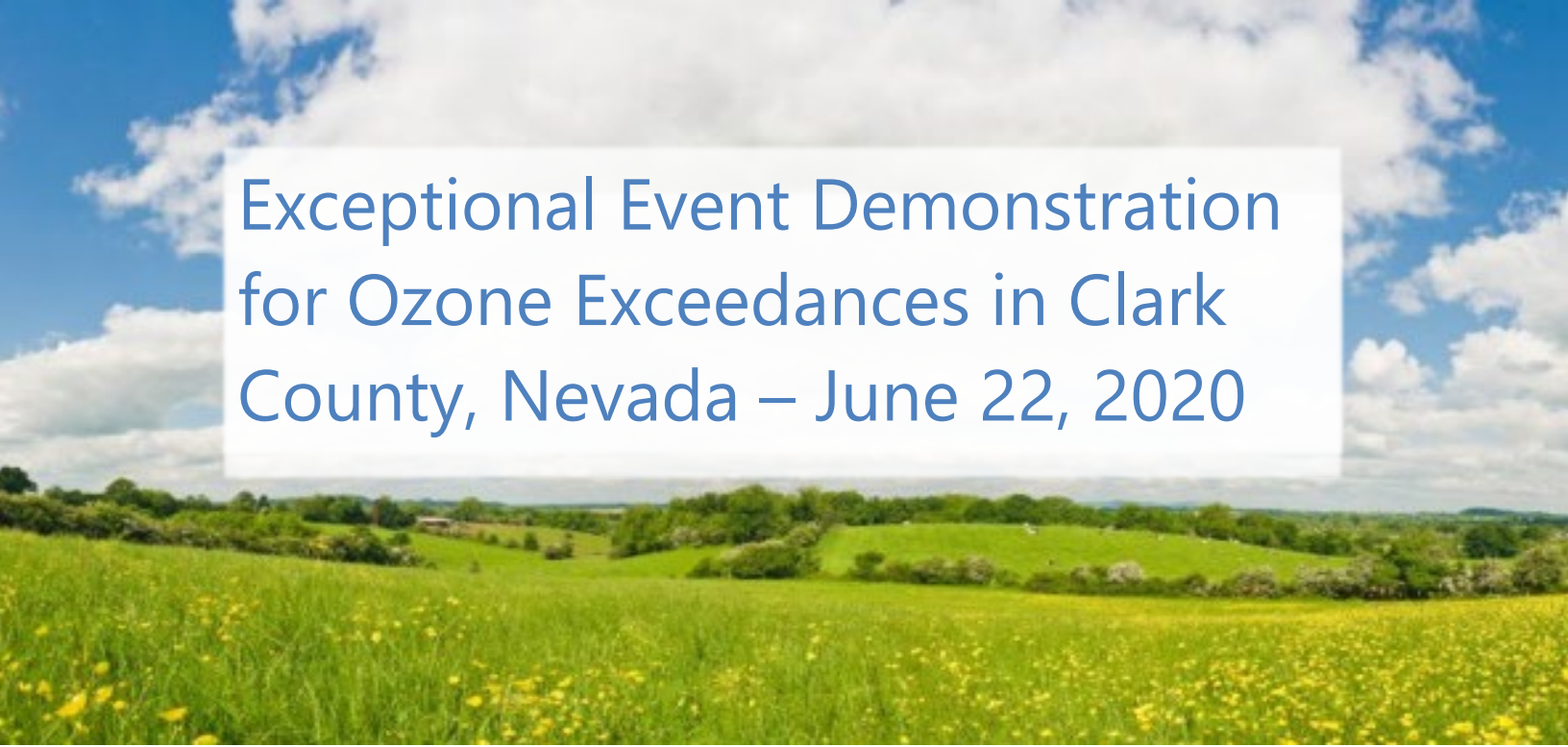# Exceptional Event Demonstration for Ozone Exceedances in Clark County, Nevada – June 22, 2020

Prepared by

Steve Brown, PhD
Crystal McClure, PhD
Cari Gostic
David Miller, PhD
Nathan Pavlovic
Charles Scarborough

Sonoma Technology
1450 N. McDowell Blvd., Suite 200
Petaluma, CA 94954
Ph 707.665.9900 | F 707.665.9800
sonomatech.com

Prepared for

Clark County Department of
Environment and Sustainability
Division of Air Quality
4701 W. Russell Road, Suite 200
Las Vegas, NV 89118
Ph 702.455.3206
www.clarkcountynv.gov

Final Report
STI-920053-7477

July 1, 2021

Cover graphic illustrates the transport from the Ivanpah Fire to Clark County, Nevada. See Section 3.1.3 for more information.

Contents

Figures

Tables

Executive Summary

On June 22, 2020, Clark County experienced an atypical, area-wide episode of elevated ambient ozone concentrations. During this episode, the 2015 8-hr ozone National Ambient Air Quality Standards (NAAQS) threshold (0.070 ppm) was exceeded at the Paul Meyer, Walter Johnson, and Joe Neal air quality monitoring sites. The exceedances at all three sites could lead to an ozone nonattainment designation for the Clark County area. Air trajectory analysis and air quality modeling suggest that this ozone exceedance was influenced by wildfire smoke that was transported to Clark County from large wildfires burning in western Arizona and a smaller fire burning in the Mojave National Preserve that began on the day of the event. The EPA Exceptional Event Rule (U.S. Environmental Protection Agency, 2016a) allows air agencies to omit air quality data from the design value calculation if it can be demonstrated that the measurement in question was caused by an exceptional event. This report describes analyses that establish a clear causal relationship between wildfire smoke and the June 22, 2020, ozone exceedance at the Paul Meyer, Walter Johnson, and Joe Neal sites.

The analyses conducted provides evidence supportive of smoke impacts on ozone concentrations in Clark County. Analyses show that (1) smoke was transported from wildfires in western Arizona and a wildfire in southern California to the surface in the Clark County area in the days leading up to the exceedance and on the day of the exceedance, respectively, (2) wildfire smoke impacted the typical diurnal profiles of ground-level pollution measurements, including CO and NO_2, in the Clark County area on June 22, (3) byproducts and tracers of wildfire combustion were present and elevated at the surface in the Clark County area on the days surrounding June 22, and (4) meteorological regression modeling and similar meteorological day analysis show that ozone observations on June 22 were unusual in the historical record given the meteorological conditions. Sources of evidence used in these analyses include air quality monitor data to show that supporting pollutant trends at the surface were influenced by wildfire smoke, air trajectory analysis to show transport of smoke-laden air to the Clark County area, media coverage of wildfires and smoke impacts, meteorological regression modeling, and meteorologically similar day analysis.

EPA guidance for exceptional event demonstrations (U.S. Environmental Protection Agency, 2016b) provides a three-tiered approach; depending on the complexity of the event, increasingly involved information may be required to demonstrate a causal relationship between wildfire smoke and an exceedance. This report documents the results of analyses conducted to address Tier 1, Tier 2, and Tier 3 exceptional event demonstration requirements.

These analyses show that smoke was transported from wildfires in western Arizona over the days leading up to June 22 and from a wildfire in the Mojave National Preserve on June 22 to the Clark County area. Combined with additional evidence, such as meteorological regression modeling and

meteorologically similar day analysis, our results show that wildfire smoke impacted ozone concentrations in Clark County on June 22, 2020.

1. Overview

1.1 Introduction

The 2020 wildfire season in California was unprecedented, with five of the six largest wildfires in California history occurring in either August or September 2020 (https://www.fire.ca.gov/media/4jandlhh/top20_acres.pdf). Smoke emissions from California wildfires can affect downwind areas, including Clark County, Nevada. This was the case on June 22, 2020, as smoke emissions from the Ivanpah Fire, which was 57 miles south of Las Vegas, and the Mangum, Bush, and Bighorn Fires (Arizona wildfires) located in western Arizona, reached Clark County. On this date, 3 of the 14 ozone (O_3) monitoring locations around Clark County recorded an exceedance of the 2015 National Ambient Air Quality Standard (NAAQS) for 8-hour ozone (0.070 ppm).

Emissions from wildfires can affect concentrations of ozone downwind by direct transport of both ozone and precursor gases (i.e., nitrogen oxides [NO_x] and volatile organic compounds [VOCs]). Each mechanism can cause an enhancement in the overall ozone concentration and/or the amount of ozone that could be produced. For example, in an area where NO_x concentrations are high, such as an urban area like Las Vegas, Nevada, the transport of VOCs from wildfire emissions can enhance the amount of ozone that can be produced, potentially driving concentrations above the ozone standard. According to U.S. Environmental Protection Agency's (EPA) exceptional event (EE) guidance (U.S. Environmental Protection Agency, 2016), EEs such as wildfires that affect ozone concentrations can be subject to exclusion from calculations of NAAQS attainment if a clear causal relationship can be established between a specific event and the exceedance.

This report describes the clear causal relationship between the Bighorn, Bush, and Mangum fires in Arizona and the Ivanpah Fire in California and the exceedance of the maximum daily 8-hour ozone average (MDA8) at the three monitoring sites in Clark County on June 22, 2020. The evidence in this report includes all three tiers of analysis required by EPA's EE guidance: for Tier 1, ground and satellite-based measurement of smoke emissions, transport of smoke from the Ivanpah Fire and Arizona wildfires to Clark County, and media coverage of the smoke event in Clark County; for Tier 2, emission vs. distance analysis, ground and satellite analysis of smoke-related pollutants, and comparison of event and non-event concentrations; and for Tier 3, vertical column analyses, meteorologically similar day analyses, and statistical Generalized Additive Modeling (GAM) of the event. The wildfires that affected ozone concentrations in Clark County could not be reasonably controlled or prevented because it was caused by accidental ignition, lightning, or an unknown cause during extremely dry and hot conditions and is unlikely to recur. Table 1-1 lists the sites affected during the June 22 event, as well as their locations and MDA8 ozone concentrations.

Table 1-1. June 22, 2020, EE information. All monitoring sites in Clark County that exceeded the 2015 NAAQS on June 22, 2020, are listed along with AQS site codes, location information, and MDA8 ozone concentrations.

AQS Site Code	Site Name	Latitude (degrees N)	Longitude (degrees W)	MDA8 O_3 Concentration (ppb)
320030075	Joe Neal	36.271	-115.238	78
320030043	Paul Meyer	36.106	-115.253	74
320030071	Walter Johnson	36.170	-115.263	73

Concurrent with this document, Clark County is submitting documentation for other ozone EEs in 2018 and 2020 that were caused by wildfires and stratospheric intrusions. These events are mentioned throughout this report and are referred to as "proposed 2018 and 2020 exceptional events," recognizing that discussion with EPA is still pending. All proposed EEs for Clark County in 2018 and 2020 are listed in Tables 1-2 and 1-3. Wherever possible, calculated statistics provide context that both includes and excludes the proposed EEs from 2018 and 2020.

Table 1-2. Proposed Clark County 2018 EEs. For each site and date combination where the 2015 NAAQS was exceeded, the MDA8 ozone concentration is shown in parts per billion (ppb). Blank cells indicate that there was no exceedance on that site/date combination.

Date	Paul Meyer	Walter Johnson	Green Valley	Jerome Mack	Joe Neal	Palo Verde	Jean	Indian Springs	Apex	Boulder City
6/19/2018	72	72	77	75						
6/20/2018	71	74			72					
6/23/2018	72	76	75	72	72	71	77	73		
6/27/2018	75	76	78	76	72	72	81	78	74	72
7/14/2018	72		78	78						
7/15/2018		71	73	73	78					
7/16/2018	75	79	71	73	80	75				
7/17/2018	74	77				74				
7/25/2018	71	72	72							
7/26/2018	72	75	77	77					71	
7/27/2018	72	74			76					
7/30/2018			73	72						
7/31/2018		73			73					
8/6/2018	79	77	74	71	76	72			74	
8/7/2018	73	74	72	71	74				71	

Table 1-3. Proposed Clark County 2020 EEs. For each site and date combination where the 2015 NAAQS was exceeded, the MDA8 ozone concentration is shown in ppb. Blank cells indicate that there was no exceedance on that site/date combination.

Date	Walter Johnson	Paul Meyer	Joe Neal	Jerome Mack	Green Valley	Boulder City	Jean	Indian Springs	Apex
5/6/2020	78	77	76	73	72		75		76
5/9/2020	71	74							
5/28/2020	71	76							
6/22/2020	73	74	78						
6/26/2020		73							
8/3/2020	82	78	81		72	72	73	71	
8/7/2020	71		72					72	
8/18/2020	82	79	78						
8/19/2020	74	74	73	71					
8/20/2020			71						
8/21/2020		71							
9/2/2020	75	73							
9/26/2020	71		75						

1.2   Exceptional Event Rule Summary

The "EPA Guidance on the Preparation of Exceptional Events Demonstration for Wildfire Events that May Influence Ozone Concentrations" (U.S. Environmental Protection Agency, 2016) describes a three-tier analysis approach to determine a "clear causal relationship" for EE demonstrations from an air agency. A summary of analysis requirements for each tier is listed in Table 1-4, and in the list below.

- Tier 1 analyses can be used when ozone exceedances are clearly influenced by a wildfire in areas of typically low ozone concentrations, are associated with ozone concentrations higher than non-event-related values, or occur outside of an area's usual ozone season.

- Tier 2 analyses are appropriate for wildfire emission cases where the impacts of the wildfire on ozone levels are less clear and require more supportive documentation than Tier 1 analyses.

- If a more complicated relationship between the wildfire and the ozone exceedance is observed, Tier 3 analyses with additional supportive documentation—such as statistical modeling of the ozone event, vertical profile analysis of smoke in the column, and meteorological analysis—should be used.

All the recommended Tier 1, Tier 2, and Tier 3 analyses were conducted in this work.

Table 1-4. Tier 1, 2, and 3 EE analysis requirements for evaluating wildfire impacts on ozone exceedances.

Tier	Requirements
1	- Comparison of fire-influenced exceedance with historical concentrations - Key factor: Evidence that fire and monitor meet one of the following criteria: - Seasonality differs from typical season, or - Ozone concentrations are 5-10 ppb higher than non-event-related concentrations - Evidence of transport of fire emissions to monitor: - Trajectories of fire emissions (reaching ground level) - Satellite images and supporting evidence from surface measurements - Media coverage and photographic evidence of smoke
2	- All Tier 1 requirements - Key Factor #1: Fire emissions and distance of fires - Key Factor #2: Comparison of the event-related ozone concentration, with non-event-related high ozone concentrations (high percentile rank over five years/seasons) - Annual and seasonal comparison - Evidence that fire emissions affected the monitor (at least one of the following): - Visibility impacts - Changes in supporting measurements - Satellite enhancements of fire-related species (i.e., NO_x, carbon monoxide [CO], aerosol optical depth [AOD], etc.) - Fire-related enhancement ratios and/or tracer species - Differences in spatial/temporal patterns
3	- All Tier 2 requirements - Evidence of fire emissions effects on monitor: - Multiple analyses from those listed for Tier 2 - Evidence of fire emissions transport to the monitor: - Trajectory or satellite plume analysis, and - Additional discussion of meteorological conditions - Additional evidence such as: - Comparison to ozone concentrations on matching (meteorologically similar) days - Statistical regression modeling - Photochemical modeling of smoke contributions to ozone concentrations

1.3   Demonstration Outline

As discussed in Section 1.2, the "clear causal relationship" analyses involve first comparing the exceedance ozone concentrations to historical values, providing evidence that the event and monitors meet the tier's key factors, providing evidence of the transport of wildfire emissions to the

monitors, and additional analyses such as ground-level measurements and various forms of modeling depending on the complexity of the event. Table 1-5 summarizes the key factors and additional supporting evidence of the tiered approach and shows the corresponding sections in this report for each analysis.

Table 1-5. Locations of Tier 1, 2, and 3 elements in this report.

Tier	Element	Section of This Report (Analysis Type)
Tier 1	Key Factor: seasonality differs from typical season and/or ozone concentrations are 5-10 ppb higher than non-event-related concentrations	Section 3.1.1 (comparison of event with historical data)
	Evidence of transport of fire emissions to monitor	Sections 3.1.2 (maps of ozone, particulate matter with a diameter less than 2.5 micrometers [$PM_{2.5}$] and fire, smoke), and 3.1.3 (Hybrid Single-Particle Lagrangian Integrated Trajectory [HYSPLIT] trajectories)
	Media coverage and photographic evidence of smoke	Section 3.1.4 (Media coverage and Images)
Tier 2	Key Factor #1: fire emissions (Q) and distance of fires (d)	Section 3.2.1 (analysis of the relationship between fire emissions and distance [Q/d])
	Key Factor #2: comparison of event concentrations with non-event-related high ozone concentrations	Section 3.2.2 (comparison of event concentrations with non-event concentrations)
	Evidence that the fire emissions affected the monitor	Sections 3.2.3 (Satellite Retrievals of Pollutant Concentrations) and 3.2.4 (changes in supporting measurements, differences in spatial/temporal patterns, and tracer measurements)
Tier 3	Evidence of fire emissions transport to the monitor	Section 3.3.1 (trajectory or satellite plume analysis, additional discussion of meteorological conditions, comparison to ozone concentrations on matching [meteorologically similar] days)
	Meteorologically similar matching day analysis	Section 3.3.2 (methodology and analysis for meteorologically similar days)
	Additional evidence	Section 3.3.3 (statistical regression modeling)

Tier 1 analyses are shown in Section 3.1. The key factor of Tier 1 analyses is the ozone concentration's uniqueness when compared to the typical seasonality and/or levels of ozone exceedance. The EPA guidance suggests providing a time series plot of 12 months of ozone concentrations overlaying more than five years of monitored data and describing how typical seasonality differs from ozone in the demonstration (U.S. Environmental Protection Agency, 2016). In addition, trajectory analysis—produced by the Hybrid Single-Particle Lagrangian Integrated Trajectory (HYSPLIT) model, together with satellite plume imagery and ground-level measurements of plume components (e.g., $PM_{2.5}$, CO, or organic and elemental carbon)—should be used to provide evidence of wildfire emissions being transported to the monitoring sites. We demonstrate the Tier 1 analysis results for the June 22, 2020, event in Section 3.1. We address the key factors in Section 3.1.1, provide evidence of wildfire smoke transport to the Clark County monitoring sites in Sections 3.1.2 and 3.1.3, and discuss the media coverage and show ground images in Section 3.1.4.

Tier 2 analyses are shown in Section 3.2. The two key factors for Tier 2 analyses are (1) fire emissions and distance of fires to the impacted monitoring sites, and (2) comparison of event-related ozone concentrations with non-event-related high ozone values. We address the first factor in Section 3.2.1 by determining the emissions divided by distance (Q/d) relationship and address the second factor in Section 3.2.2 by comparing the six-year percentiles and yearly rank-order analysis of ozone concentrations. The Tier 2 analyses also require evidence of wildfire smoke transport to affected monitoring sites; we provide this evidence in Section 3.2.3 through satellite measurements of pollutant concentrations. In Section 3.2.4, we discuss supporting pollutant trends and diurnal patterns of surface-measured $PM_{2.5}$, CO, NO_x, and total nonmethane organic compounds (TNMOC) compared with ozone concentrations and wildfire tracer measurements. The Tier 2 analyses are included in this demonstration for completeness and to inform the Tier 3 analyses but, alone, are not expected to clearly demonstrate a relationship between the wildfire emissions and the monitored exceedances (see Section 3.2). We performed Tier 3 analyses to provide clear causal weight of evidence of this relationship.

Tier 3 analyses are shown in Section 3.3. For this tier, total column information and event-related meteorological conditions (Section 3.3.1) were investigated, and a Generalized Additive Statistical Model (GAM) was developed to estimate the wildfire's contribution to ozone concentrations (Section 3.3.2).

Following the EPA's EE guidance, we performed Tier 1, Tier 2, and Tier 3 analyses to show the "clear causal relationship" between the Ivanpah Fire and Arizona wildfires and the exceedance event in Clark County on June 22, 2020. Focusing on the characterization of the meteorology, smoke, transport, and air quality on the days leading up to the event, the following specific analyses were conducted (results of these analyses are presented in Section 3):

- Developed time series plots that show the June 22 ozone concentrations at each affected monitoring site in historical context for 2020 and the past six years

- Compiled maps of (1) ozone and $PM_{2.5}$ concentrations in the area, (2) smoke plumes, and (3) fire locations from satellite data

- Showed the transport patterns via HYSPLIT modeling, and identified where the back trajectory air mass intersected with smoke plumes or passed over or near fires

- Discussed media coverage of the June 22 event and showed ground images

- Quantified total fire emissions and calculated emissions/distance ratio (Q/d) for the fire

- Performed statistical analysis to compare event ozone concentrations to non-event concentrations

- Provided maps showing satellite retrievals of NO_x, AOD, and CO

- Developed plots to show diurnal patterns of ozone and supporting pollutants such as $PM_{2.5}$, CO, NO_x, and TNMOC

- Examined wildfire tracer species and their background concentrations vs. event concentrations

- Assessed vertical transport of smoke using satellite-observed aerosol vertical profiles and ceilometer mixing height retrievals

- Created a GAM model of MDA8 ozone concentrations to assess the enhancement of ozone concentrations due to wildfire influence

1.4   Conceptual Model

The conceptual model for the EE on June 22, 2020, that lead to the ozone exceedances at the Paul Meyer, Walter Johnson, and Joe Neal monitoring sites is outlined in Table 1-5. We provide the analysis techniques performed and evidence for each Tier. This establishes a weight of evidence for the clear causal relationship between wildfire emissions in Arizona and California and the June 22, 2020, exceptional ozone event. We assert that wildfire emissions from Arizona wildfires that arrived the night of June 21 led to enhanced ozone concentrations in Clark County on June 22 and exceedances at the Paul Meyer, Walter Johnson, and Joe Neal sites. Additionally, the Ivanpah Fire in California likely extended the duration of high daytime ozone on June 22, but the timing of smoke impact on Clark County is less certain. In support of this assertion, the key points of evidence for the conceptual model are summarized below.

1. The June 22, 2020, ozone exceedance occurred during a typical ozone season, but event concentrations at the Paul Meyer, Walter Johnson, and Joe Neal exceedance sites were significantly higher than non-event concentrations. Ozone concentrations at the three exceedance sites showed a high percentile rank when compared with the past six years and ozone seasons.

2. HMS smoke and fire detections and modeled emission tracer dispersion show that wildfire emissions from the Bighorn, Bush, and Mangum fires in Arizona covered a region south and east of Clark County that coincided with transport from the south into Clark County on June 21, 2020. HMS smoke and fire reports also constrain the initiation of the Ivanpah fire in the

Mojave National Preserve to mid-day on June 22.

3. Near-surface back and forward trajectories at the exceedance sites at the time of maximum ozone concentration show consistent transport patterns intersecting with boundary layer smoke. This smoke was from the western Arizona fires that arrived in Clark County in the late evening on June 21 during low wind conditions, which favor air circulation within the Las Vegas Valley. Trajectories on the event day also demonstrate near-surface, short-range transport from the Ivanpah fire into Clark County in the mid-afternoon on June 22 that possibly extended the duration of high daytime ozone.

4. Meteorological conditions on June 22 did not favor enhanced local ozone production when compared with meteorologically similar ozone season days. Average MDA8 ozone across similar days was well below the ozone NAAQS and >10 ppb lower than the June 22 ozone exceedances.

5. GAM model predictions of MDA8 ozone on June 22 are all well below the 70-ppb ozone NAAQS for each EE-affected site. Using the 75th-95th quantile of positive residuals (observed MDA8 ozone minus GAM-predicted MDA8 ozone) we find a minimum wildfire effect on ozone of 2-10 ppb in Clark County from an atypical source; in this case, the Arizona wildfires and Ivanpah Fire.

6. Wildfire smoke impacted the typical diurnal profiles of ground-level $PM_{2.5}$, CO, NO_2, and TNMOC on the evening preceding June 22. The anomalous, concurrent, sharp evening enhancement observed in these pollutants suggest that wildfire emissions were transported into Clark County, diluted in the nighttime boundary layer, and circulated in the valley overnight before the EE. Elevated carbonaceous aerosol (OC+EC) contributions to $PM_{2.5}$ and levoglucosan wildfire tracers persisted in the Clark County area based on June 23 observations.

2.   Historical and Non-Event Model

2.1   Regional Description

Clark County is located in the southern portion of Nevada and borders California and Arizona. Clark County includes the City of Las Vegas, one of the fastest growing metropolitan areas in the United States with a population of approximately 2 million (U.S. Census Bureau, 2010). Las Vegas is located in a 1,600 km^2 desert valley basin at 500 to 900 m above sea level (Langford et al., 2015). It is surrounded by the Spring Mountains to the west (3,000 m elevation), the Sheep Mountain Range to the north (2,500 m elevation), and three mountain ranges to the south. The valley floor slopes downward from west to east, which influences surface wind, temperature, precipitation, and runoff patterns. The Cajon Pass and I-15 corridor to the west is an important atmospheric transport pathway from the Los Angeles Basin into the Las Vegas Valley (Langford et al., 2015). **Figures 2-1 and 2-2** show the topography of the Clark County area and surrounding areas.

The Las Vegas Valley climatology features abundant sunshine and hot summertime temperatures, with average summer month high temperatures of 34-40°C. Because of the mountain barriers to moisture inflow, the region experiences dry conditions year-round (~107 mm annual precipitation, 22% of which occurs during the summer monsoon season in July through September). The urban heat island effect in Las Vegas during the summer leads to large temperature gradients within the valley, with generally cooler temperatures on the eastern side. During the summer season, monsoon moisture brings high humidity and thunderstorms to the region, typically in July and August (National Weather Service Forecast Office, 2020). Winds in the Las Vegas basin tend to be out of the southwest during spring and summer (Los Angeles is upwind), while winds in the fall and winter tend to be out of the northwest, with air transported between the neighboring mountain ranges and along the valley.
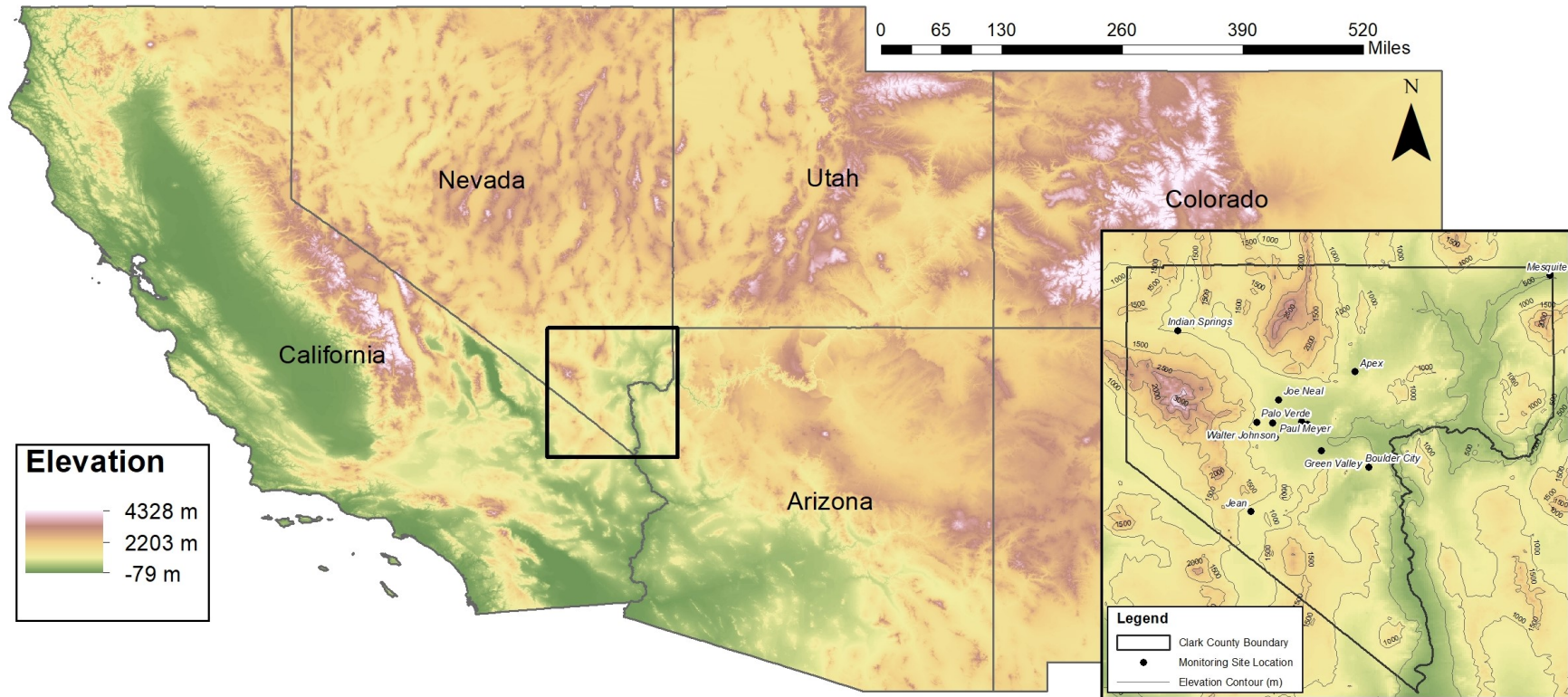
Figure 2-1. Regional topography around Clark County, with an inset showing county boundaries and the air quality monitoring sites analyzed in this report.
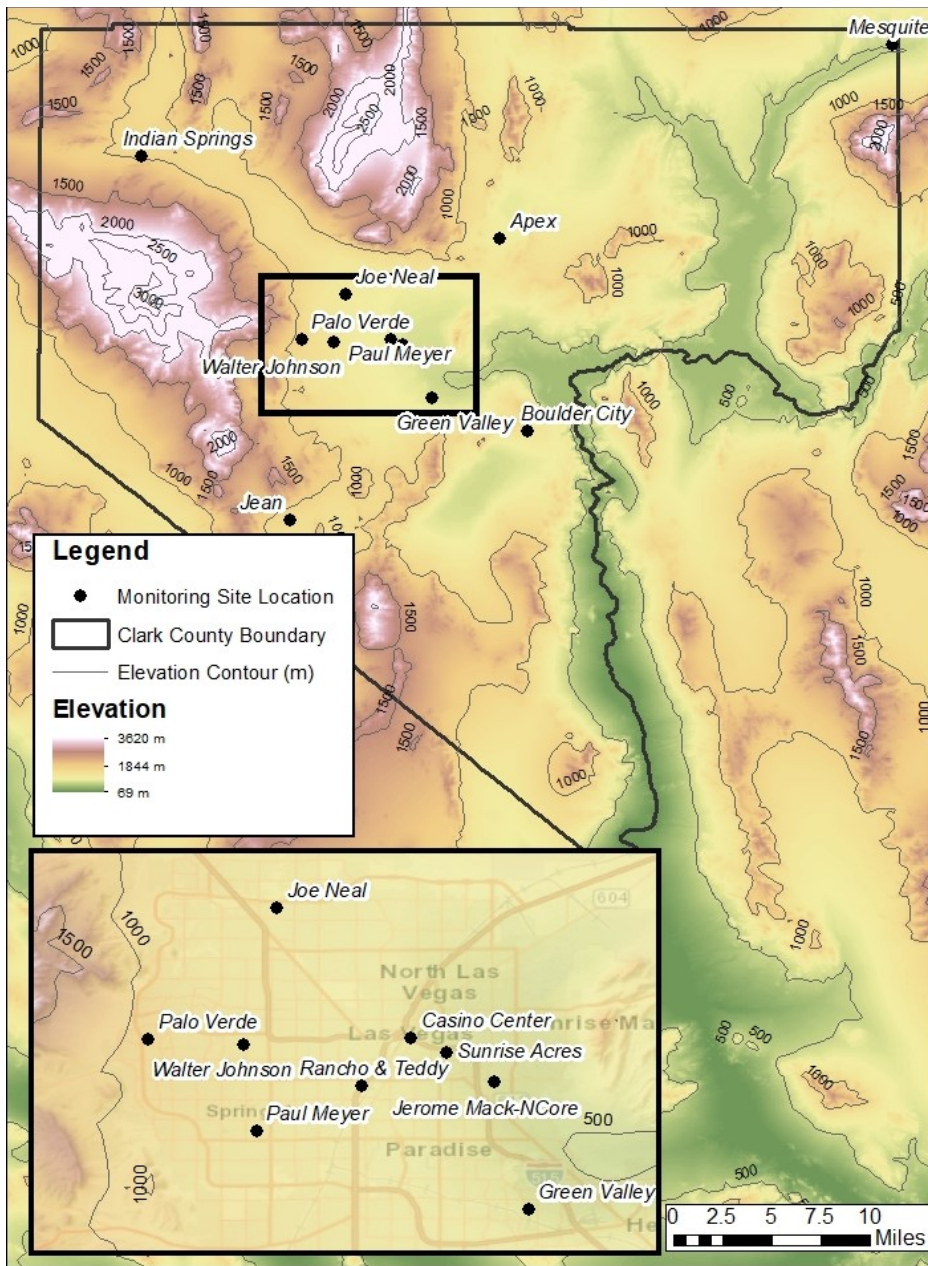
Figure 2-2. Clark County topography, with an inset showing all air quality monitoring sites in the Clark County area.

2.2 Overview of Monitoring Network

The Clark County Department of Environment and Sustainability, Division of Air Quality (DAQ) operated 14 ambient air monitoring sites in the region during 2020 (Figure 2-2). These sites measure

hourly ozone, PM$_{2.5}$, particulate matter with a diameter less than 10 micrometers (PM$_{10}$), NO$_x$, TNMOC, and CO concentrations along with meteorological parameters. Table 2-1 presents the monitoring data coverage across time and space for criteria pollutants and surface meteorological parameters (barometric pressure, temperature, wind speed and direction), as well as mixing height. Ozone and other criteria pollutants at 11 sites around Clark County were examined to investigate the high ozone event observed on June 22, 2020. DAQ's ambient air monitoring network meets the monitoring requirements for criteria pollutants pursuant to Title 40, Part 58, of the Code of Federal Regulations (CFR), Appendix D (40 CFR Part 50, Appendix U). Data are quality-assured in accordance with 40 CFR 58 and submitted to the EPA's Air Quality System (AQS). The spatial distribution of monitoring sites characterizes the regional air quality in Las Vegas, as well as air quality upwind and downwind of the urban valley region (Figure 2-2). The Jean monitoring site along the I-15 corridor is generally upwind such that it captures atmospheric transport into the region and is least impacted by local sources (Figure 2-2).

Table 2-1. Clark County monitoring site data. The available date ranges of all parameters and monitoring sites used in this report for Clark County, Nevada, are shown. Casino Center and RT are near-road sites and are not used for the EE analysis.

Site	AQS Sitecode	O₃	PM₂.₅	CO	NO	NO₂	TNMOC	Temp.	Wind Speed	Wind Direction	Barom. Pressure	Mixing Height
Apex	320030022	2014-2020						2014-2020	2014-2020	2014-2020		
Boulder City	320030601	2014-2020									2014-2016	
Casino Center	320031502							2014-2020	2016-2020	2016-2020		
Green Valley	320030298	2015-2020	2014-2020	2020				2016-2020	2014-2020	2014-2020	2014-2016	
Indian Springs	320037772	2014-2020										
Jean	320031019	2014-2020	2014-2020					2014-2020	2014-2020	2014-2020	2014-2016	
Jerome Mack	320030540	2014-2020	2014-2020	2015-2020[1,2]	2015-2020	2015-2020	2020	2014-2020	2014-2020	2014-2020	2014-2020	2020
Joe Neal	320030075	2020	2018-2020	2019-2020		2015-2020		2014-2020	2014-2020	2014-2020	2014-2016	
Mesquite	320030023	2014-2020						2014-2020	2014-2020	2014-2020		
Palo Verde	320030073	2014-2020	2020					2014-2020	2014-2020	2014-2020	2014-2016	
Paul Meyer	320030043	2014-2020	2017-2020					2014-2020	2014-2020	2014-2020	2014-2016	
RT	320031501							2015-2020	2015-2020	2015-2020	2014-2016	
Sunrise Acres	320030561			2020				2014-2020	2014-2020	2014-2020	2014-2016	
Walter Johnson	320030071	2014-2020	2020					2015-2020	2015-2020	2015-2020	2014-2016	

[1] CO data invalid at Jerome Mack on Sep. 2, 2020

[2] CO data invalid at Jerome Mack Apr. 28, 2020 – May 20, 2020

2.3   Characteristics of Non-Event Historical Ozone Formation

During the ozone season (April–September) in Clark County, Nevada, ozone concentrations are typically influenced by local formation, transport into the region, and on occasion by EEs such as wildfires and stratospheric intrusions. Transport from upwind source regions (e.g., Los Angeles Basin, Mojave Desert, Asia) occurs with southwesterly winds, and southerly transport dominates the later portion of the season due to the summer monsoon (Langford et al., 2015; Zhang et al., 2020). Local precursor emissions in Clark County include mobile NO_x and VOC sources, coal and natural-gas fueled power generation NO_x sources, and biogenic VOC emissions. Based on 2017 emission inventories in Las Vegas, there are 98 tons of NO_x and 238 tons of VOC emissions per day on a typical ozone season weekday (Clark County Department of Environment and Sustainability, 2020). On-road mobile sources comprise 40% of NO_x emissions and total mobile source emissions comprise 88% of total NO_x emissions during the ozone season. In contrast, 52% of VOC emissions originate from biogenic sources within Clark County. Local emissions and/or precursors transported into the region contribute to ozone formation within Clark County (Langford et al., 2015; Clark County Department of Air Quality, 2019).

In this demonstration, the impacts of wildfire smoke on ozone concentrations in Clark County on June 22, 2020, are discussed. In order to fully discern the effect of wildfire smoke on ozone concentrations in Clark County on June 22, 2020, the historical ozone record for all affected sites (see Table 1-1 in Section 1) are examined. *Non-event days* refer to all days other than the June 22 event. Because percentile rankings are sensitive to including the relatively large number of potential EE days during 2018 and 2020, statistics *excluding potential EE days* (i.e., without including the 2018 and 2020 potential EE days as defined in Tables 1-2 and 1-3 in Section 1) are also provided. The 8-hour ozone design value (DV) is the three-year running average of the fourth-highest daily maximum 8-hour (MDA8) ozone concentration (40 CFR Part 50, Appendix U). Within Clark County, Las Vegas is classified as an EPA Region 9 marginal nonattainment region with a 73 ppb ozone DV for 2017-2019 (U.S. Environmental Protection Agency, 2020).

Ozone EE days are identified as days with significant wildfire or stratospheric intrusion influence in addition to an MDA8 concentration greater than 70 ppb. By this criterion, there were 15 possible EE days in 2018, 13 possible EE days in 2020, and no EE days in 2019.

The EE on June 22, 2020, occurred early in the ozone season under hot, dry air, upper-level high pressure and surface low-pressure meteorological conditions. These conditions favor subsidence and enhanced vertical mixing of wildfire smoke-influenced ozone and precursors to ground level (see Section 3.3.1). Compared with a non-event conceptual model of local precursor emissions contributing to ozone formation at ground level under similar conditions, the June 22 conditions indicate additional local boundary transport of wildfire-influenced air parcels on the event date via surface westerly winds.

Figures 2-3 through 2-8 depict the six-year historical record and seasonality of MDA8 ozone concentrations at each EE affected monitoring site, along with the 99th percentile and NAAQS ozone concentrations. June 22 ranks in the top 1% for daily maximum ozone concentration in the six-year historical record at two of the three EE affected sites. June 22 also ranks in the top 5% for MDA8 ozone during the ozone season at each of the three EE affected sites. **Figure 2-9** depicts a two-week ozone diurnal cycle of 1-hour ozone beginning one week before the June 22 event and ending one week after. On June 22, daily maximum 1-hour ozone concentrations were the highest during this two-week period at each of the three EE affected sites (Table 1-1).
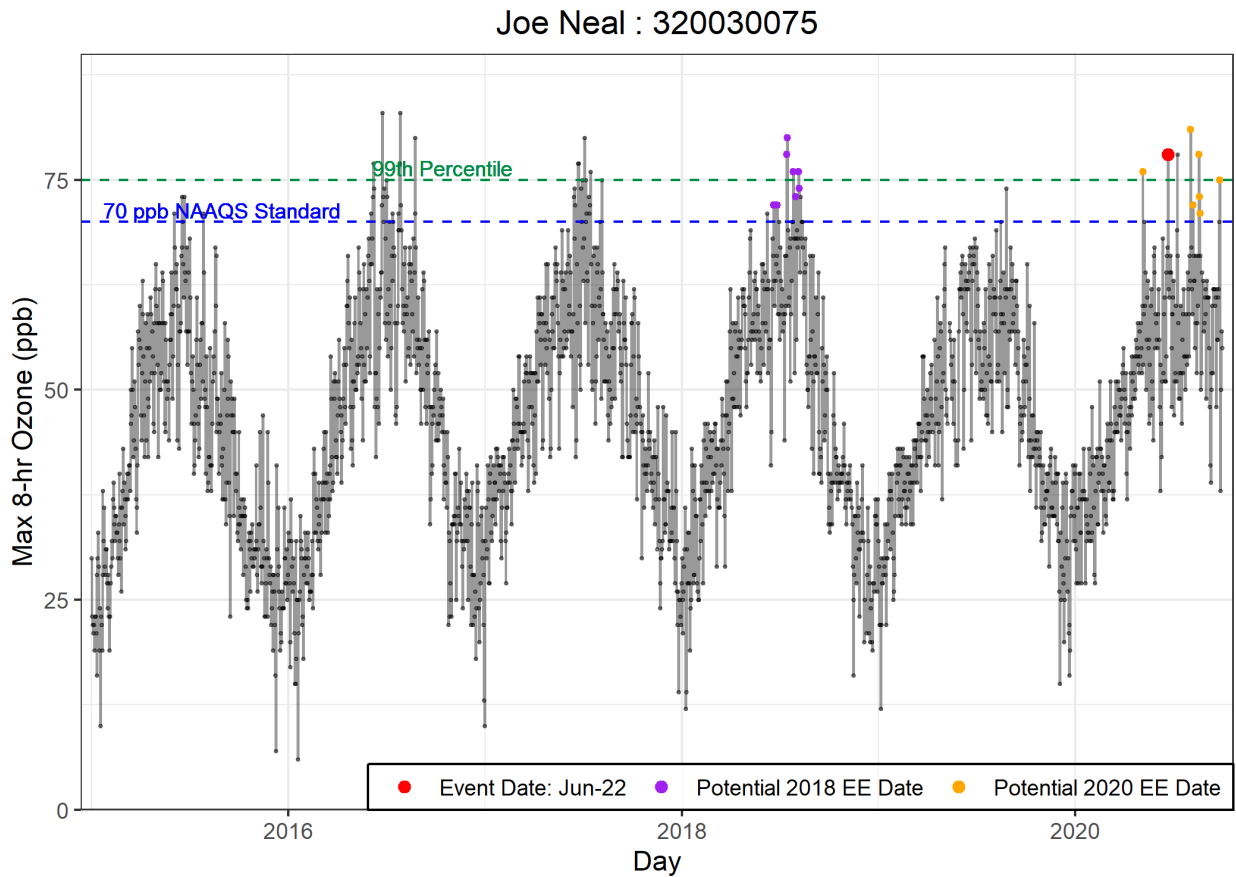
Figure 2-3. Time series of 2015-2020 ozone concentrations at the Joe Neal site. June 22, 2020, is shown in red.
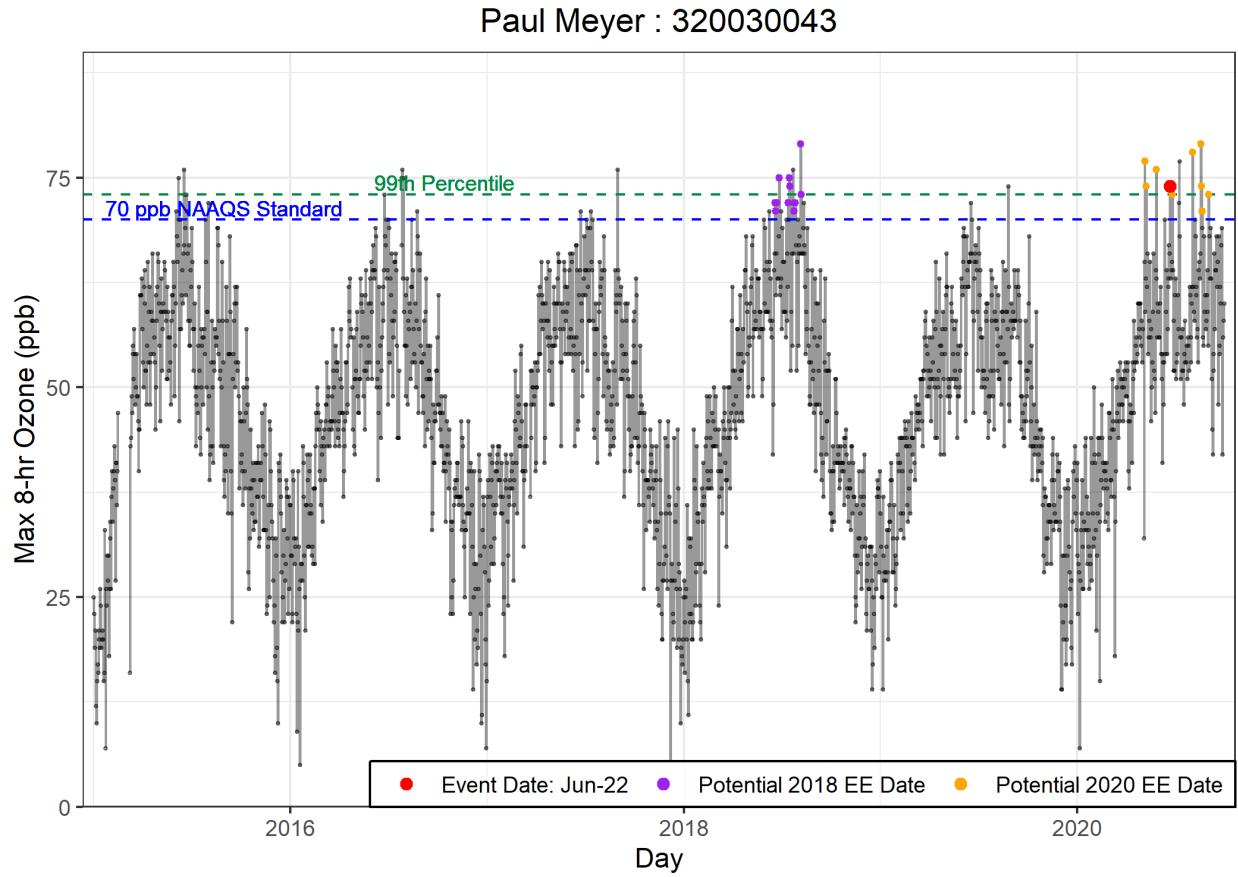
Figure 2-4. Time series of 2015-2020 ozone concentrations at the Paul Meyer site. June 22, 2020, is shown in red.

Walter Johnson : 320030071
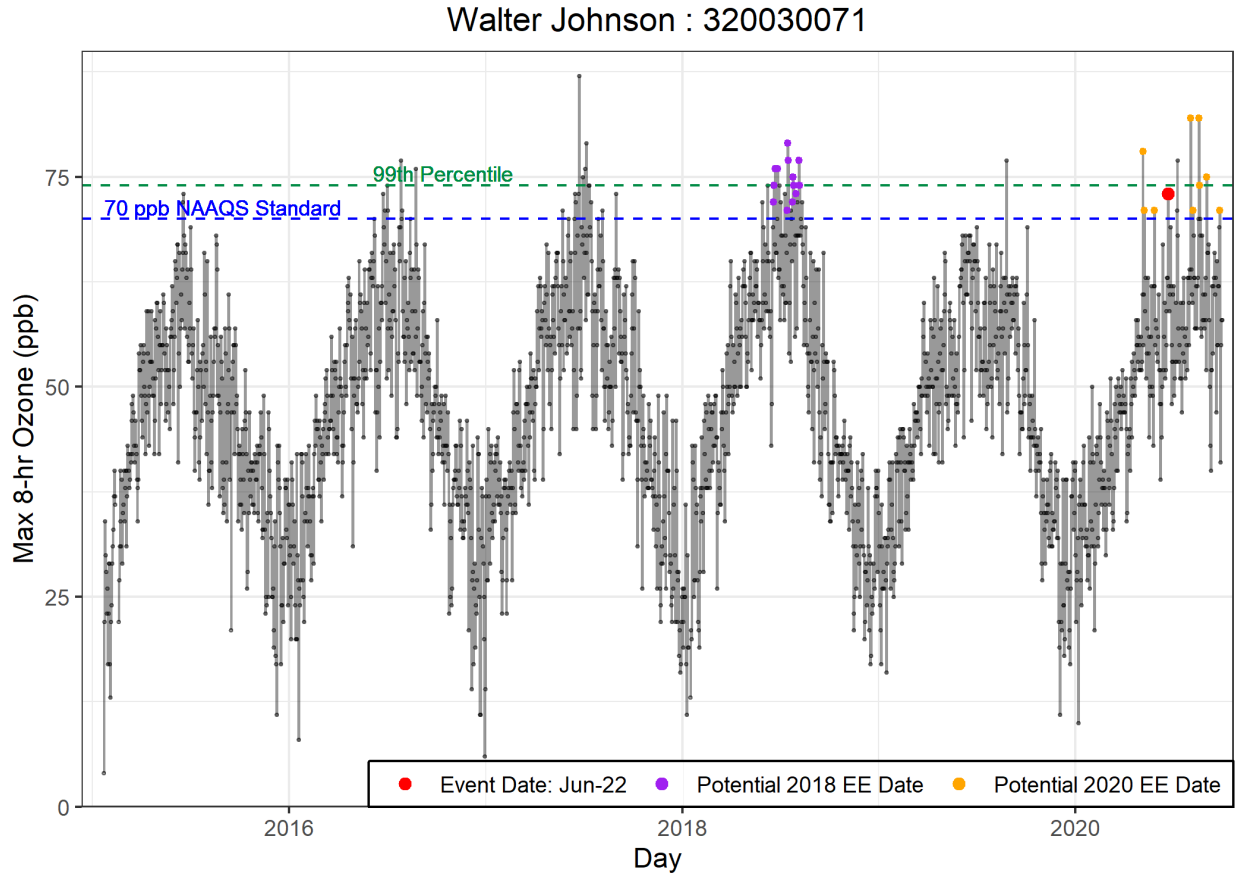
Figure 2-5. Time series of 2015-2020 ozone concentrations at the Walter Johnson site. June 22, 2020, is shown in red.
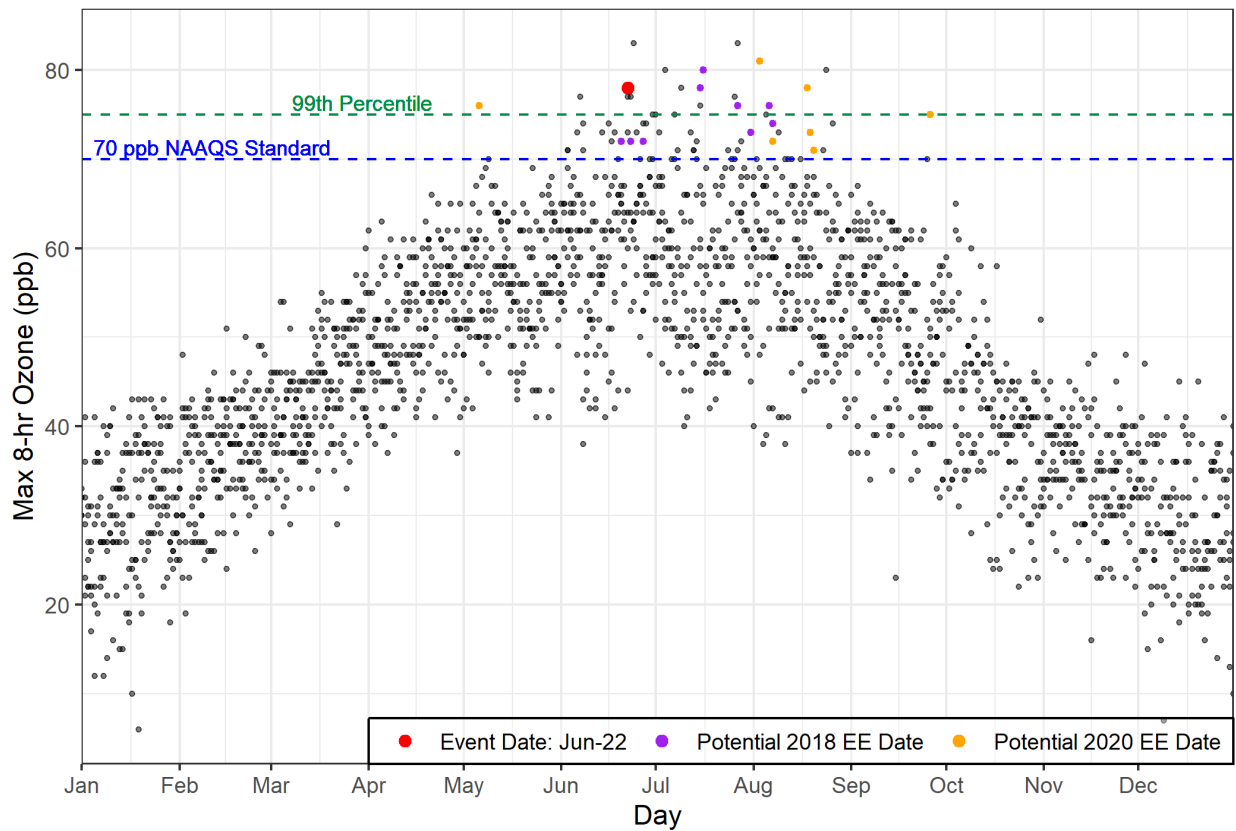
Figure 2-6. Seasonality of 2015-2020 ozone concentrations from the Joe Neal site. June 22, 2020, is shown in red.
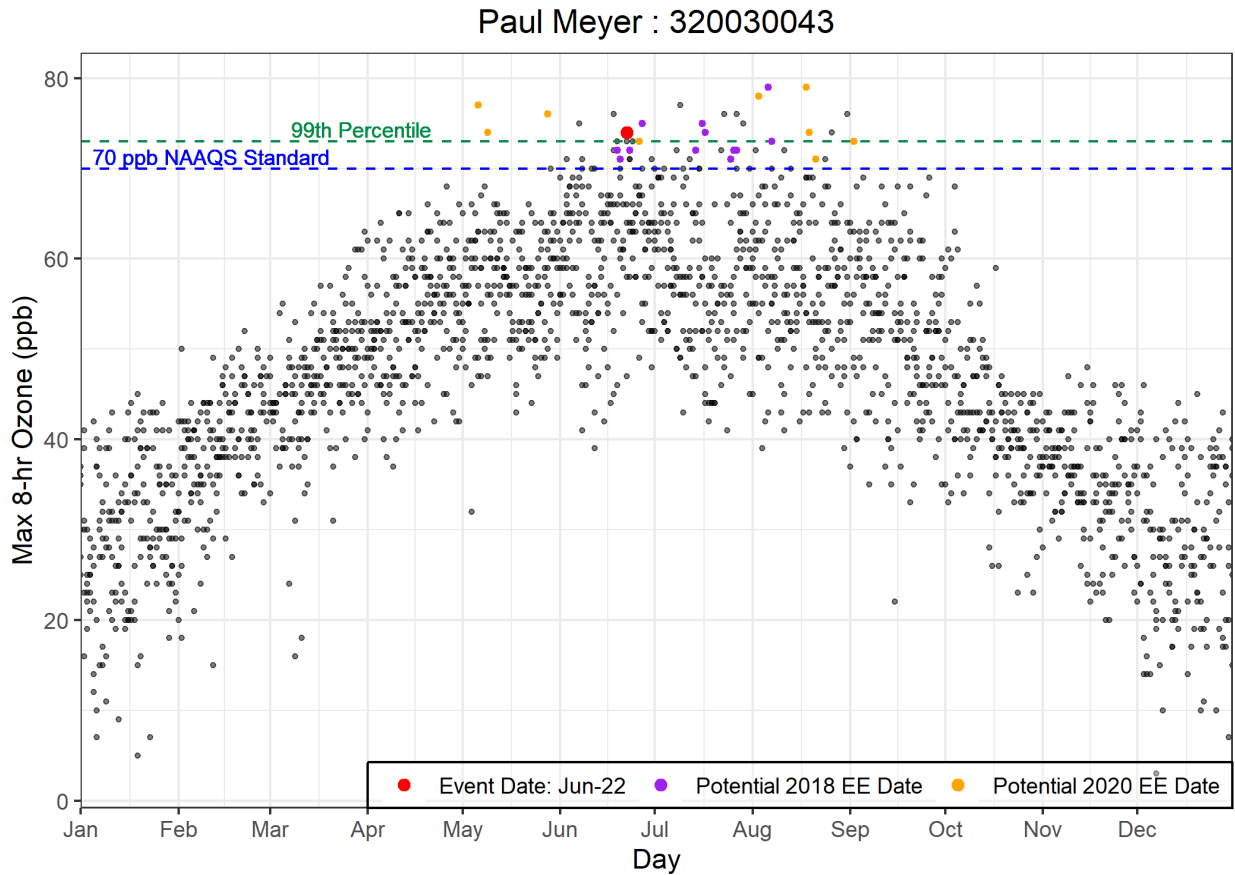
Figure 2-7. Seasonality of 2015-2020 ozone concentrations from the Paul Meyer site. June 22, 2020, is shown in red.
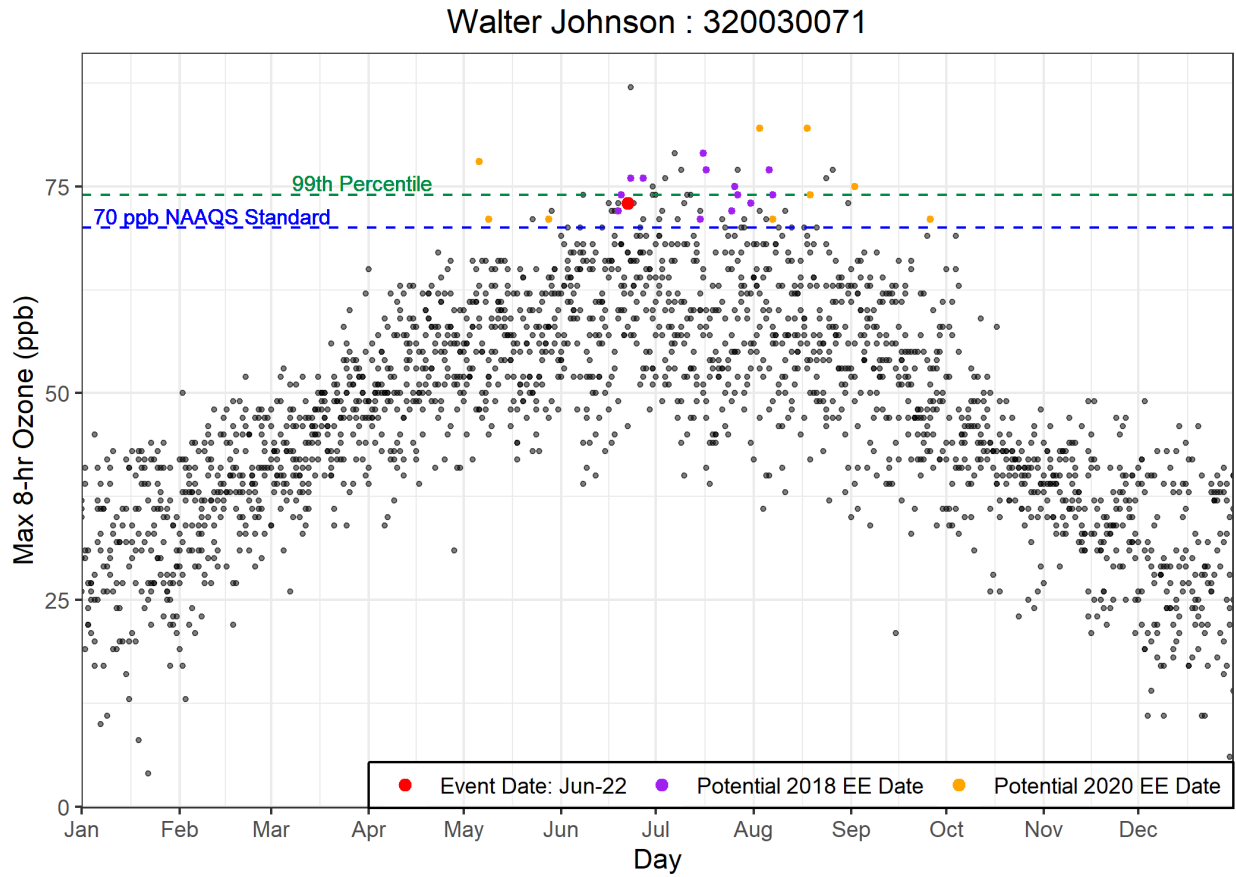
Figure 2-8. Seasonality of 2015-2020 ozone concentrations from the Walter Johnson site. June 22, 2020, is shown in red.
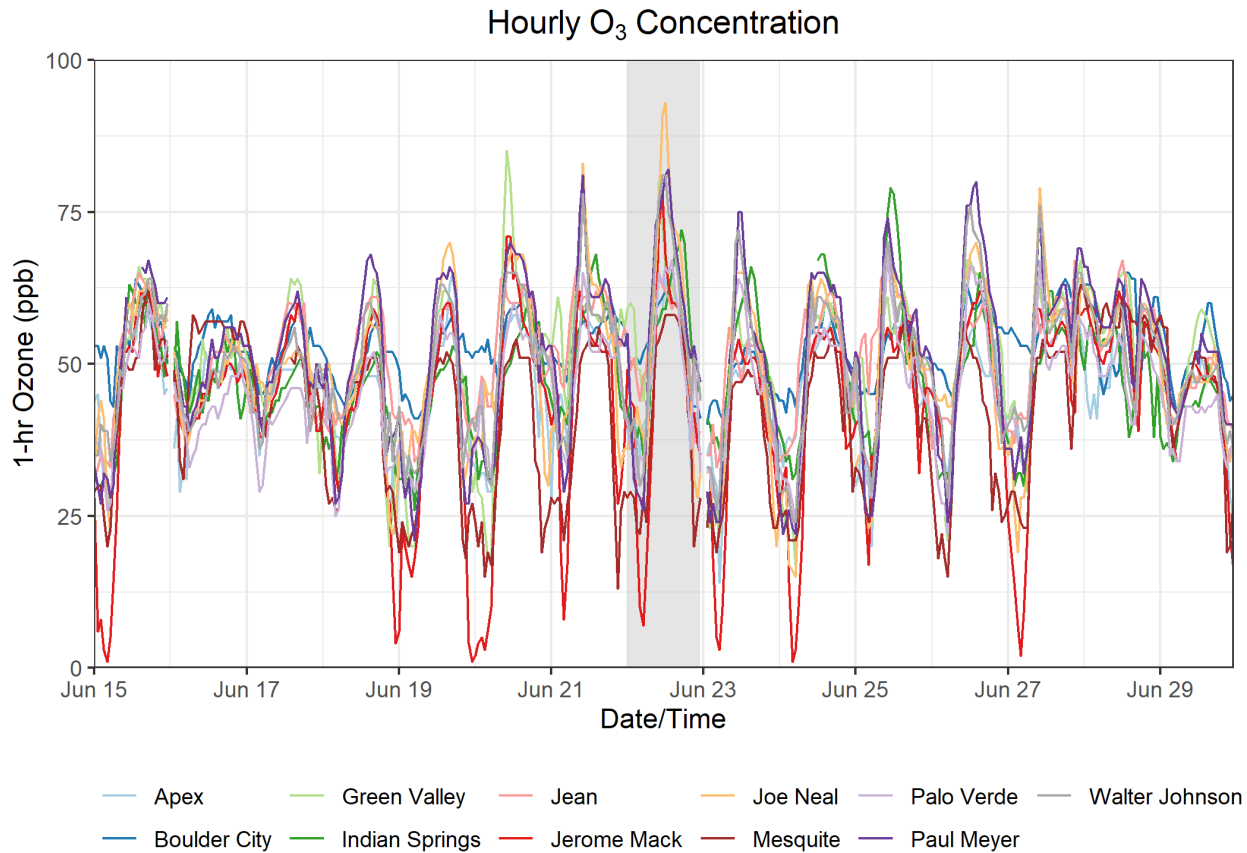
Figure 2-9. Ozone time series at all monitoring sites. Time series of hourly ozone concentrations at monitoring sites in Clark County for one week before and after the June 22 event are shown. June 22, 2020, is shaded for reference.

3. Clear Causal Relationship Analyses

3.1 Tier 1 Analyses

3.1.1 Comparison of Event with Historical Data

To address the Tier 1 EE criterion of comparison with historical ozone, the June 22 EE ozone concentrations at each site were compared with the 2020 ozone record, focusing mainly on the ozone season when the highest ozone concentrations occur. **Figures 3-1 through 3-3** depict the 2020 daily maximum ozone record at each monitoring site, along with the 99th percentile of previous 5-year MDA8 ozone and NAAQS criteria ozone concentrations. During 2020, June 22 ranks in the top 1% for daily maximum ozone concentration at the Paul Meyer and Joe Neal monitoring sites. When compared with daily ozone rankings on June 22 over the six-year ozone record at all EE affected sites (Figures 2-6 through 2-8), the 2020 rankings indicate that June 22, 2020, was an extreme ozone event.
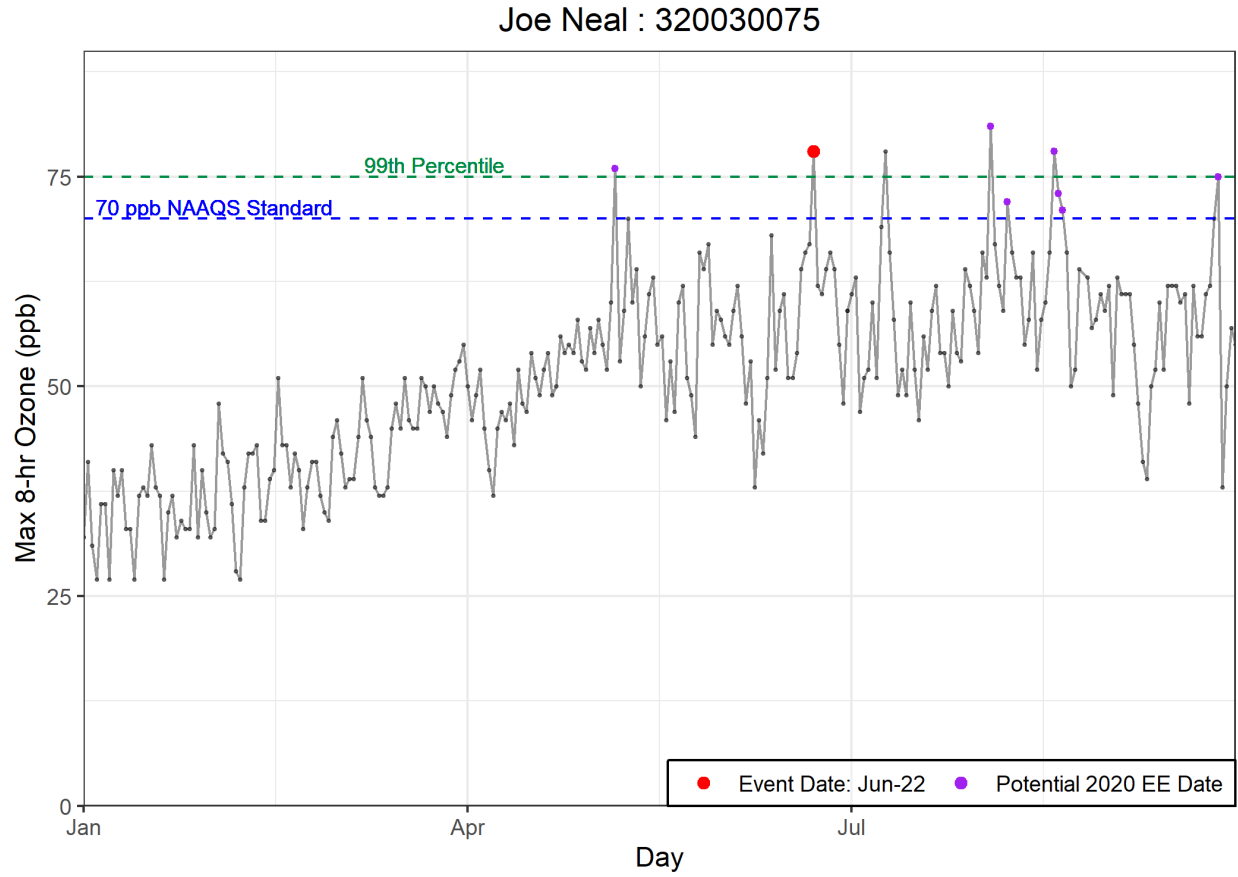
Figure 3-1. Time series of 2020 MDA8 ozone concentrations from the Joe Neal site. June 22, 2020, is shown in red.
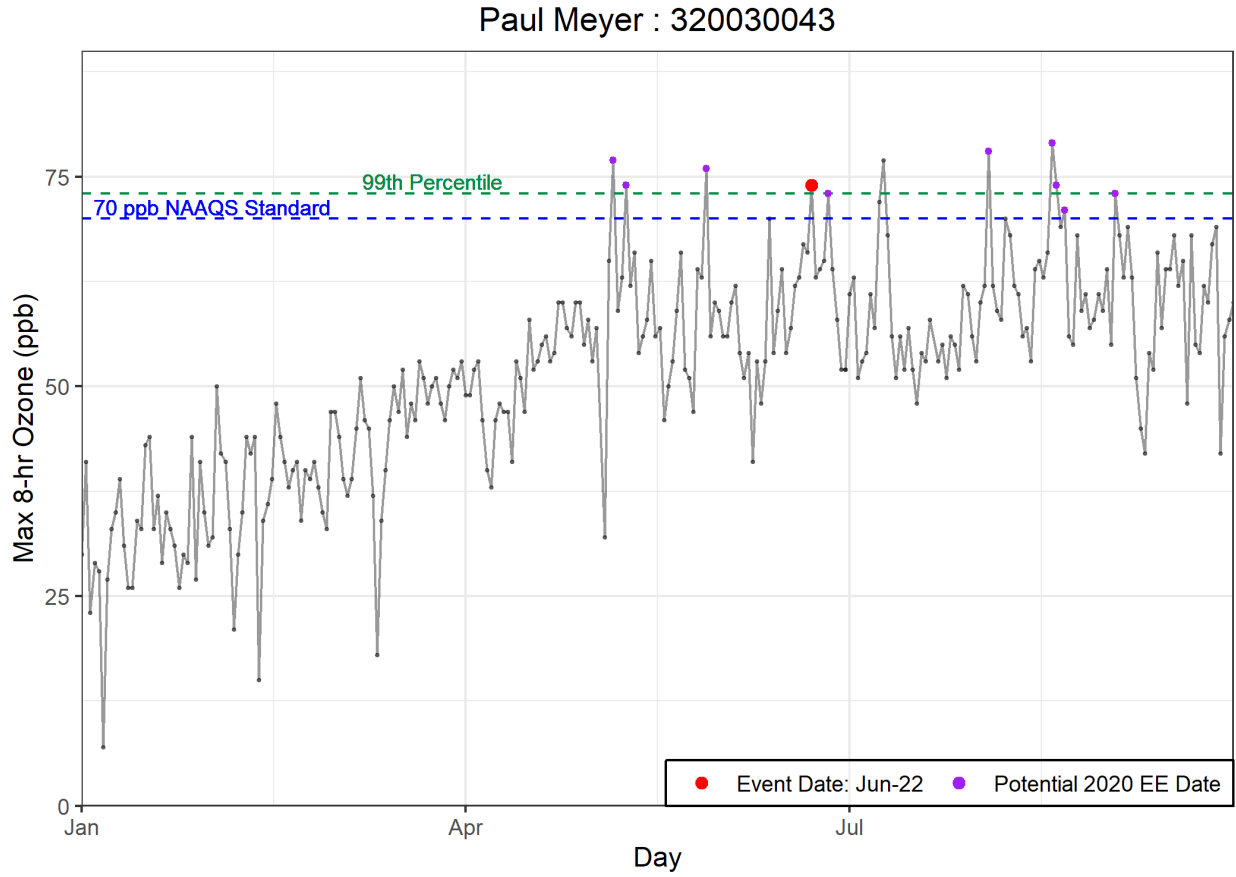
Figure 3-2. Time series of 2020 MDA8 ozone concentrations from the Paul Meyer site. June 22, 2020, is shown in red.
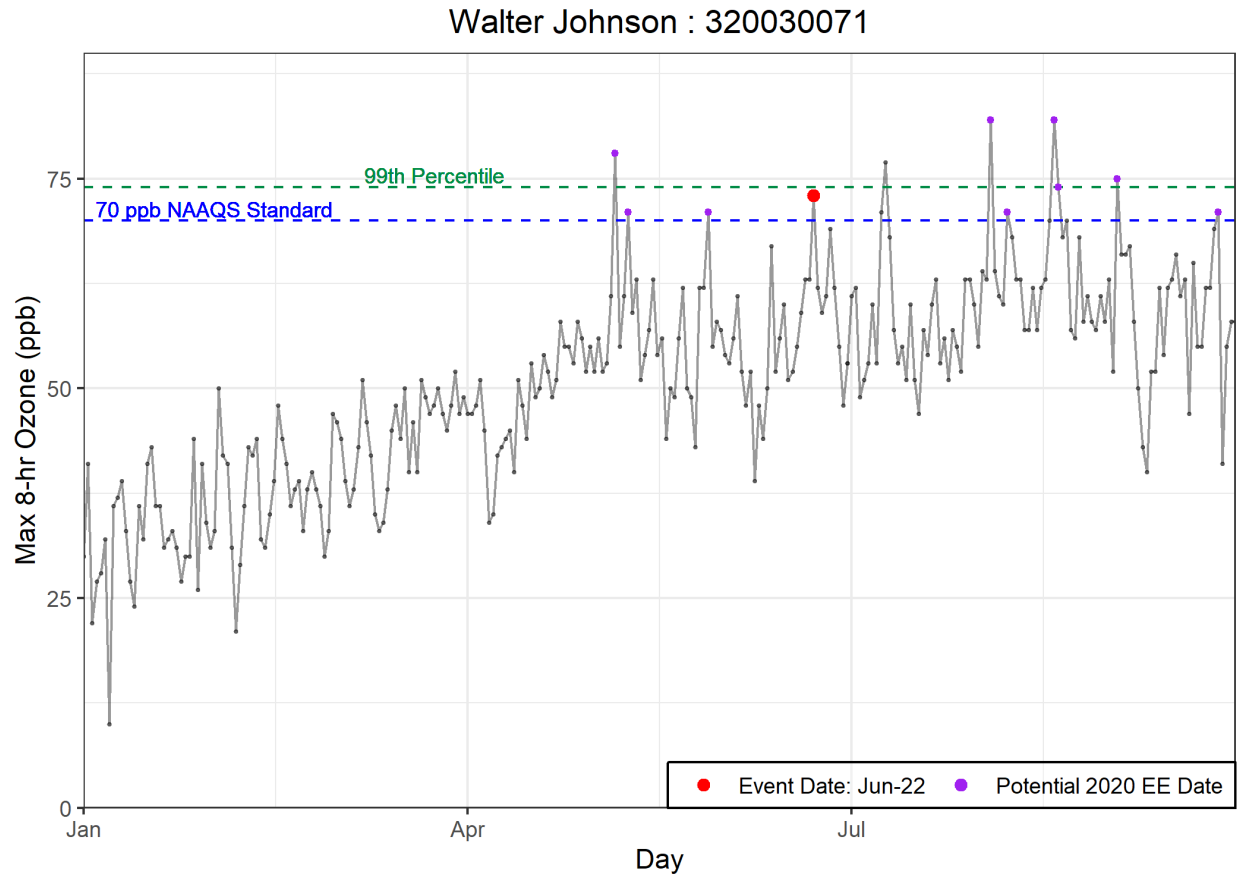
Figure 3-3. Time series of 2020 MDA8 ozone concentrations from the Walter Johnson site. June 22, 2020, is shown in red.

The June 22, 2020, ozone exceedance occurred during a typical ozone season, but June 22 MDA8 ozone concentrations were the second highest compared with daily ozone concentrations excluding potential EE days (Figures 3-1 through 3-3). Table 3-1 provides historical monitoring site statistics for each affected site on June 22, 2020. The statistics shown are for May through September in 2015-2019; proposed 2018 EE ozone concentrations are included. The MDA8 ozone concentrations on June 22 were >10 ppb above the mean and median ozone concentrations for the historical ozone season at all EE affected sites. The Joe Neal site exhibited ozone concentrations 6 ppb above the 95th percentile of ozone concentrations when compared with historical ozone season non-event days, while ozone concentrations at other EE affected sites were < 5 ppb above the 95th percentile of non-event day historical ozone (Table 3-1). Because June 22 is during the normal ozone season and MDA8 ozone concentration at two of three EE affected sites could not be clearly distinguished from the 95th percentile ozone concentration during the non-event historical ozone season, the June 22, 2020, event does not satisfy the key factor for a Tier 1 EE. Tier 2 comparison of the event-related ozone concentrations with non-event-related high ozone concentrations (> 99th percentile over five years or top four highest daily ozone measurements) are described in Section 3.2.2.

Table 3-1. Ozone season non-event comparison for June 22, 2020. MDA8 ozone concentrations (ppb) for each affected site are shown in the top row. Five-year (2015-2019) average MDA8 ozone statistics for May through September ozone season are shown for each affected site around Clark County to compare with the event ozone concentrations.

	Joe Neal 320030075	Paul Meyer 320030043	Walter Johnson 320030071
Jun. 22	78	74	73
Mean	57	57	57
Median	57	58	57
Mode	62	58	57
St. Dev	9	8	9
Minimum	23	22	21
95 %ile	72	70	71
99 %ile	78	76	77
Maximum	83	79	87
Range	60	57	66
Count	912	911	917

3.1.2 Ozone, Fire, and Smoke Maps

Ozone and PM$_{2.5}$ Maps

We produced maps of ozone Air Quality Index (AQI), PM$_{2.5}$ AQI levels, active fire and smoke detections from satellites, and visible satellite imagery that show the transport of smoke from California to Las Vegas on June 22, 2020. These maps also show that high ozone concentrations occurred across southern Nevada and Arizona corresponding with the presence of wildfire smoke.

From June 21-22, 2020, moderate and unhealthy ground-level ozone concentrations (indicated by the yellow, orange, and red areas) were detected in the western United States (**Figure 3-4**), especially in California, Arizona, and certain parts of Nevada and New Mexico. On June 21, high ozone concentrations (i.e., the orange and red areas) were seen in central and southern California, and these high concentrations continued to persist on June 22. On these two days, ozone and ozone precursors from the southern California region were transported northeast, reaching the California/Nevada state border. On June 22, the region of high ozone concentrations persisted over the northwest corner of Arizona and a large portion of southern Nevada, covering Las Vegas.
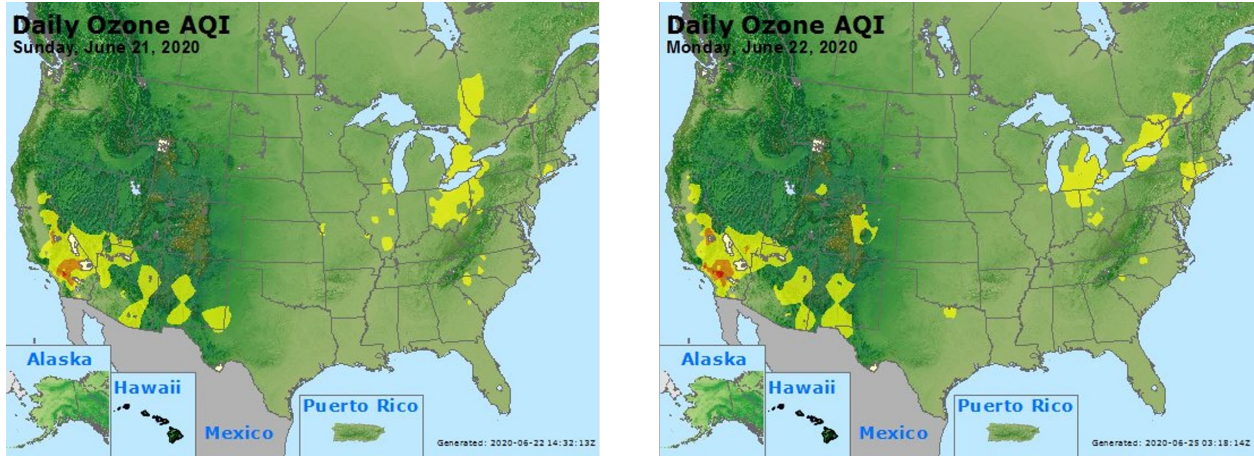
Figure 3-4. Daily ozone AQI for June 22 event (right) and the day before the event. Source: AirNow

From June 21 to 22, 2020, moderate PM$_{2.5}$ concentrations (indicated by the yellow areas) were detected in the western United States (**Figure 3-5**), mostly in southern California. On June 21, moderate PM$_{2.5}$ concentrations (i.e., yellow areas) were seen in southern California near the Los Angeles area, and these moderate concentrations continued on June 22 but encompassed a smaller area. The area between Los Angeles and Las Vegas is mostly devoid of PM$_{2.5}$ monitors. Therefore, enhanced PM$_{2.5}$ concentrations from the Ivanpah fire would not have been observed on June 22.
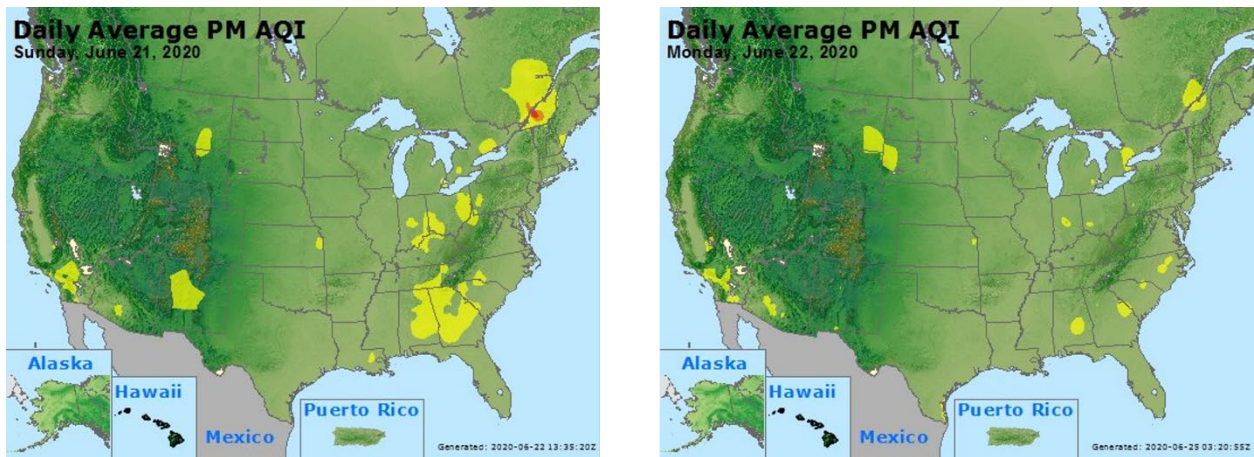
Figure 3-5. Daily PM$_{2.5}$ AQI for June 22 event (right) and the day before the event. Source: AirNow

HMS Fire Detection Maps

According to EPA's guidance on Tier 1 analysis requirements (U.S. Environmental Protection Agency, 2016), the National Oceanic and Atmospheric Administration (NOAA) Hazard Mapping System (HMS) Fire and Smoke Product can be used to demonstrate the transport of fire emissions to the impacted monitors. The HMS Fire and Smoke Product consists of

1. A daily fire detection product derived from three satellite data products[1] to spatially and temporally map fire locations at 1 km grid resolution, and

2. A daily smoke product derived from visible satellite imagery[2] that consists of polygons showing regions impacted by smoke.

The HMS smoke plume dataset is based on measurements from several environmental satellites and is reviewed by trained NOAA analysts to identify cases where smoke is dispersed by transport. The NOAA Satellite and Information Service website (**ospo.noaa.gov/Products/land/hms.html**) allows users to download real-time and archived HMS fire detection and smoke products.

Figure 3-6 shows the HMS smoke plume and fire detection data over the southwestern United States from June 19 to June 22, 2020, including southern California where the Ivanpah Fire started on June 22. As the daily plots indicate, there was fire activity throughout Arizona. The daily maps also show substantial smoke plumes forming in and covering western Arizona on June 19 through June 22. On June 22, the Ivanpah fire is visible in the Mojave National Preserve along the California-Nevada border, with smoke plumes extending into Clark County. No other smoke plumes are visible in the Las Vegas region. Although the HMS smoke plumes (as drawn by the HMS analysts) from the regional Arizona wildfires (the Mangum, Bush, and Bighorn fires) do not extend into Clark County on June 22, based on variable wind speeds and the significant amount of smoke produced, it is likely that these regional fires contributed ozone and/or ozone precursors to Clark County immediately preceding the EE.

[1] The HMS fire detection product is developed using data from the Moderate Resolution Imaging Spectroradiometer (MODIS), Geostationary Operational Environmental Satellite system (GOES), Advanced Very High-Resolution Radiometer (AVHRR) and Visible Infrared Imaging Radiometer Suite (VIIRS) satellite instruments.
[2] The HMS smoke product is derived from GOES-EAST and GOES-WEST visible satellite imagery.
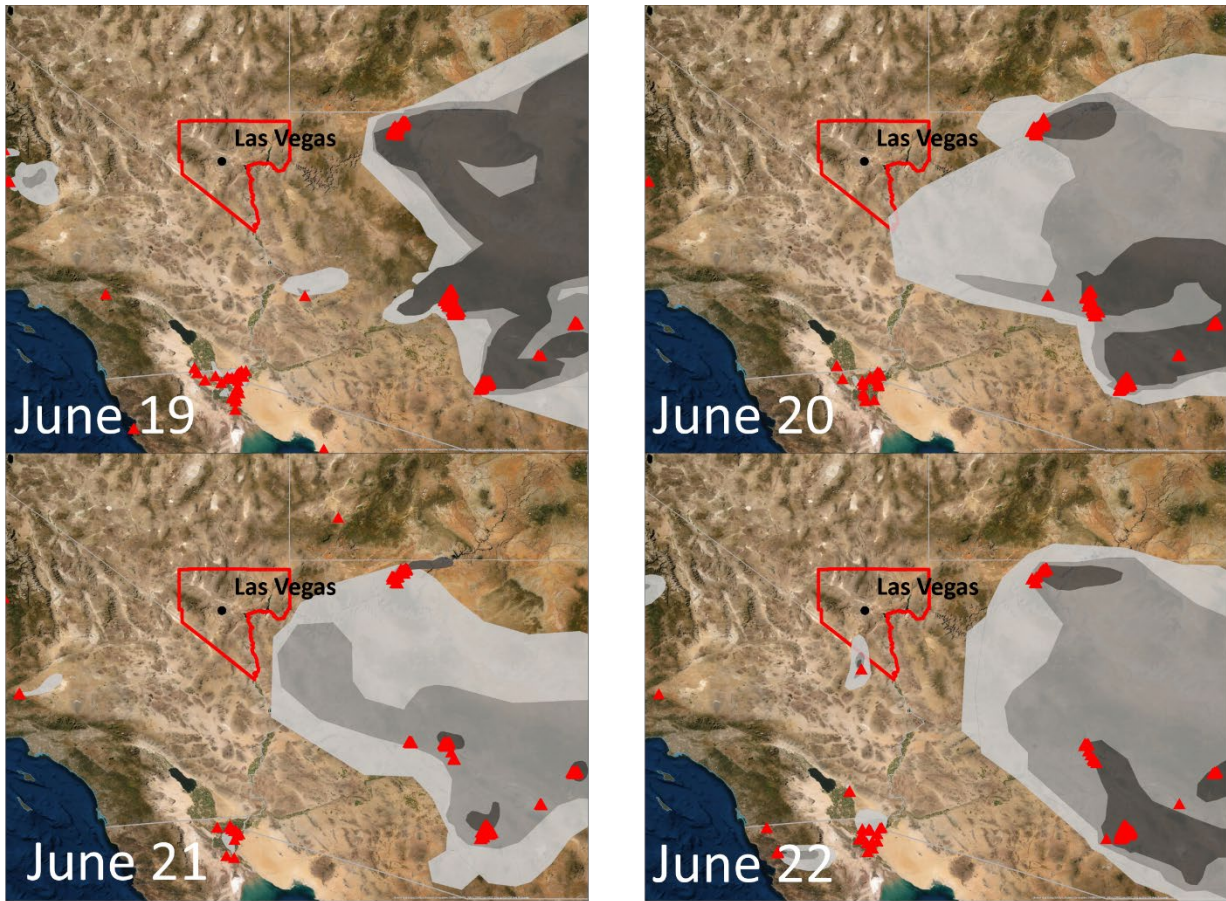
Figure 3-6. Daily HMS smoke over the United States for the June 22 event and three days before the event. Fire detections are shown as red triangles, smoke is shown in gray, and Clark County is outlined in red.

The HMS smoke plume data for June 21, the day before the EE, was obtained and combined with HYSPLIT back trajectories on high ozone concentration days to identify intersections and assess potential smoke impacts (Section 3.1.3). The rest of this section provides information on smoke transport, based on HYSPLIT trajectories and satellite data.

Modeled Smoke

Fire detection data were used from the Moderate Resolution Imaging Spectroradiometer (MODIS) instrument onboard the Aqua and Terra satellites to model the spatial extent of non-conserved smoke from the Mangum, Bighorn, and Bush fires in Arizona on June 21, 2020. A particulate matter tracer was chosen for dispersion, however, due to dry deposition in the model, the extent of the tracer would be a conservative estimate compared to gas-phase species. After fire detections from these fires were aggregated, the fire size and location were input into the BlueSky Pipeline which

estimates fuels burned based on landcover type at the fire location. The BlueSky Pipeline is utilized operationally by the U.S. Forest Service Research and Development Division, AirFire (https://tools.airfire.org/websky/v1/#status) to model smoke emissions and to initialize HYSPLIT smoke dispersion from fire locations. The Bighorn, Bush, and Mangum fires were modeled with the BlueSky Pipeline version available from AirFire (https://github.com/pnwairfire/bluesky). The results shown in Figure 3-7 indicate smoke impacts from the Arizona fires on June 21 in the mixed layer and show that wildfire smoke from these fires intruded into Clark County, Nevada. This finding is consistent with the HYSPLIT trajectories in Section 3.1.3 and HMS smoke maps in Section 3.1.2.
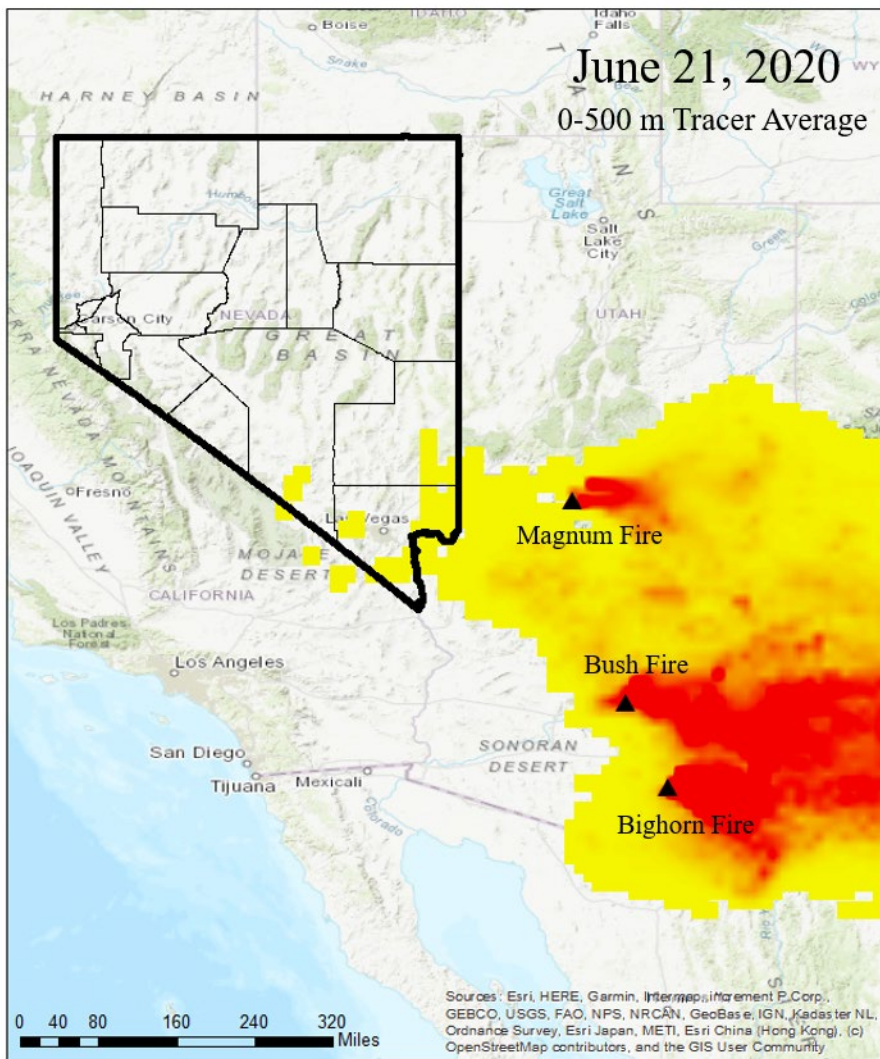
Figure 3-7. The average tracer concentration between 0-500 m for June 21, 2020, modeled in the BlueSky Pipeline initialized with the Mangum, Bush, and Bighorn fires.

3.1.3 HYSPLIT Trajectories

HYSPLIT trajectories were run to (1) demonstrate the transport of air parcels to Las Vegas from upwind areas, and (2) show transport of smoke-containing air parcels from wildfires toward the affected monitors. These trajectories show that air was transported from the Ivanpah Fire in southern California, located in the Mojave National Preserve, to the Clark County area on the day of the event, June 22, 2020, and that air was transported from smoke plumes from fires in Arizona (i.e., Mangum, Bush, and Bighorn fires) to Clark County in the hours leading up to the event.

NOAA's online HYSPLIT model tool was used for the trajectory modeling (http://ready.arl.noaa.gov/HYSPLIT.php). HYSPLIT is a commonly used model that calculates the path of a single air parcel from a specific location and height above the ground over a period of time; this path is the modeled trajectory. HYSPLIT trajectories can be used as evidence that fire emissions were transported to an air quality monitor. This type of analysis is important for meeting Tier 1 requirements and is required under Tier 3.

The model options used for this study are summarized in Table 3-2. The meteorological data from the North American Mesoscale Forecast System (NAM, 12-km resolution) and High-Resolution Rapid Refresh (HRRR, 3-km resolution) model were used (ready.noaa.gov/archives.php). These data have high spatial resolution, are readily available for HYSPLIT modeling over the desired lengths of time, and are expected to capture fine-scale meteorological variability. Single-site backward trajectory start times were selected to be the average time of peak ozone of the Paul Meyer, Walter Johnson, and Joe Neal sites (20:00 UTC or 12:00 p.m. local standard time) and later in the afternoon when the smoke from the Ivanpah fire would affect Clark County (23:00 UTC or 3:00 p.m. local standard time). To capture transport from the smoke plumes produced by the Mangum, Bush, and Bighorn fires in Arizona, single-site backward trajectories were initiated in the late afternoon on June 21 (00:00 UTC or 4:00 p.m. local standard time) because ozone precursors from those fires were transported to the area in the evening before the EE date (see Section 3.2.4 for more details). The backward trajectory matrix analysis was also initiated at noon (20:00 UTC or 12:00 p.m. local standard time). Another backward trajectory matrix was initiated in the late afternoon on June 21 (00:00 UTC or 4:00 p.m. local standard time) to understand transport from the fires in western Arizona.

As suggested in the EPA's EE guidance (U.S. Environmental Protection Agency, 2016), a backward trajectory length of 72 hours was selected to assess whether smoke from the current day or from the previous two days may have been transported over a long distance to the monitoring sites. Investigation showed that one of the fires leading to elevated ozone levels in the Las Vegas Valley began on June 22, 2020 (the same day as the ozone event). Therefore, in the results below, only the backward trajectory for the prior 24 hours is shown. Backward trajectories, including single site and matrix, that captured smoke transport from the fires in western Arizona were run for the previous 48 hours. Trajectories were initiated at 50, 100, 500, and 1,000 m, above ground level to capture transport throughout the mixed boundary layer, as ozone precursors may be transported aloft and influence concentrations at the surface through vertical mixing. Three backward trajectory

approaches available in the HYSPLIT model were used in this analysis, including site-specific trajectories, trajectory matrix, and trajectory frequency. Site-specific back trajectories were run to show direct transport from the wildfire smoke to the affected site(s) – this analysis is useful in linking smoke impacts at a single location (i.e., an air quality monitor) to wildfire smoke. Matrix back trajectories were run to show the general air parcel transport patterns from the Las Vegas area to the wildfire smoke plumes. Similarly, matrix forward trajectories were run to show air parcel transport patterns from the fires to the Las Vegas area. Matrix trajectories are useful in analyzing air transport over areas larger than a single air quality site. Trajectory frequency analysis show the frequency with which multiple trajectories initiated over multiple hours pass over a grid cell on a map. Trajectory frequencies are useful in estimating the temporal and spatial patterns of air transport from a source region to a specific air quality monitor. Together, these trajectory analyses indicate the transport patterns into Clark County on June 22, 2020.

Table 3-2. HYSPLIT run configurations for each analysis type, including meteorology data set, time period of run, starting location(s), trajectory time length, starting height(s), starting time(s), vertical motion methodology, and top of model height.

HYSPLIT Parameters	Backward Trajectory Analysis – Site-Specific	Back Trajectory Analysis – Matrix	Backward Trajectory Analysis – Frequency	Forward Trajectory Analysis – Matrix	Backward Trajectory Analysis – High Resolution
Meteorology	12-km NAM	3-km HRRR & 12-km NAM	12-km NAM	3-km HRRR	3-km HRRR
Time Period	June 21–22, 2020	June 22, 2020	June 21–22, 2020	June 21–22, 2020	June 22, 2020
Starting Location	36.1822 N, 115.2516 W	Evenly spaced grid covering Las Vegas, Nevada	36.1822 N, 115.2516 W	Evenly spaced grid covering Ivanpah Fire	36.1822 N, 115.2516 W
Trajectory Time Length	72 & 24 hours	24 hours, 48 hours	24 hours	10 hours	24 hours
Starting Heights (AGL)	50 m, 100 m, 500 m, 1,000 m	100 m, 500 m	500 m	250 m	1000 m
Starting Times	00:00, 20:00, 23:00 UTC	00:00 UTC, 20:00 UTC	20:00 UTC	19:00 UTC	20:00 UTC
Vertical Motion Method	Model Vertical Velocity	Model Vertical Velocity	Model Vertical Velocity	Model Vertical Velocity	Model Vertical Velocity
Top of Model	10,000 m	10,000 m	10,000 m	10,000 m	10,000 m

Site-specific and matrix backward trajectories were calculated from the Las Vegas Valley on June 22, 2020. The hour of 20:00 UTC (i.e., 12:00 p.m. local standard time) was chosen as the model starting time because it is the average time of peak ozone for the Paul Meyer, Walter Johnson, and Joe Neal sites on June 22. These trajectories showed air circling in the Las Vegas Valley for most of the morning on June 22, but were inconclusive in showing impact from either the Arizona or Ivanpah fires, and have been moved to Appendix A. Based on our conceptual model, ozone precursors were transported into the Las Vegas area in the evening/overnight on June 21. Figure 3-8 shows a backward trajectory from the Las Vegas Valley on June 22 at 00:00 UTC (i.e., 4:00 p.m. local standard time), together with measured ozone (8-hour begin time averages) and HMS smoke plume data from June 20 and 21 overlaid. This figure shows the trajectory intersecting smoke on June 20 and 21 before entering Las Vegas beginning in the evening of June 21. Winds in the evening and overnight

were light on June 21 and 22, allowing air to circulate through the Las Vegas Valley (consistent with the trajectories shown in Appendix A and meteorological data in Section 3.3.1).

To identify variations in meteorological patterns of transported air to Las Vegas, a HYSPLIT trajectory matrix was generated. For this approach, trajectories are run in an evenly spaced grid of source locations. **Figure 3-9** shows the 48-hour backward trajectory matrix with source locations encompassing Las Vegas. The backward trajectories were initiated in the early evening of June 21 at 00:00 UTC (i.e., 4:00 p.m. local standard time) to capture smoke transport in the hours leading up to the day of ozone exceedance. Consistent with Figure 3-8, some trajectories originate from northern Mexico, pass through the smoke plumes from the fires in western Arizona on June 20-21, then move into Clark County by early evening on June 21.

The conceptual model suggests that emissions from the Ivanpah Fire entered Clark County in the afternoon on June 22 and kept ozone concentrations high, leading to a high MDA8 ozone concentration. **Figure 3-10** shows the high-resolution (3-km) backward trajectories from the Las Vegas Valley during the afternoon (June 22 23:00 UTC or 3:00 p.m. local standard time) for this event. The higher resolution meteorology was chosen for this case because the fire was much closer to Clark County. On June 22, the Ivanpah Fire in the Mojave National Preserve became active in the late morning/early afternoon (see Section 3.2.1 for more details), creating a smoke plume near the California-Nevada state line. This plume was observed during the afternoon overpass of MODIS and shown in the HMS smoke figures in Section 3.1.2 as a smoke plume reaching into Clark County by 2:30 p.m. local time. The HYSPLIT results show the trajectory from Las Vegas passing directly over the Mojave National Preserve where the Ivanpah fire was burning. We chose low heights to model this trajectory because it was unlikely that the smoke from the Ivanpah fire (a grass fire) would be lofted high into the atmosphere. The timings in the trajectory analysis do not exactly match the start time of the Ivanpah Fire; however, they do show the afternoon flow from the Ivanpah Fire into Clark County. We do know that a significant amount of smoke built up between the 10:30 a.m. local standard time overpass of Terra (no fire signal from the Ivanpah Fire) and the 2:30 p.m. local standard time overpass of Aqua (positive fire signal from the Ivanpah Fire and smoke plume that stretched into Clark County). Based on the trajectory flow and the shape of the smoke plume (smoke moving to the northeast towards Clark County from the fire), the trajectory flow and the shape of the smoke plume show that the Ivanpah Fire could have an impact on ozone concentrations in Clark County during the afternoon of June 22. This effect could keep ozone levels high, as shown in Section 3.2.4 (where the surrounding days show a decrease in ozone in the afternoon), and subsequently cause a higher-than-normal MDA8 ozone concentration on June 22. **Figure 3-11** shows the accompanying 24-hour backward trajectory matrix with source locations encompassing Las Vegas relating to the Ivanpah Fire case. The backward trajectories were initiated in the afternoon at 3:00 p.m. local standard time (23:00 UTC) of June 22, 2020, at a starting height of 100 m above ground level (AGL). As shown in the plot, the transported air intersecting Las Vegas during the afternoon of June 22 follows a similar southwestern pattern. Consistent with the trajectory depicted in Figure 3-10, transported air intersecting Las Vegas during the afternoon on June 22 traveled from the southwest,

with multiple trajectories passing over the Mojave National Preserve in southern California where the Ivanpah Fire was burning.
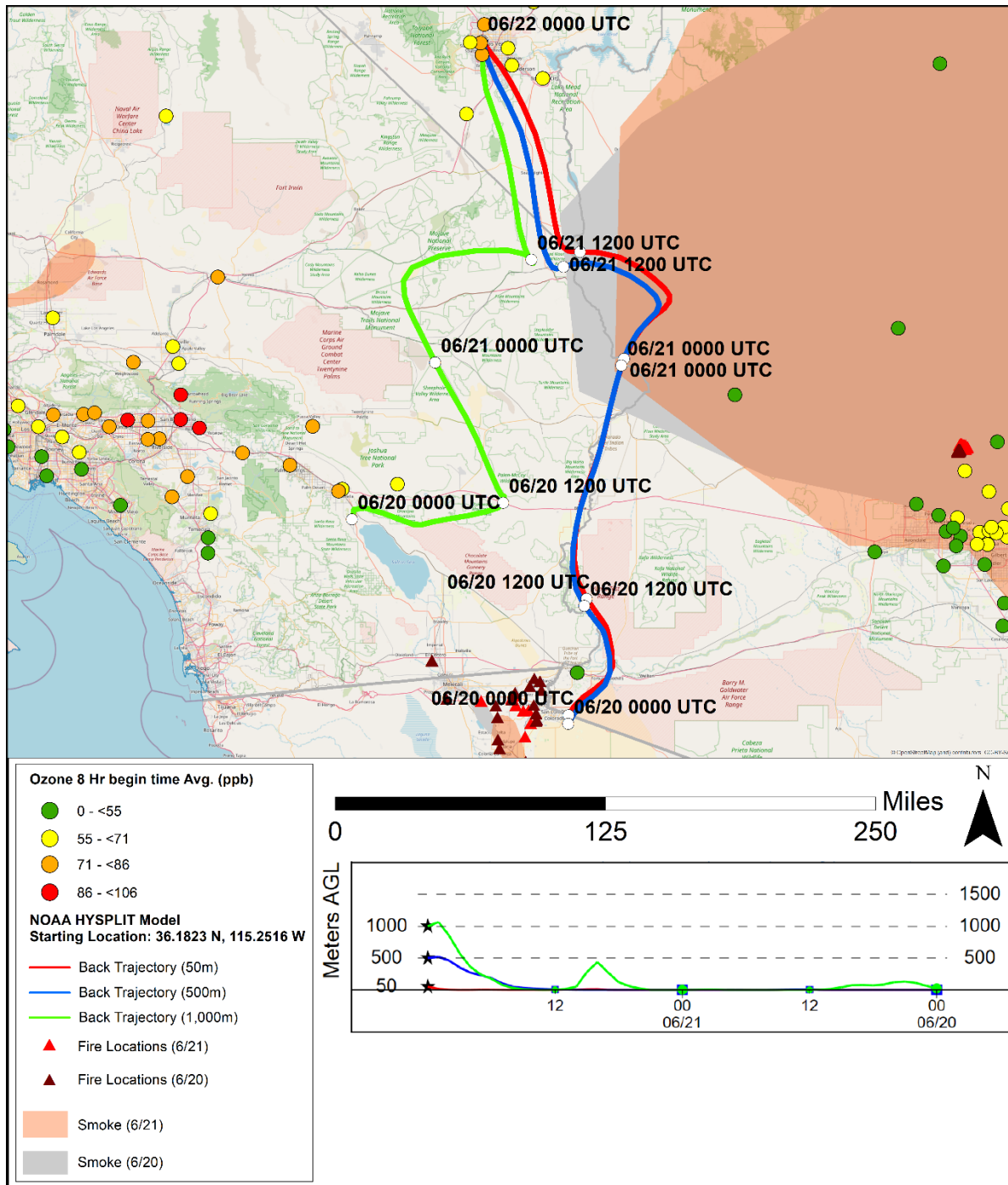
Figure 3-8. 48-hour HYSPLIT back trajectories with smoke from the Las Vegas Valley, ending on June 22, 2020, at 00:00 UTC (4:00 p.m. Local Standard Time). NAM 12-km back trajectories are shown for 50 m, 500 m, and 1,000 m above ground level. Smoke layers represent smoke on June 20 and 21 at approximately 2:30 p.m. local time.
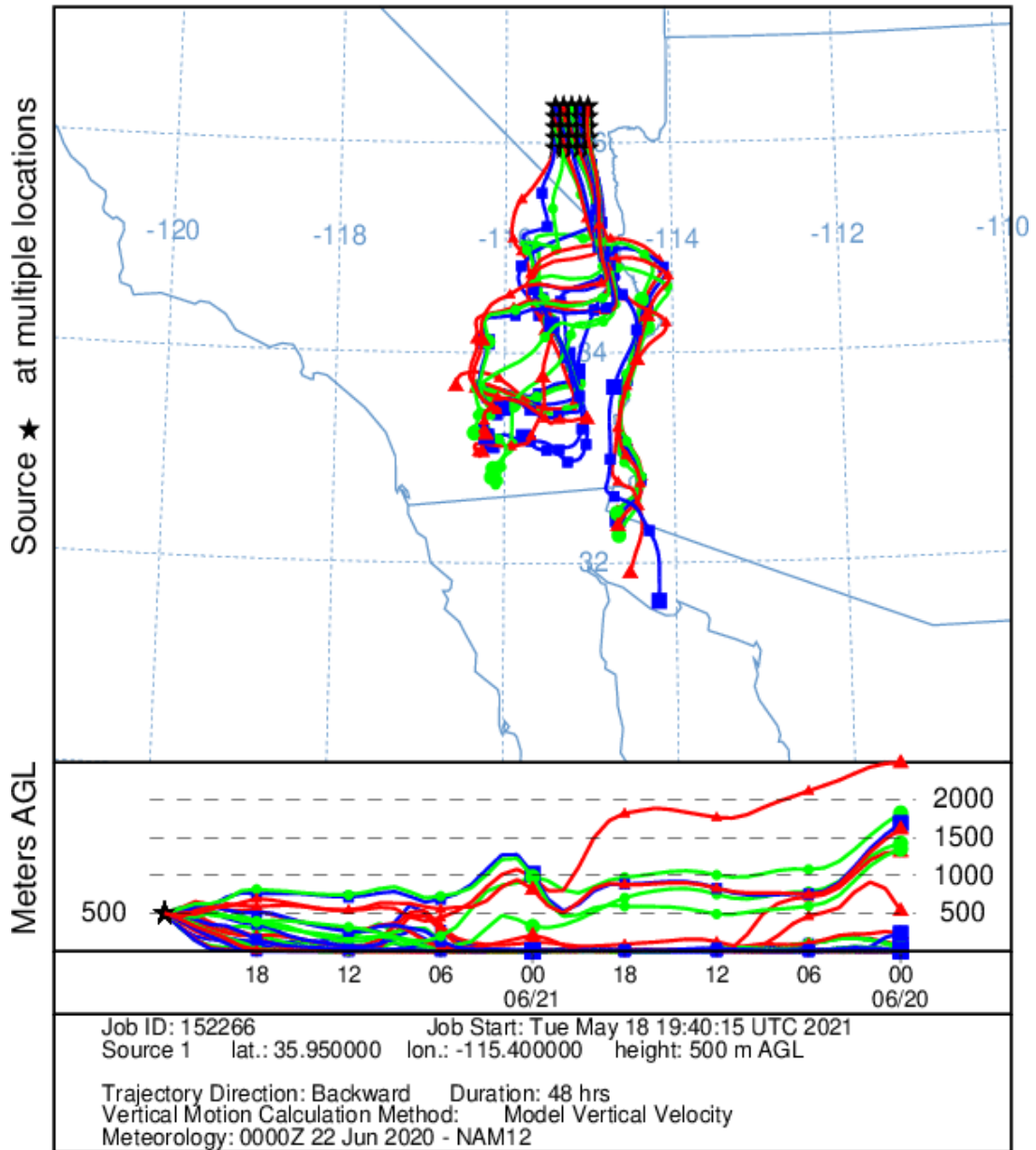
Figure 3-9. HYSPLIT back trajectory matrix. A 24-hour, NAM 12-km back trajectory matrix was initiated on June 22, 2020, at 00:00 UTC (6:00 p.m. Local Time on June 21) from Las Vegas Valley at 500 m above ground level.
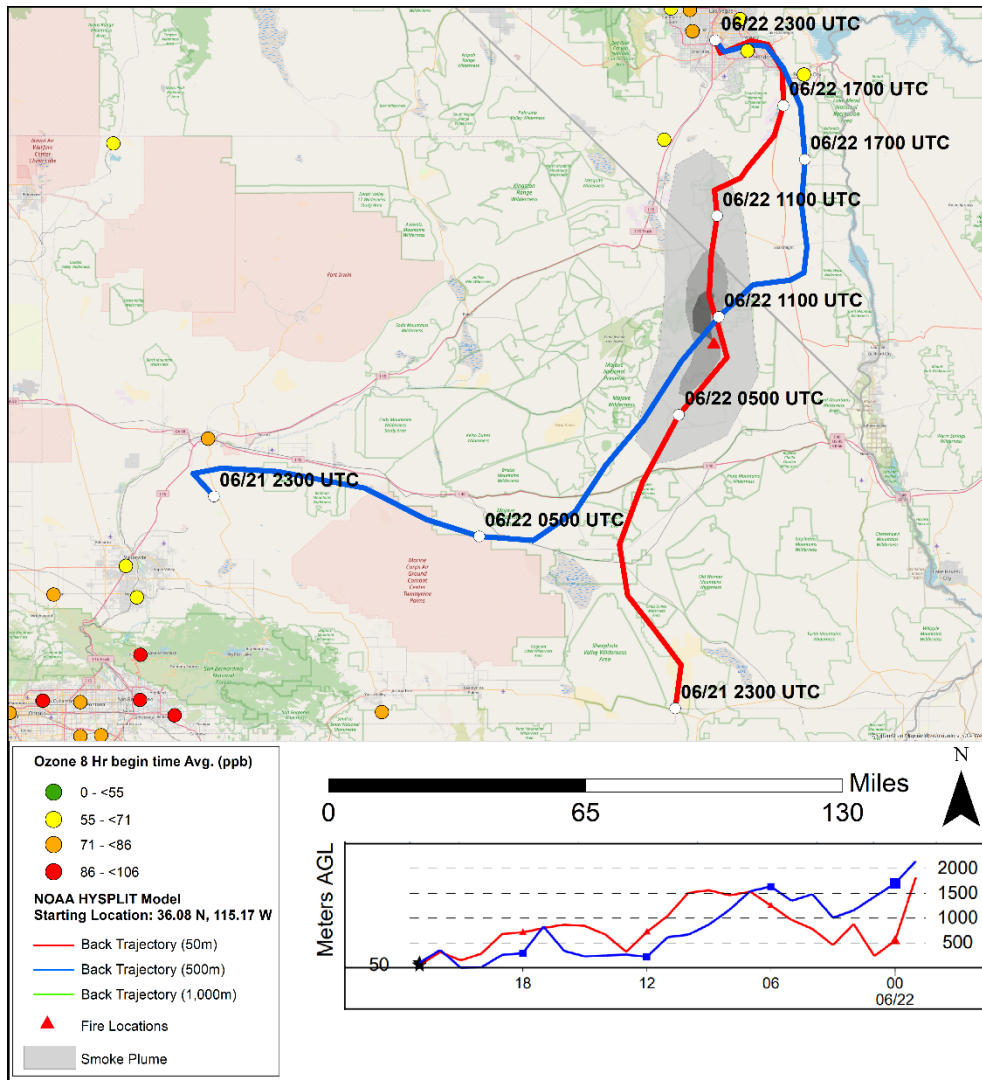
Figure 3-10. 24-hour HYSPLIT back trajectories with smoke from the Las Vegas Valley, ending on June 22, 2020, at 23:00 UTC (3:00 p.m. Local Standard Time). HRRR 3-km back trajectories are shown for 50 m and 100 m above ground level. Smoke layers represent smoke on June 22 at approximately 2:30 p.m. local standard time.
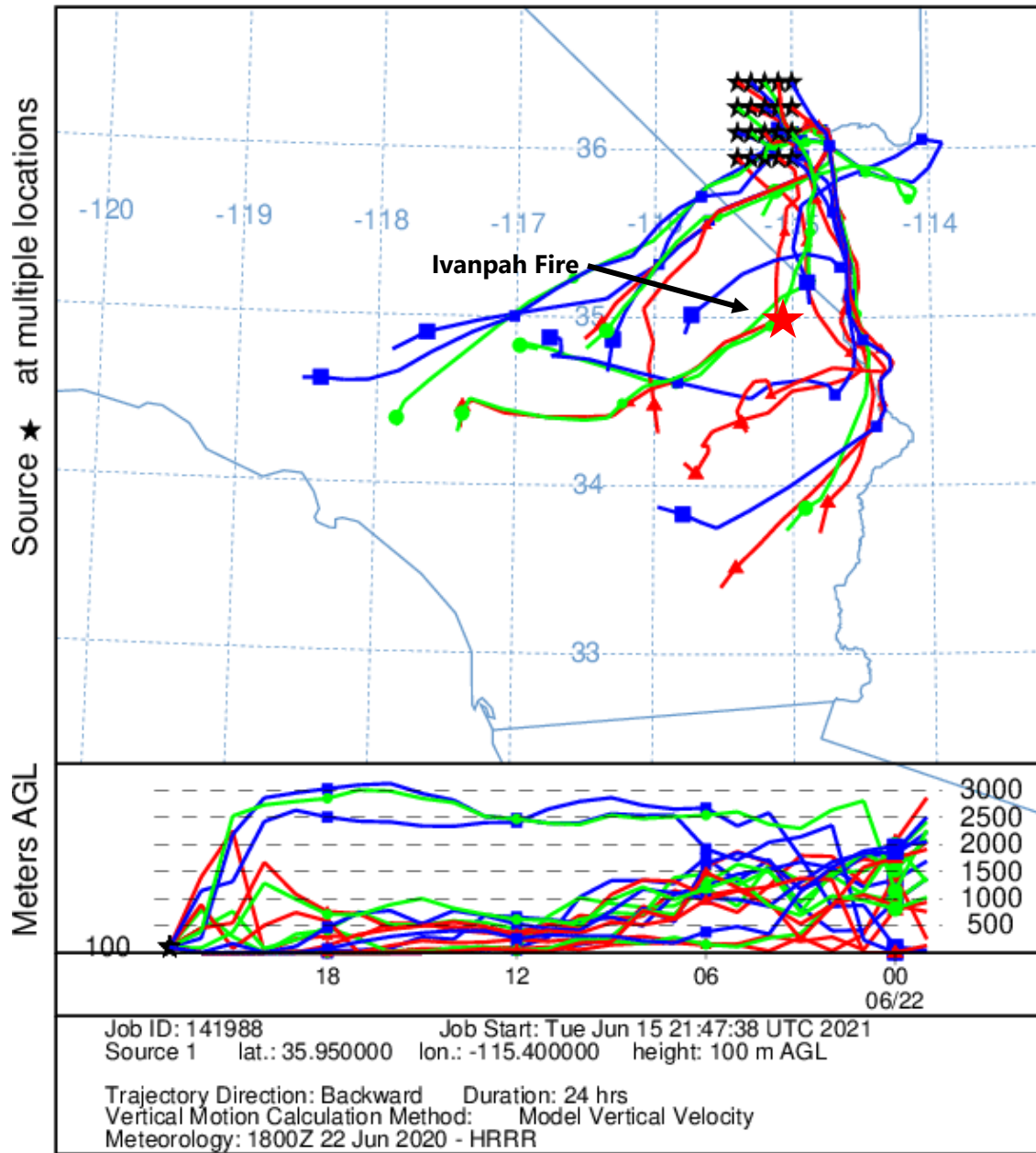
Figure 3-11. HYSPLIT back trajectory matrix for the Ivanpah Fire. A 24-hour, HRRR 3-km back trajectory matrix was initiated on June 22, 2020, at 23:00 UTC (3:00 p.m. Local Standard Time) from Las Vegas Valley at 100 m above ground level. The approximate location of the Ivanpah Fire is indicated by a red star.

The third trajectory approach used in this analysis was HYSPLIT trajectory frequency. In this option, a trajectory from a single location and height starts every three hours. Using a continuous 0.25-degree grid, the frequency of trajectories passing through each grid cell is totaled and then normalized by the total number of trajectories. **Figure 3-12** shows a 24-hour backward trajectory frequency plot starting from the Las Vegas Valley and 500 m AGL on June 22, 2020 (500 m was chosen because it is more likely to show regional transport). The trajectory frequency plot yields similar results as those from the previous two approaches for the Ivanpah case; transported air impacting the Las Vegas Valley on June 22 traversed the Mojave National Preserve where the Ivanpah Fire was burning. **Figure 3-13** shows the previous day backward trajectory frequency plots at a starting height of 500 m AGL. The air transport pattern shows air reaching Las Vegas Valley from the southern California region and from where the Arizona wildfire (i.e., Bighorn, Mangum, and Bush fires) smoke was shown in Section 3.1.2. **Figure 3-14** shows the back trajectory from 00:00 UTC on June 22 (4:00 p.m. local standard time on 6/21) at a starting height of 500 m AGL. The trajectory frequency plot is consistent with Figure 3-12, which also shows transport from southern California and western Arizona (where smoke from the Arizona fires was shown in Section 3.1.2).
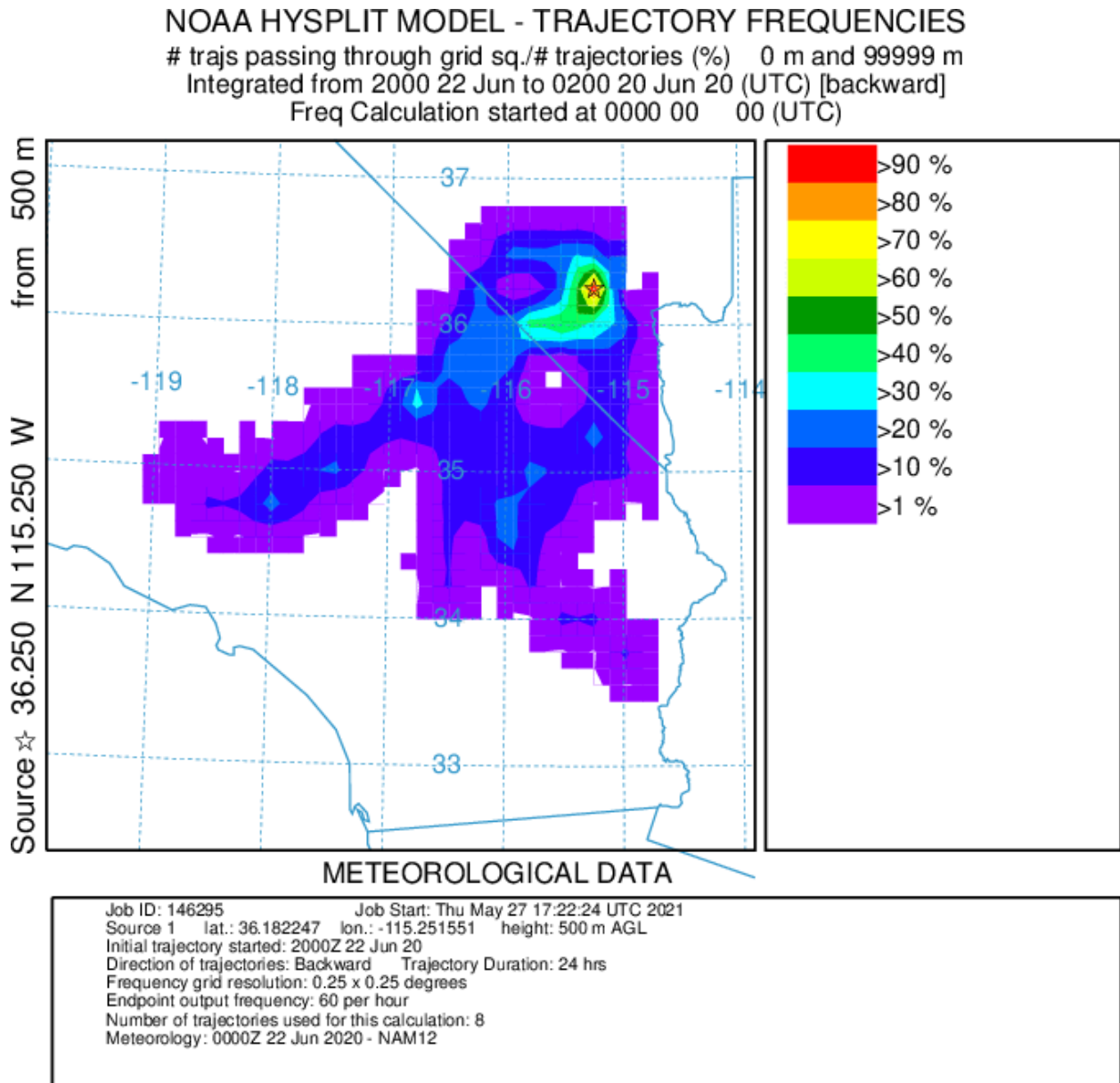
Figure 3-12. 24-hour, NAM 12 km frequency of HYSPLIT back trajectories initiated on June 22, 2020, at 20:00 UTC (12:00 p.m. Local Time) from Las Vegas Valley at 500 m above ground level. The colors within the frequency plot indicate the percent of trajectories that pass through a grid square.

Figure 3-13. 24-hour, NAM 12-km frequency of HYSPLIT back trajectories initiated on June 21, 2020, at 20:00 UTC (12:00 p.m. Local Time) from Las Vegas Valley at 500 m above ground level. The colors within the frequency plot indicate the percent of trajectories that pass through a grid square.
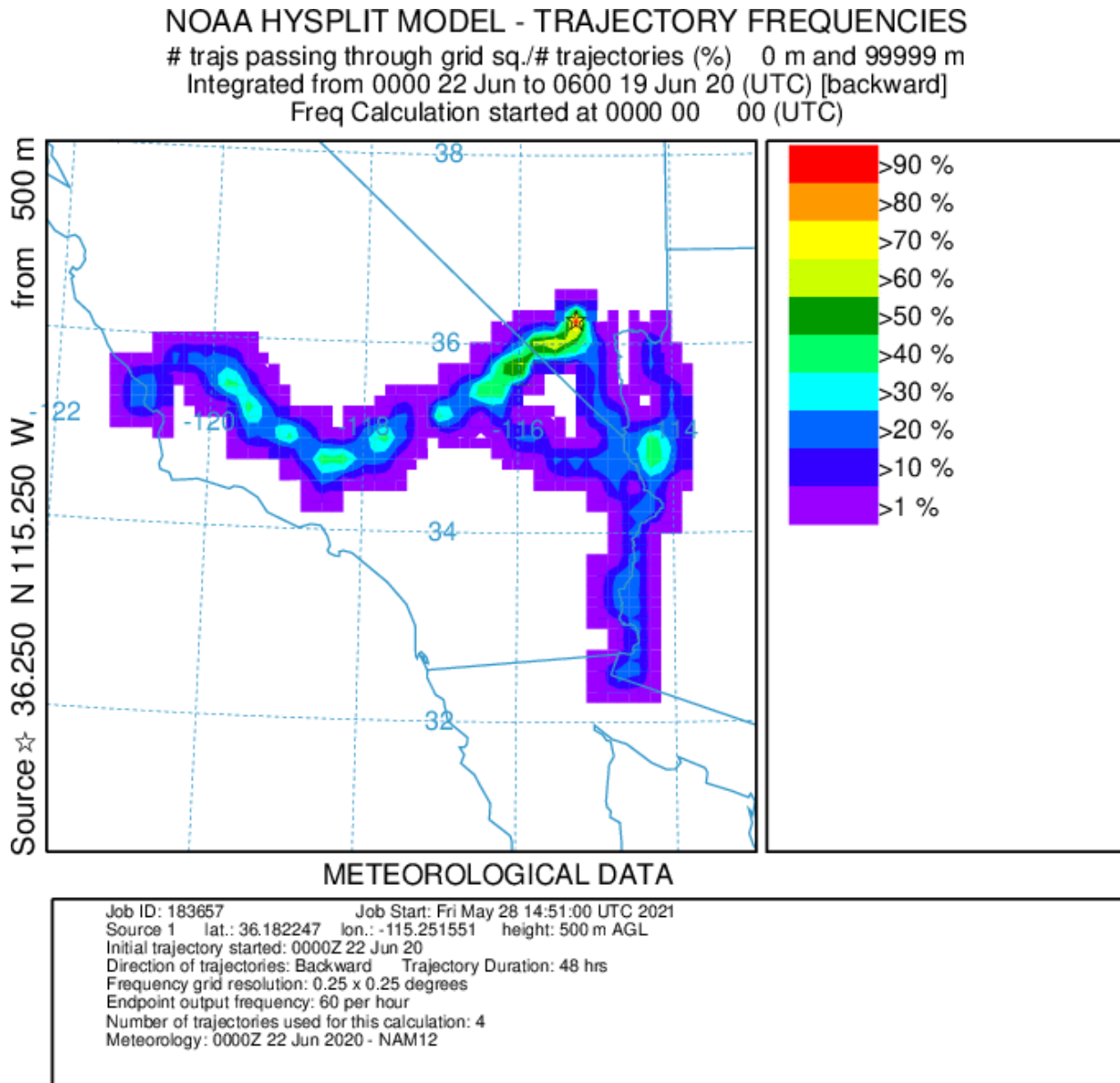
Figure 3-14. 24-hour, NAM 12-km frequency of HYSPLIT back trajectories initiated on June 21 at 00:00 UTC (6:00 p.m. Local Time on June 21) from Las Vegas Valley at 500 m above ground level. The colors within the frequency plot indicate the percent of trajectories that pass through a grid square.

Forward trajectories were run from the Ivanpah Fire location starting at 19:00 UTC on June 22, 2020 (11:00 a.m. local standard time, presumably the earliest the Ivanpah fire could have started), are shown in **Figure 3-15**. We choose 250 m as a modeling height because this fire grew rapidly (consuming around 1,000 acres in a day) but was unlikely to inject smoke above the boundary layer. These trajectories show that smoke was transported from the Ivanpah Fire in southern California to Clark County between noon and the early evening on June 22. This is consistent with our conceptual

model that smoke from the Ivanpah Fire could have affected ozone in the Clark County area during the afternoon on June 22. Ozone production can occur quickly at short distances from wildfire smoke plumes at ≥2 hours transport downwind (Jaffe and Wigder, 2012), especially for smaller fires with relatively low NO_x concentrations downwind and minimal ozone titration. These forward trajectories, combined with the back trajectories shown above, further support the transport of smoke from the southern California Ivanpah Fire to Clark County, Nevada. Forward trajectories were run from the fires in western Arizona, but single trajectories did not pass over Clark County. Therefore, forward trajectories from the fires in western Arizona are not included in this demonstration. However, modeled smoke dispersion from the fires in western Arizona (see Section 3.1.2 Modeled Smoke) showed some transport into Clark County.
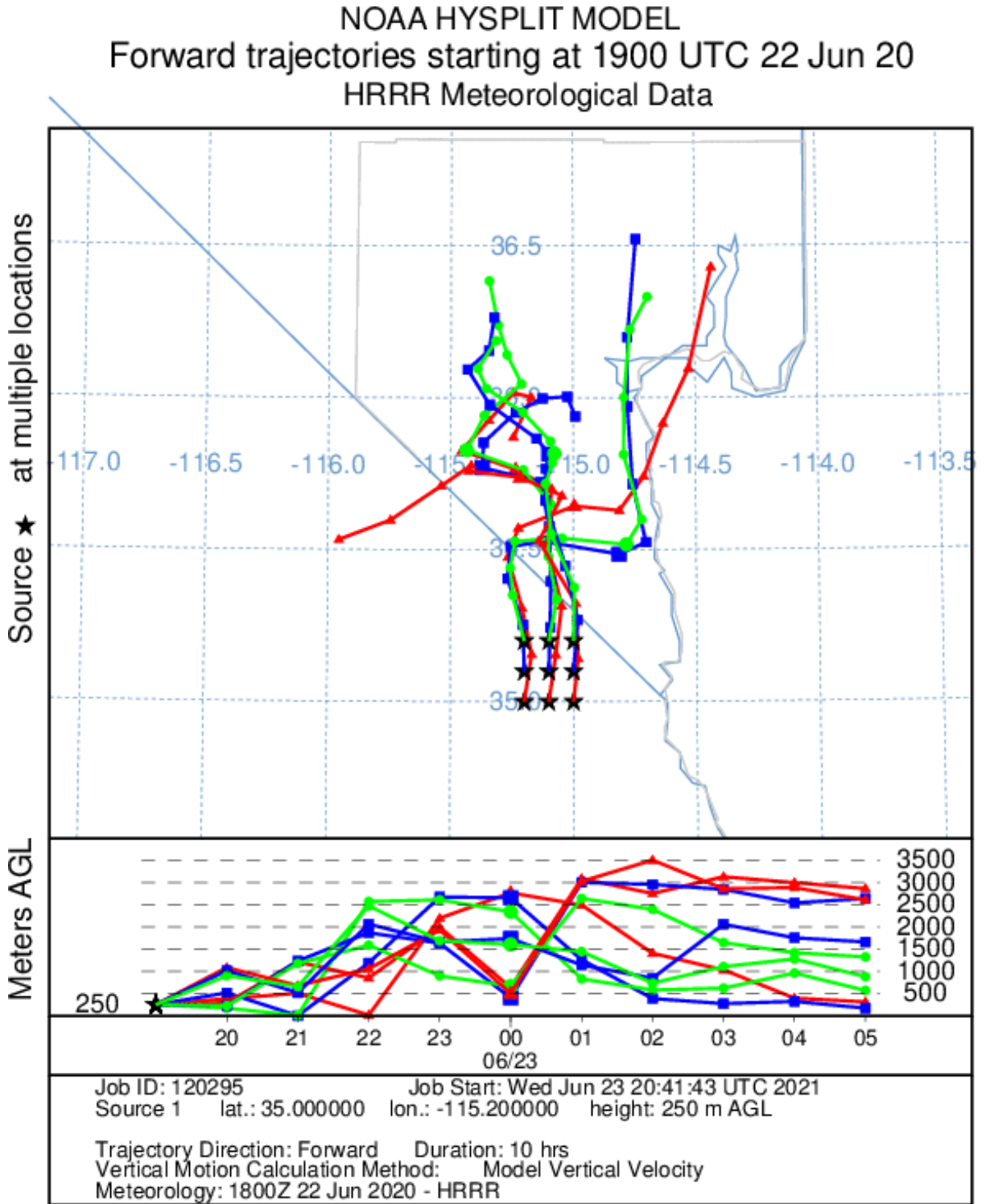
Figure 3-15. HYSPLIT forward trajectory matrix. A 10-hour, HRRR 3km forward trajectory matrix was initiated on June 22, 2020, at 19:00 UTC (11:00 a.m. Local Standard Time) from the Ivanpah Fire at 250 m above ground level.

3.1.4 Media Coverage and Ground Images

News, weather, and environmental organizations provided coverage of the fires that caused smoky conditions in Clark County. Media articles mentioned in this section are included in Appendix B. The National Weather Service (NWS), Las Vegas, posted a tweet (Figure 3-16) on June 21, 2020, showing satellite imagery of smoke from the Bush fire moving westward towards Clark County.[3] CNN reported on the Bush Fire as it spread to become the fifth largest fire in Arizona's history, noting in the same article that two other large fires, the Bighorn Fire and the Mangum Fire, were concurrently burning in Arizona.[4]

Figure 3-16. Tweet posted by NWS Las Vegas showing satellite imagery of smoke from the Bush Fire in Arizona being transported westward towards southern Nevada.

---

[3] https://twitter.com/NWSVegas/status/1274754867534262272?s=20
[4] https://www.cnn.com/2020/06/23/us/arizona-bush-fire-tuesday/index.html (see Appendix B)

In addition to these large fires in Arizona, fires burned across the southwestern U.S. around the time of this EE. The Ivanpah Fire was reported in a news release on June 23 by San Bernardino County after reaching a size of 1,000 acres.[5] The abundance of disparate fires burning across the southwest created widespread smoky conditions throughout the region.

Ground images from visibility cameras (operated by the Clark County DES, Division of Air Quality) located on the roof of the M Hotel in Las Vegas clearly show the smoky conditions that persisted on June 22 (Figure 3-17). When compared to images taken on a clear day during ozone season (May 21, 2020) (Figure 3-18), the June 22 images show drastically reduced visibility and an opaque gray haze in every direction due to wildfire smoke.
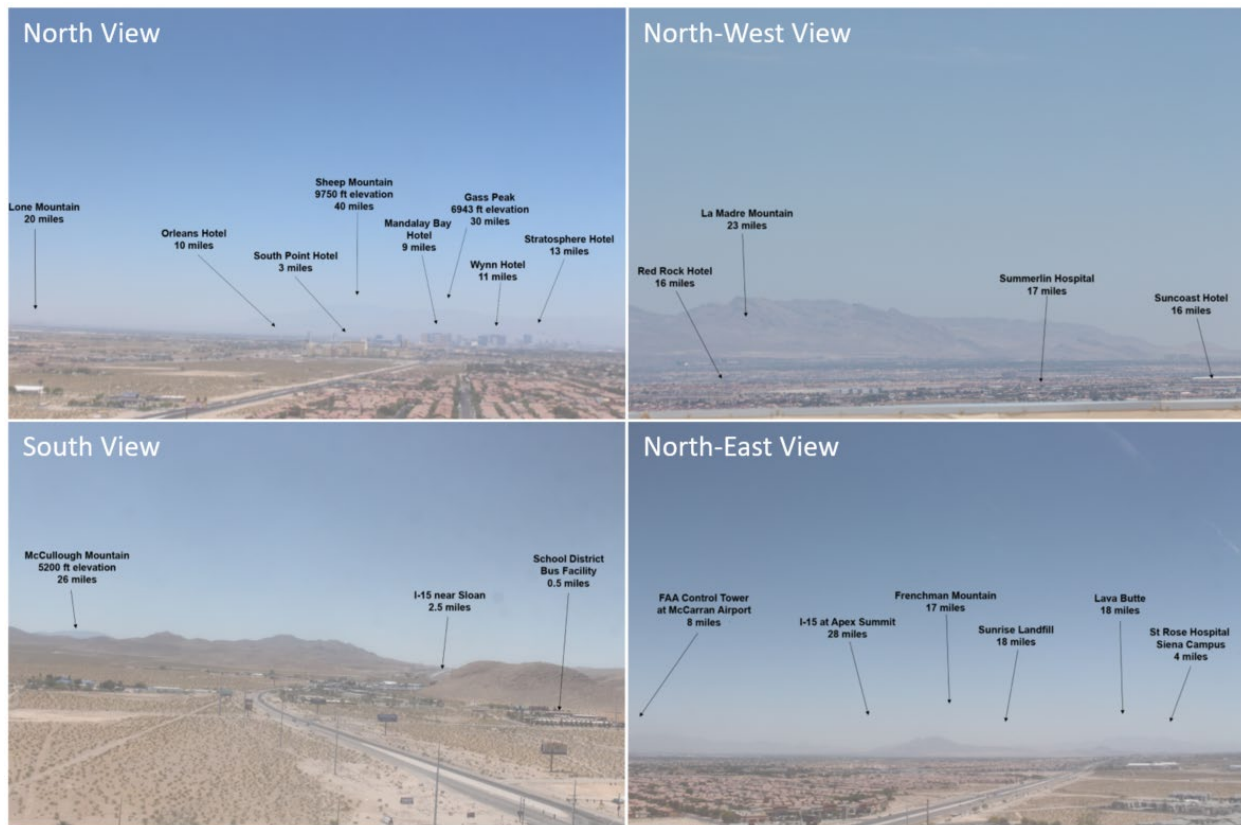
Figure 3-17. Clark County visibility images from June 22, 2020. Images taken from webcams set up in Clark County are shown for the EE on June 22. Each image is labeled with the viewing direction and landmarks.

---

[5] https://www.sbcounty.gov/sbcfire/media/viewer/attachment.ashx?ID=33c32bc8-129e-4514-9e90-974f6ca9c0c2 (see Appendix B)
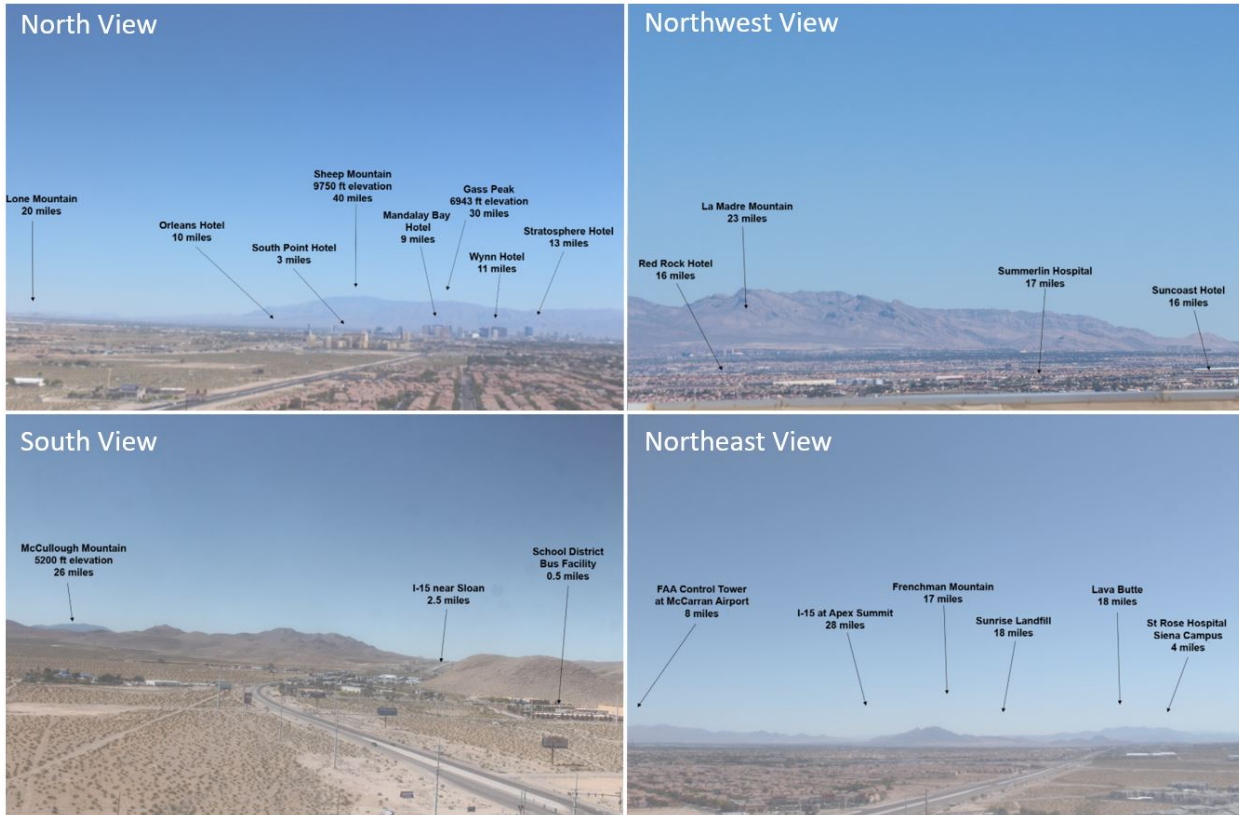
Figure 3-18. Visibility images taken from webcams set up in Clark County on a clear day (May 21, 2020). Each image is labeled with the viewing direction and landmarks.

3.2 Tier 2 Analyses

This exceptional event demonstration meets the clear causal relationship criterion of the Exceptional Events Rule through a Tier 3 weight of evidence showing. EPA guidance says that "As part of the weight of evidence showing for the clear causal relationship rule element [for a tier 3 demonstration], air agencies should explain how the events, monitor and exceedance compare with the key factors outlined in Section 3.5.1 [Evidence that the Event, Monitor(s), and Exceedance Meet the Key Factors for Tier 2 Clear Causal Analyses]. The relationship of the event to the Tier 2 key factors may help inform the amount of additional information that will be needed to support Tier 3 analyses...") (U.S. Environmental Protection Agency, 2016). Tier 2 analyses include two key factors—Q/D analysis and comparison of event ozone concentrations with non-event concentrations—and select additional evidence to show that the fire emissions affected the monitor. This section of the demonstration presents the Tier 2 analysis results, which were used to guide the Tier 3 analyses. The Tier 2 results

are consistent with the Tier 3 analyses, and both sets of analyses contribute to the weight of evidence for the September 2 exceptional event.[6]

3.2.1 Key Factor #1: Q/d Analysis

The EE guidance (U.S. Environmental Protection Agency, 2016) describes a method to relate the quantity of smoke emissions and distance of the fire to an exceeding monitor. The resulting quantity, called Q/d, may be used to screen fires that meet a conservative threshold of air quality impacts.[7] This section provides the results of the Q/d analyses for fires that were likely to have contributed to the June 22 ozone event in Clark County.

Based on media coverage, dispersion and trajectory analysis, and ground/satellite-based analyses in Section 3.1, smoke from large wildfires in Arizona was transported into Clark County and influenced ozone concentrations. We also suspect that the Ivanpah Fire in the Mojave National Preserve contributed to prolonged high ozone concentrations in Clark County, Nevada, on June 22 in the late afternoon. Figure 3-19 shows large fires burning in Arizona and California on June 22, 2020, which includes the fires attributed in this demonstration. Table 3-3 shows agency data available for the Ivanpah, Bighorn, Bush, and Mangum wildfires (as of December 2020). The Ivanpah Fire started on June 22, 2020, in the late morning/early afternoon during extremely hot and dry conditions in the Mojave National Preserve.[8] According to the first responder (Aragon, 2021), the fire was reported at 14:42 hrs PDT, and the responding engine reported "a column of black smoke while still approximately 40 minutes from the incident." The first responder estimates the initial time of the fire was within an hour of the initial report, which would be approximately noon to 1:00 p.m. local standard time. The MODIS smoke images shown in Section 3.1.2 were taken by 2:30 p.m. local standard time (PST) on June 22, which show an already large column of smoke extending into Nevada from the Ivanpah Fire. Since the first responder and satellite images indicate a highly visible (via satellite and 40 minutes away by ground) smoke plume by early afternoon, we suggest that the fire likely started in late morning or early afternoon (with no definitive time). Smoke from the Ivanpah fire was not visible in the Terra overpass (10:30 a.m. local standard time), but had a large smoke plume by the time of the Aqua overpass (2:30 p.m. local standard time). This fire was mostly contained by June 23. The large Arizona wildfires that caused regional smoke in the area started

---

[6] As noted in the ozone exceptional event guidance (U.S. Environmental Protection Agency, 2016), a Tier 3 demonstration must be presented when "the relationship between the wildfire-related emissions and the monitored exceedance or violation cannot clearly be shown using Tier 1 or Tier 2 analyses." Therefore, while the analyses presented in Section 3.2 provides evidence that is supportive of a clear causal relationship between the fires identified and the monitored exceedance, these analyses alone are not expected to be sufficient to demonstrate such a relationship in the absence of the Tier 3 analyses.

[7] Specifically, fires with a Q/d value meeting the 100 tons/km threshold may qualify for a tier 2 demonstration of a clear causal relationship. However, this threshold is insufficient to identify all cases where ozone impacts from smoke may have occurred. Pages 16-17 of the guidance state "To determine an appropriate and conservative value for the Q/D threshold (below which the EPA recommends Tier 3 analyses for the clear causal relationship), the EPA conducted a review... The reviews and analyses did not conclude that particular O_3 impacts will always occur above a particular value for Q/D. For this reason, a Q/D screening step alone is not sufficient to delineate conditions where sizable O_3 impacts are likely to occur." (U.S. Environmental Protection Agency, 2016).

[8] https://www.fireweatheravalanche.org/wildfire/incident/119448/california/ivanpah-fire

prior to June 22 and were caused by lightning, accidental human ignition, or unknown events. These fires were:

- Bighorn Fire: **https://inciweb.nwcg.gov/incident/6741/**

- Bush Fire: **https://inciweb.nwcg.gov/incident/6773/**

- Mangum Fire: **https://inciweb.nwcg.gov/incident/6748/**

Figure 3-19. Large fires burning on June 22, 2020, in the vicinity of Clark County are shown in red. The Clark County boundary is shown in black.

Table 3-3. Fire data for the Ivanpah Fire and wildfires in Arizona associated with the June 22 EE. Information includes start/containment date, cause of the fire, and the total reported acres burned. NA means a date has not officially been determined.

Fire Name	Start Date	Contained Date	Cause	Total Area Burned (acres)
Ivanpah Fire	6/22/2020	NA	Unknown	1,088
Mangum Fire	6/8/2020	7/27/2020	Unknown	71,450
Bush Fire	6/13/2020	7/6/2020	Human	193,455
Bighorn Fire	6/5/2020	7/23/2020	Lightning	119,987

Overall, these fires burned almost 400,000 acres through July 2020. On June 22, 2020, based on agency estimates, the Ivanpah Fire and wildfires in Arizona had burned around 350,000 acres.

Key factor #1 for a Tier 2 demonstration requires an analysis of wildfire smoke emissions from a qualifying fire and the distance of the fire to the affected monitor or monitors. To identify qualifying fires, the guidance "recommends generating 24-hour back trajectories from the affected O_3 monitoring site(s) beginning at each hour of these two or three dates" (U.S. Environmental Protection Agency, 2016). Three dates would be used only if the 8-hour averaging period for the daily maximum 8-hour ozone data include hours falling on two dates (i.e., the 8-hour average includes at least 11 p.m. and midnight on two distinct calendar days). For this demonstration, 24-hour HYSPLIT back trajectories were generated from the monitor location starting on each hour of the day of the exceedance, as well as the day prior to the exceedance (June 21 and June 22). The guidance states that "...fires that are close to any of these back trajectories" may be used to calculate Q/d (U.S. Environmental Protection Agency, 2016). To identify fires that fall near the HYSPLIT trajectories, trajectories were buffered by a distance of 25% of the distance traveled by the trajectory, which is consistent with uncertainty reported for HYSPLIT trajectory modeling (Draxler, 1991). **Figure 3-20** shows the back trajectories and buffer of uncertainty from Clark County, Nevada. All fires falling within the uncertainty buffer of one or more trajectories were considered candidates for calculating Q/d. The only candidate fire for Q/d identified based in 24-hour back trajectories was the Ivanpah Fire. However, Section 3.1 analyses indicate that the Bush, Mangum, and Bighorn fires contributed to regional smoke conditions. An extended assessment of emissions from these fires is provided in **Appendix C**.

Automated Smoke Exceptional Event Screening for Fire Report for June 22, 2020 LasVegasNevada
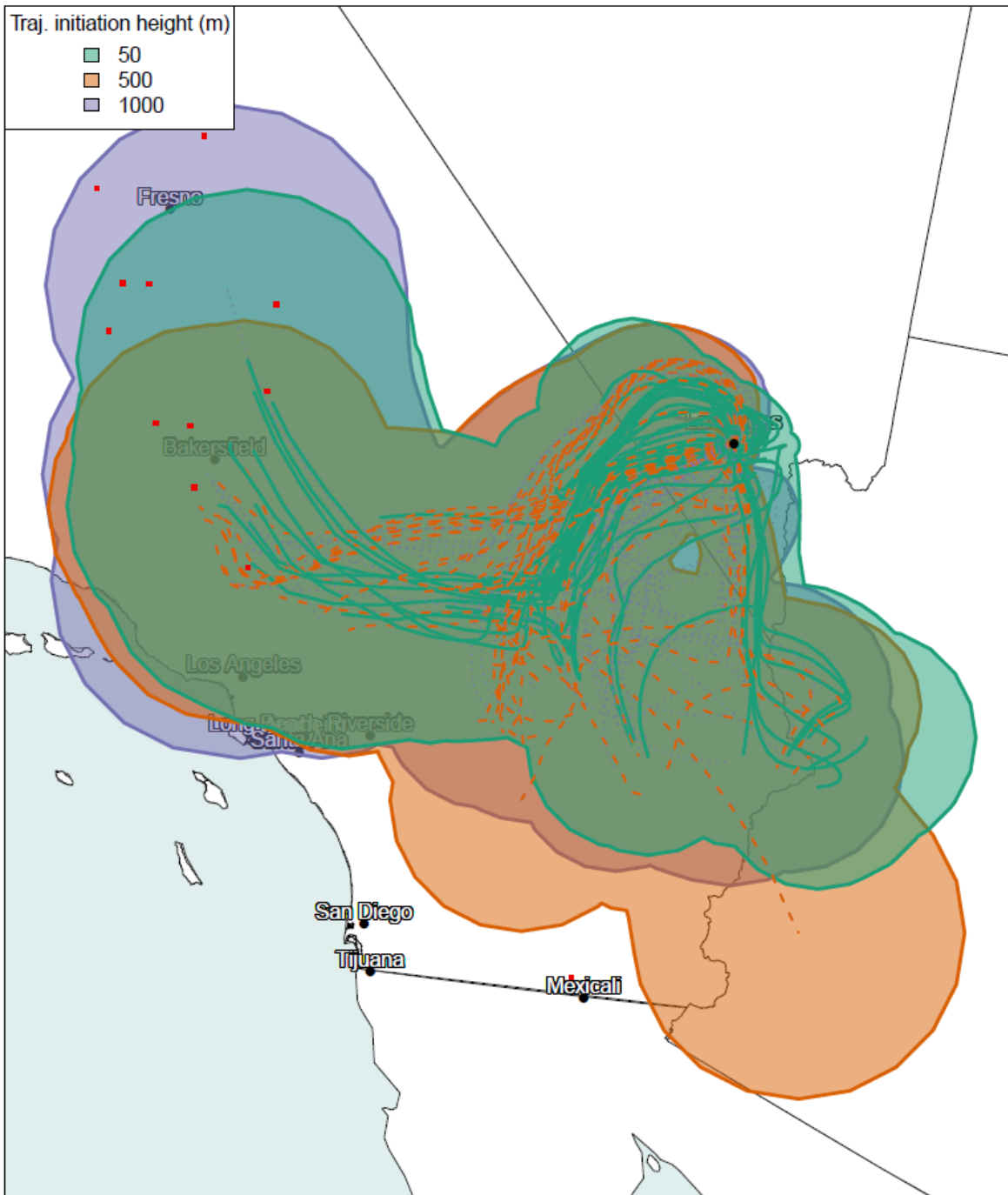
Figure 3-20. Q/d analysis. 24-hour back trajectories are shown as solid or dotted lines. The starting height of the back trajectory is indicated by the color. Uncertainty buffers, calculated as 25% of the distance traveled by the trajectory, are shown in colored polygons. Active fires on June 22 are shown as red squares. Fires falling within one or more uncertainty buffer(s) were used to calculate individual and aggregate Q/d values.

To calculate Q/d for qualifying fires, the total daily emissions of NO_x and reactive VOCs (rVOCs) in tons is divided by the distance from the fire to impacted monitors. BlueSky Playground Version 3.0.1 (https://tools.airfire.org/playground/v3/) was used to estimate emissions of NO_x and VOCs for the Ivanpah Fire on a daily basis for June 21 and 22. Daily fire growth was identified using news reports citing official sources. The fire's location was used to identify the distance to the impacted monitors and fuelbed type. Emissions calculations were based on very dry conditions.

EPA guidance recommends that an event may qualify for a Tier 2 demonstration if the Q/d value for a fire, or the aggregate Q/d across multiple fires, exceeds a conservative value of 100 tons/km. Daily Q/d results indicate that emissions of NO_x and rVOCs occurred from the Ivanpah Fire during the day of the exceedance (Table 3-4). However, the emissions were not large enough to reach the Q/d threshold of 100 tons/km for a Tier 2 demonstration, and it was determined that Tier 3 analyses were needed to demonstrate a clear causal relationship.

The Q/d analysis, as described in the ozone exceptional event guidance (U.S. Environmental Protection Agency, 2016) and presented here, would not reflect the impact of transport occurring over more than 24 hours. The analyses provided in Section 3.1.3 show that the Bush, Bighorn, and Mangum Fires contributed to regional smoke conditions in Clark County. To quantify this contribution, we conducted an extended analysis to investigate emissions from these fires. The results are presented in Appendix C. These analyses provide evidence that the identified fires emitted ozone precursors in the days leading up to the June 22 wildfire smoke event, including June 20 and June 21.

The results of the Q/d analysis presented in this section, as well as the extended emissions assessment included in Appendix C, agree with and further strengthen the conceptual model and Tier 3 weight of evidence of a clear causal relationship between the identified wildfires smoke emissions and the monitored ozone exceedance identified in this demonstration.

Table 3-4. Daily growth, emissions, and Q/d for the Ivanpah Fire on June 22, 2020. Growth and location for the fire were obtained from agency estimates available from news sources. Column "E (Tons)" represents the sum of NO_x and reactive VOC emissions.

Fire Name	Area (Acres)	Daily Growth (Acres)	NO_x (Tons)	VOCs (Tons)	Reactive VOCs (Tons)	E (Tons)	Distance (Km)	Q/d (Tons/km)	Fuel Loading	Fire Size Data Source
Ivanpah Fire	1,000	1,000	3.7	19.4	12	15	110	0.1	Creosote bush shrubland	https://www.fireweatheravalanche.org/wildfire/incident/119448/california/ivanpah-fire

3.2.2 Key Factor #2: Comparison of Event Concentrations with Non-Event Concentrations

Another key factor in determining whether the June 22, 2020, exceedance event is exceptional is to compare event ozone concentrations with non-event concentrations via percentile and rank-order analysis. Table 3-5 shows June 22, 2020, concentrations as a percentile in comparison with the last six years of data (with and without the other proposed 2018 and 2020 EE days included) at each site in Clark County. For the three monitoring sites (i.e., Paul Meyer, Walter Johnson, and Joe Neal) that show a NAAQS standard exceedance on June 22, all of the exceedances are greater than or equal to the 98th percentile when compared to the last six years of data, even with all other proposed 2018 and 2020 EE days included. Without the other EE days included, the percentiles are slightly higher (>99th percentile). Table 3-6 shows the June 22 percentile ranks for all monitoring sites around Clark County in comparison with the last six years of ozone season (May to September) data. All three monitoring sites show percentile ranks above the 97th percentile (with all proposed 2018 and 2020 EE days included). When the other possible EE days are excluded, the percentile ranks for Paul Meyer and Joe Neal increase to above the 99th percentile, while the Walter Johnson site shows a 98th percentile rank. Although not all of the sites showed above the 99th percentile rank for June 22 compared with the last six ozone seasons, this analysis confirms that the June 22 EE included unusually high concentrations of ozone when compared with the last six years of data and the last six ozone seasons.

Table 3-5. Six-year percentile ozone. The June 22 EE ozone concentration at each site is calculated as a percentile of the last six years with and without other 2018 and 2020 EEs included in the historical record.

AQS Site Code	Site Name	6-Year Percentile	6-Year Percentile w/o EE Dates
320030071	Walter Johnson	98.7	*99.4*
320030043	Paul Meyer	99.3	*99.7*
320030075	Joe Neal	99.7	*99.8*

Table 3-6. Six-year ozone-season percentile ozone. The June 22 EE ozone concentration at each site is calculated as a percentile of the last six years' ozone season (May-September) with and without other 2018 and 2020 EEs included in the historical record.

AQS Site Code	Site Name	6-Year Percentile	6-Year Percentile w/o EE Dates
320030071	Walter Johnson	97.1	*98.5*
320030043	Paul Meyer	98.5	*99.2*
320030075	Joe Neal	99.3	*99.6*

We also compared the rank-ordered concentrations at each site for 2020. To ensure that our rank-ordered statistics would not be biased by an abnormally low ozone year, we re-examined Figures 2-3 through 2-9 and concluded that 2020 ozone concentrations were not atypically low. **Tables 3-7 through 3-9** show the rank-ordered ozone concentrations for 2018 through 2020 and the design values for 2020, with the proposed 2018 and 2020 EEs included. For the Joe Neal monitoring site, June 22 is tied as the second highest MDA8 ozone concentration for 2020. However, for the Paul Meyer and Walter Johnson monitoring sites, June 22 was not in the top five highest MDA8 ozone days for 2020 when all 2020 EE dates are included. If we remove the other 2020 EE days, June 22 is then the highest ozone day at Joe Neal and the second highest ozone day at Paul Meyer and Walter Johnson.

Table 3-7. Site-specific ozone design values for the Joe Neal monitoring site. The top five highest ozone concentrations for 2018-2020 at Joe Neal are shown, and proposed EE days in 2018 and 2020 are included.

Joe Neal Rank	2018	2019	2020
Highest	80	74	81
Second Highest	78	70	78
Third Highest	76	69	78
Fourth Highest	76	68	78
Fifth Highest	74	67	76
Design Value		74	

Table 3-8. Site-specific ozone design values for the Paul Meyer monitoring site. The top five highest ozone concentrations for 2018-2020 at Paul Meyer are shown, and proposed EE days in 2018 and 2020 are included.

Paul Meyer Rank	2018	2019	2020
Highest	79	74	79
Second Highest	76	72	78
Third Highest	75	70	77
Fourth Highest	75	69	77
Fifth Highest	74	69	76
Design Value		73	

Table 3-9. Site-specific ozone design values for the Walter Johnson monitoring site. The top five highest ozone concentrations for 2018-2020 at Walter Johnson are shown, and proposed EE days in 2018 and 2020 are included.

Walter Johnson Rank	2018	2019	2020
Highest	79	77	82
Second Highest	77	69	82
Third Highest	77	69	78
Fourth Highest	76	68	77
Fifth Highest	76	68	75
Design Value		73	

For further comparison with non-event ozone concentrations, Table 3-10 shows five-year (2015-2019, proposed 2018 EE events included) MDA8 ozone statistics for the week before and after June 22. This two-week window analysis shows that each affected monitoring site shows MDA8 ozone concentrations on June 22 to be well above the average and at or above the 95th percentile (except for the Walter Johnson site, which is 1 ppb below the 95th percentile) of the last five years of data.

Table 3-10. Two-week non-event comparison. June 22, 2020, MDA8 ozone concentrations for each affected site are shown in the top row ppb. Five-year (2015-2019) average MDA8 ozone statistics for June 8 through July 6 are shown for each affected site around Clark County to compare with the event ozone concentrations.

	Joe Neal 320030075	Paul Meyer 320030043	Walter Johnson 320030071
Jun. 22	78	74	73
Mean	63	62	62
Median	64	64	64
Mode	64	64	66
St. Dev	8	8	8
Minimum	41	42	43
95 %ile	74	73	74
99 %ile	78	75	76
Maximum	83	76	87
Range	42	34	44
Count	97	97	97

The percentile, rank-ordered analyses, and the two-week window analysis, indicate that all affected monitoring sites on June 22, 2020, showed unusually high ozone concentrations compared with non-event concentrations. This conclusion supports a key factor, suggesting that June 22 was an EE in Clark County, Nevada.

3.2.3 Satellite Retrievals of Pollutant Concentrations

Satellite retrievals of pollutants associated with wildfire smoke, such as AOD, CO, and NO_x, can provide evidence that smoke was present at a monitoring site. We examined maps of Multi-Angle Implementation of Atmospheric Correction (MAIAC) AOD from the MODIS instrument onboard the Aqua and Terra satellites, CO retrievals from the Atmospheric Infrared Sounder (AIRS) instrument onboard the Aqua satellite, and NO_2 retrievals from the Ozone Monitoring Instrument (OMI). NO_2 retrievals were determined to be inconclusive and moved to Appendix D. MODIS AOD measurements indicate the concentration of light-absorbing aerosols, including those emitted by wildfires, in the total atmospheric column. On June 20 and 21, 2020, MODIS AOD was elevated over the locations of fires in Arizona. On June 20 through June 23, AOD measurements were not enhanced over southern California (Figure 3-21). Because the Ivanpah Fire in the Mojave National Preserve was relatively small, it is difficult for the low spatial resolution of MODIS to detect a relatively small magnitude smoke plume close to the surface that does not fill the entire atmospheric column. The June 21 MODIS AOD image does show enhanced AOD in northwestern and midwestern Arizona (compared with southwestern Arizona), which is consistent with HMS and BlueSky modeled smoke tracers in Section 3.1.2. MODIS AOD retrievals indicate normal levels of aerosols in the Clark County area on June 22 (Figure 3-22).
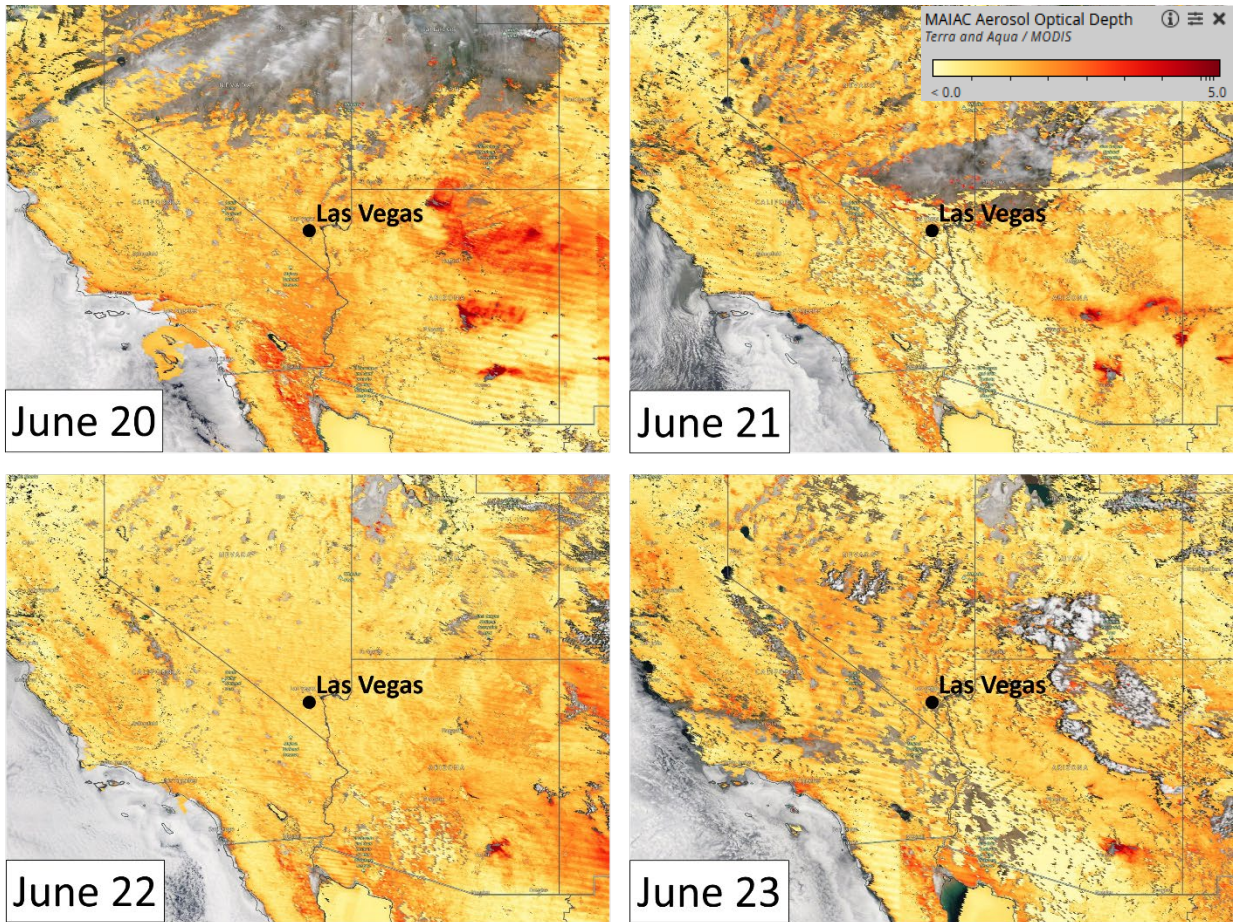
Figure 3-21. MAIAC MODIS Aqua/Terra combined AOD retrievals for two days before, during the EE on June 22, and the day after the EE.
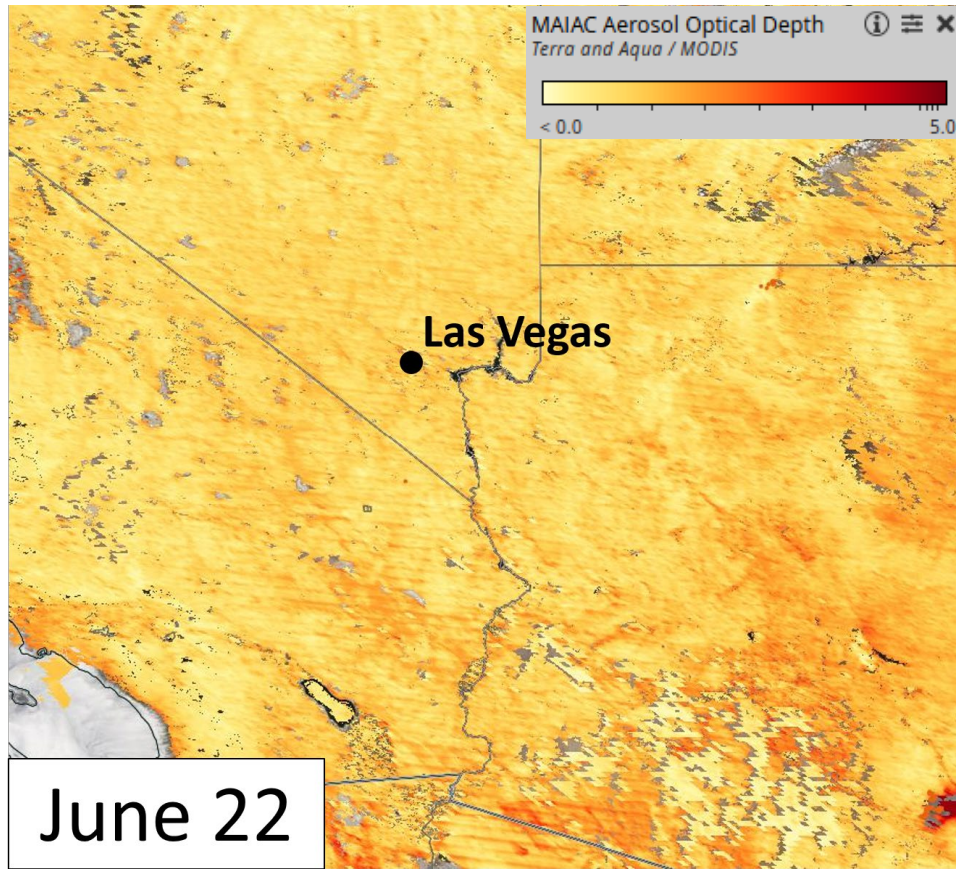
Figure 3-22. A zoomed-in view (over Clark County and the Ivanpah Fire) of the MAIAC MODIS Aqua/Terra combined AOD retrieval during the EE on June 22, 2020.

CO measurements at 500 hPa from AIRS show no enhancement in CO concentrations over Nevada and the Clark County area on June 21 and 22 (**Figures 3-23 and 3-24**). Unfortunately, CO measurements from AIRS were unavailable over Clark County on June 22. On June 21, CO concentrations in areas of Clark County were up to approximately 100 ppb at 500 hPa. Again, consistent with the MODIS AOD images, higher CO concentrations are seen stretching towards Las Vegas on June 21 from the Arizona fires.
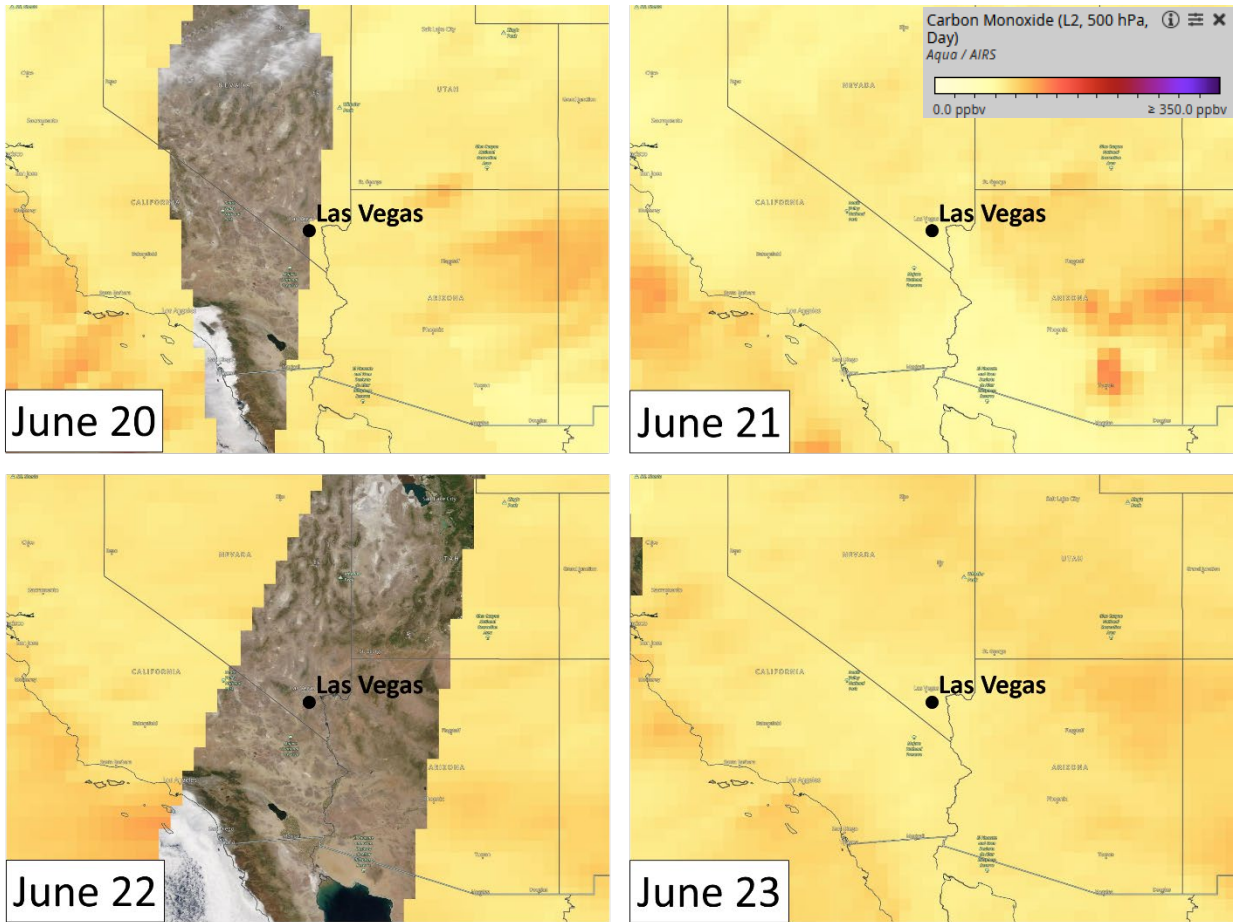
Figure 3-23. MODIS Aqua AIRS CO retrievals for the two days before, during the EE on June 22, and the day after the EE.
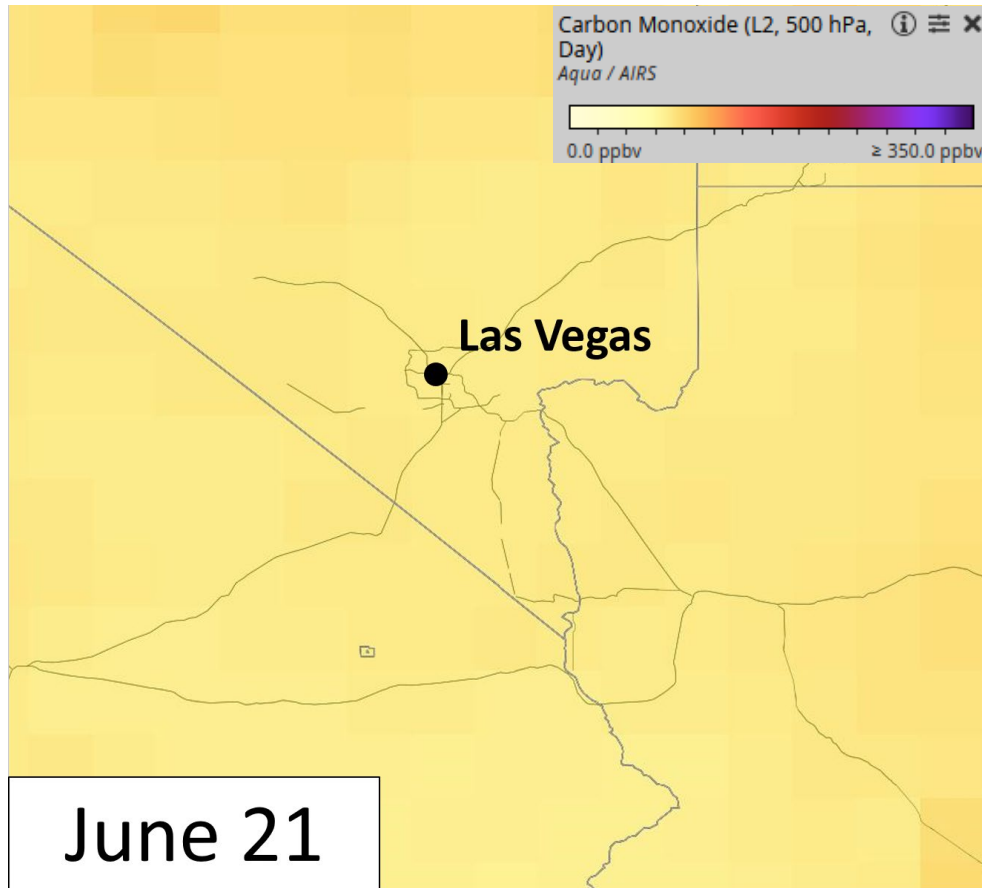
Figure 3-24. A zoomed-in view (over Clark County and the Ivanpah Fire) of the Aqua AIRS CO retrieval the day before the EE on June 21, 2020.

3.2.4 Supporting Pollutant Trends and Diurnal Patterns

Ground measurements of wildfire plume components (e.g., PM$_{2.5}$, CO, NO$_x$, and VOCs) can be used to further demonstrate that enhanced concentrations or unusual diurnal patterns indicate that smoke impacted ground-level air quality. Concentrations of PM$_{2.5}$, CO, NO$_2$, and TNMOC measured at all exceedance sites, as well as other nearby sites in Clark County, were examined. The nitric oxide (NO) data were unavailable at all exceedance sites, so this pollutant is not included in this analysis. If PM$_{2.5}$, CO, NO$_x$, and VOCs were enhanced at the time the smoke plume arrived in Clark County, these measurements would provide additional supporting evidence of smoke impacts in Clark County.

Ideally, at least five years of data are used to calculate average and percentile concentrations for a pollutant. Five years of data are unavailable from monitoring sites in Clark County for multiple parameters at various sites within the network. Where an average or percentile of data is displayed in this section, the number of years of available data used in the calculation is noted when less than five years is available.

Figure 3-25 shows an overall view of pollutants measured around Clark County in the period surrounding the June 22 event. Outlined in a dotted blue line is the night of June 21, during which examined wildfire plume components increased between 7:00 p.m. and 11:00 p.m. local standard time. The peak of all supporting pollutants occurred at 9:00 p.m. except TNMOC, which showed an apex at 10:00 p.m., though this disparity is possibly due to analyzing GC in the hour after sampling. The simultaneous peak in supporting pollutant concentrations at a subset of monitoring sites is indicative of wildfire smoke arriving at Clark County. Concurrently, ozone showed a dip in concentration over these few hours, a possible result of titration due to increased NO_x. Though a nighttime decrease in the planetary boundary layer (PBL) height could contribute to increased pollutant concentrations at the surface, HYSPLIT trajectories show that air arriving in Clark County between 8:00 p.m. and 10:00 p.m. local time was transported northward from the western border of Arizona (**Figure 3-26**), and HMS smoke maps from June 20 and 21 show this region immersed in wildfire smoke (see Figure 3-6 in Section 3.1.2). Furthermore, the sharp evening enhancements in tracers of the wildfire plumes did not persist throughout the night, as the transported wildfire emissions plume mixed into the nighttime boundary layer in Clark County. This finding aligns with the assertion that the 9:00 p.m. spike in supporting pollutants was consistent with wildfire smoke from the Arizona fires. Additional evidence of wildfire smoke in Clark County can be found in deviations from average diurnal concentrations of supporting pollutants. The diurnal average captures expected patterns in pollutant concentrations, such as a typical nightly increase due to a lowered PBL. The discussion below examines $PM_{2.5}$, CO, and NO_2 on a site-by-site basis to show that concentrations of supporting pollutants deviated from expected diurnal patterns during the event period, providing further evidence of smoke impact on Clark County air quality on June 22.
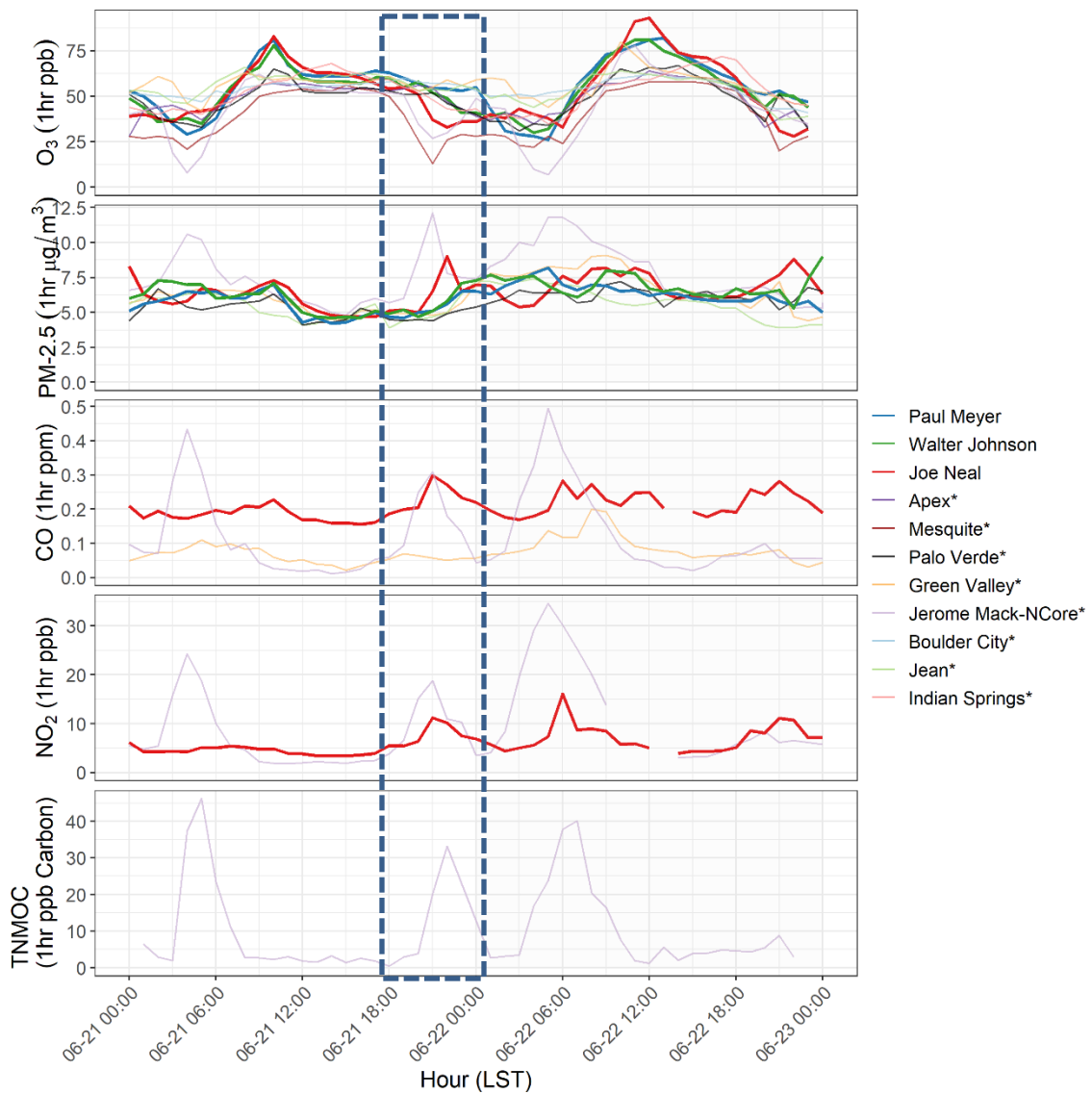
Figure 3-25. Hourly concentrations of ozone, PM$_{2.5}$, CO, NO$_2$, and TNMOC. Unstarred sites in the legend represent sites with an exceedance on June 22. Starred sites represent supporting sites in Clark County. The gray area marks June 22, the event date. The dashed blue box highlights the proposed time window of smoke arrival in Clark County.
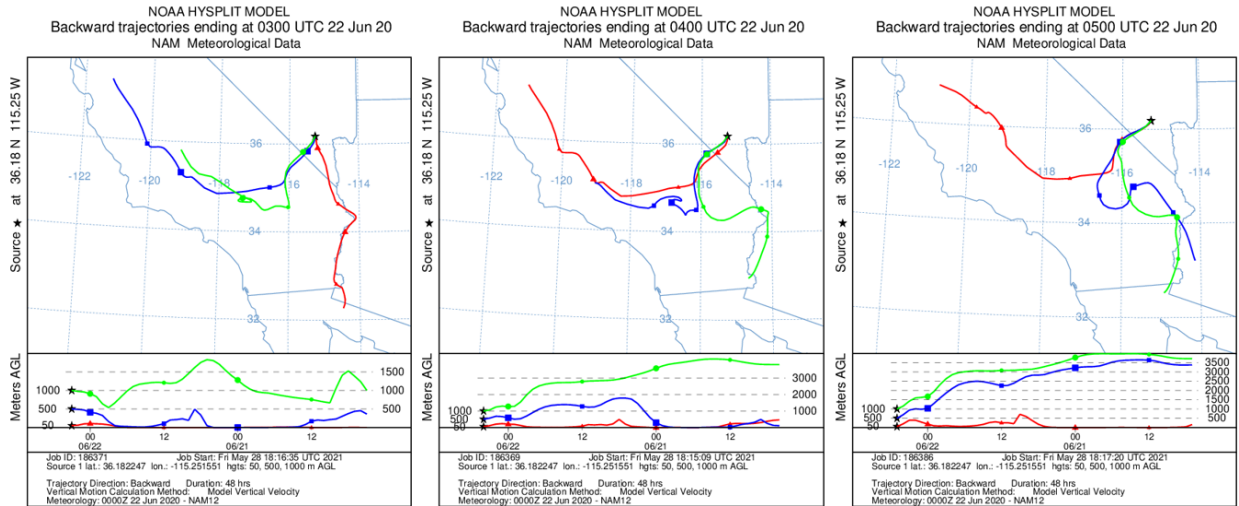
Figure 3-26. 48-hour NAM HYSPLIT back-trajectories at 50 m (red), 500 m (blue), and 1,000 m (green) above ground level. From left to right, trajectories end in Las Vegas at 8:00 p.m., 9:00 p.m., and 10:00 p.m. local time on June 21, 2020.

Figures 3-27 through 3-29 display the diurnal profile and average seasonal diurnal profile of ozone and PM$_{2.5}$ at each event-affected monitoring site. The 5th to 95th percentile range of ozone and PM$_{2.5}$ concentrations is also displayed as a shaded ribbon. Average and percentiles of ozone concentrations are calculated from five years of data at each site. Availability of PM$_{2.5}$ data varies per site: three years of data are available at Joe Neal, four years at Paul Meyer, and one year at Walter Johnson. On June 22, the daily peak value for ozone rose well above the seasonal diurnal average, exceeding the 95th percentile concentration at its maximum at each event-affected site. PM$_{2.5}$ concentrations showed slight deviations from normal at each site, but did not approach concentrations that would be considered abnormal. Late morning to early afternoon concentrations remained elevated above average at each site during a period when concentrations would typically decrease. This deviation is most pronounced at Joe Neal between 6:00 a.m. and 12:00 p.m. A spike in PM$_{2.5}$ concentrations was also observed at Joe Neal on the night of June 21. Though an increase in PM$_{2.5}$ concentrations is expected during evening hours due to commuter travel, the spike that occurred on June 21 occurred at a later hour and rose to an above-average level. Though modest abnormalities appeared in PM$_{2.5}$ concentrations at exceedance sites during the June 22 event period, values did not rise to abnormal levels.
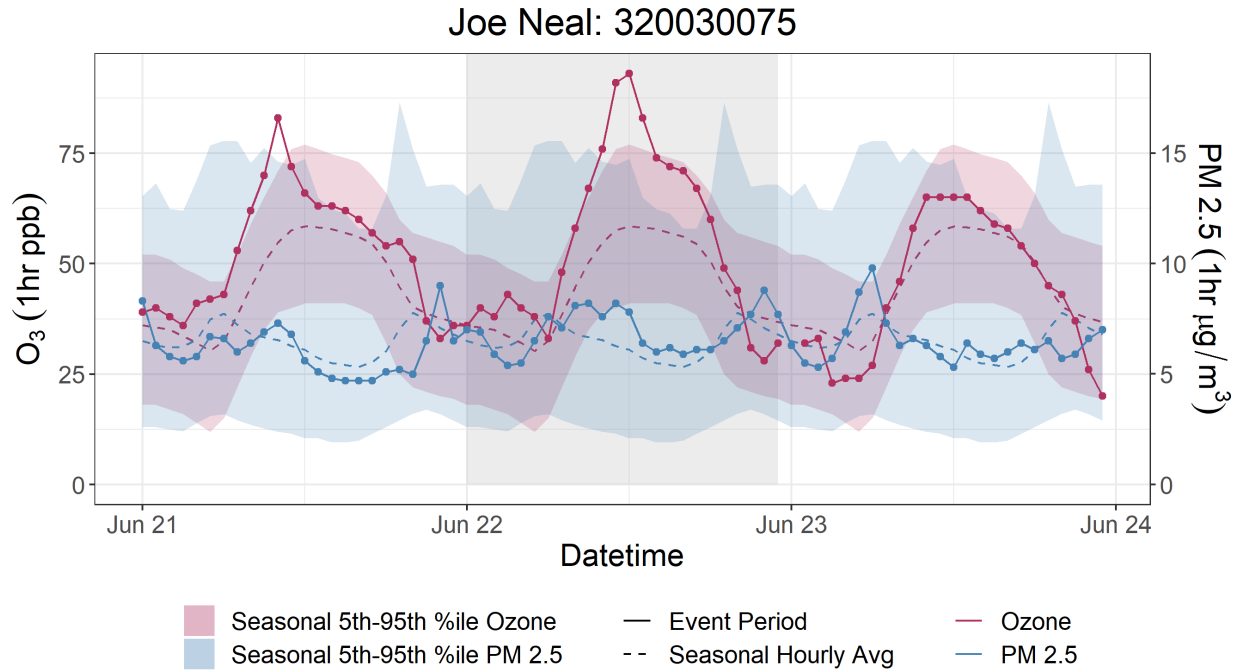
Figure 3-27. Diurnal profile of hourly ozone (red) and PM$_{2.5}$ (blue) concentrations at the Joe Neal site, including concentrations on June 22 (solid) and the seasonal (May-Sept.) diurnal average (dotted). Shaded ribbons represent the five-year 5th to 95th percentile range. Five years of ozone data is available, and three years of PM$_{2.5}$ data is available at Joe Neal. The gray area marks the event date.
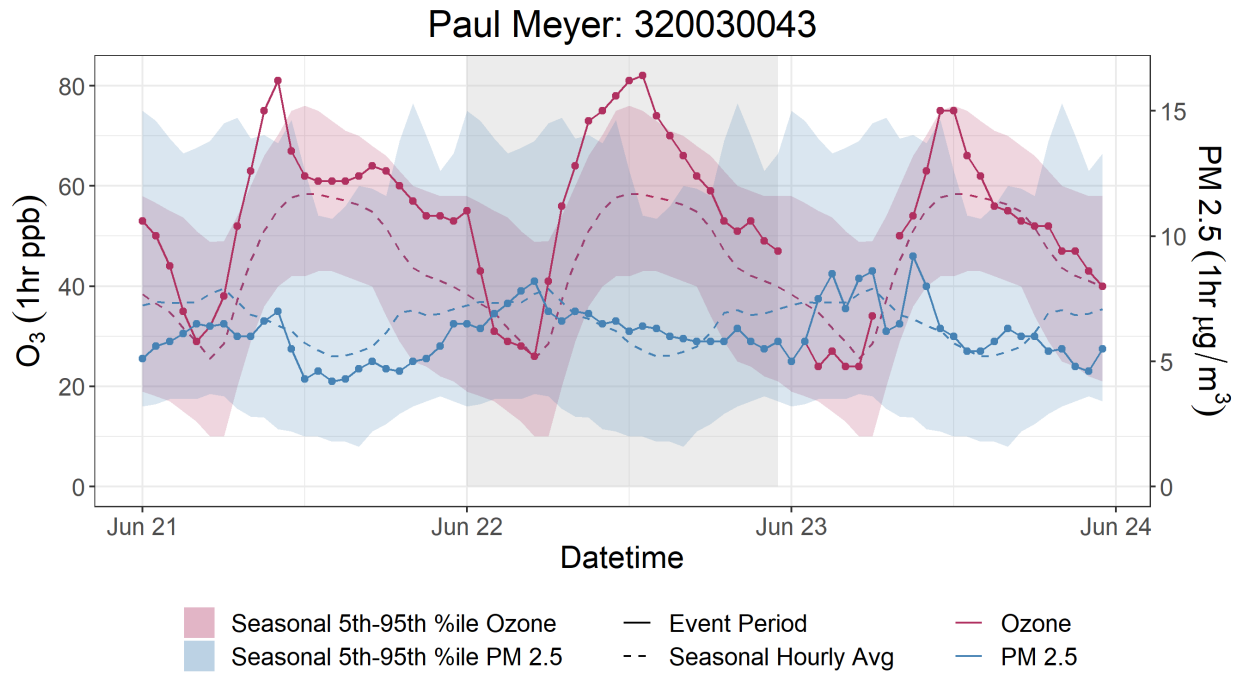
Figure 3-28. Diurnal profile of hourly ozone (red) and PM$_{2.5}$ (blue) concentrations at the Paul Meyer site, including concentrations on June 22 (solid) and the seasonal (May-Sept.) diurnal average (dotted). Shaded ribbons represent the five-year 5th to 95th percentile range. Five years of ozone data are available, and four years of PM$_{2.5}$ data are available at Paul Meyer. The gray area marks the event date.
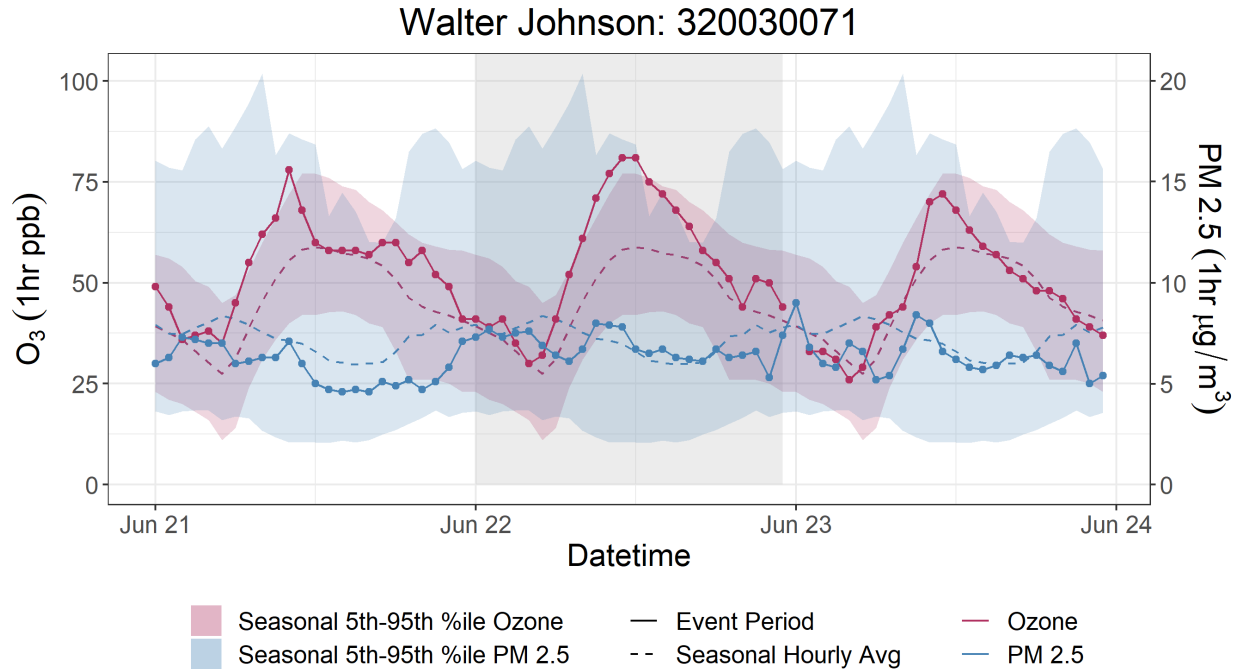
Figure 3-29. Diurnal profile of hourly ozone (red) and PM$_{2.5}$ (blue) concentrations at the Walter Johnson site, including concentrations on June 22 (solid) and the seasonal (May-Sept.) diurnal average (dotted). Shaded ribbons represent the five-year 5th to 95th percentile range. Five years of ozone data is available, and one year of PM$_{2.5}$ data is available at Walter Johnson. The gray area marks the event date.

The lack of significant increase in PM$_{2.5}$ concentrations on the event date does not rule out wildfire smoke influence in Clark County. Though the PM$_{2.5}$ concentration in a smoke plume decreases as the distance from a fire or the age of a smoke plume increases, the ozone mixing ratio may continue to increase due to persistent aerosols and secondary reactions within the plume (Jaffe and Widger, 2017). An examination of the concentrations of PM$_{2.5}$ elemental carbon (EC) and organic carbon (OC) that contribute to total PM$_{2.5}$ can identify the effects of combustion in ambient air even when the direct effect of increased PM$_{2.5}$ concentration has dwindled upon transport. Speciated PM$_{2.5}$ measurements are available from the Jerome Mack–NCore site for 24-hour periods every three days. **Figure 3-30** shows EC plus OC and the percent of total PM$_{2.5}$ made up by EC plus OC between June 17 and June 29, 2020. There is a gap in data between June 3 and June 17, and between June 29 and July 8, that prevents the display of a larger period surrounding the event date. Figure 3-30 is similar to that shown in the *State of Arizona Exceptional Event Documentation for Wildfire-Caused Ozone Exceedances on June 20, 2015, in the Maricopa Nonattainment Area* report prepared by the Arizona Department of Environmental Quality (ADEQ). The presence of wildfire smoke in Clark County is accompanied by an increase in the percentage of total PM$_{2.5}$ constituted by EC and OC from 20% on June 17 to 39% on June 20. HYSPLIT back trajectories ending in Las Vegas on June 20 (**Figure 3-31**) show that air transport paths intersected with smoke-affected areas in western Arizona, and

Figure 3-6 in Section 3.1.2 shows smoke plumes directly entering the southern tip of Clark County on June 20. This increase in the percent of PM$_{2.5}$ constituted by EC plus OC is more drastic than that presented in the 2015 ADEQ demonstration. Interpolation between June 20 and June 23 and data through June 29 indicate that this percentage remained enhanced for a week after June 22. This is not surprising because June 26, 2020, is another date with suspected wildfire smoke influence, but represents a shift in transport sector from the Arizona fires to the Utah and southern Nevada fires. Any compounding effect the fast-burning Ivanpah Fire had on PM$_{2.5}$ speciation on June 22 cannot be determined due to the lack of data on the event date. However, the greater fraction of EC and OC seen during the event period identifies byproducts of combustion within Clark County due to fires burning in Arizona (see Section 3.1.3).
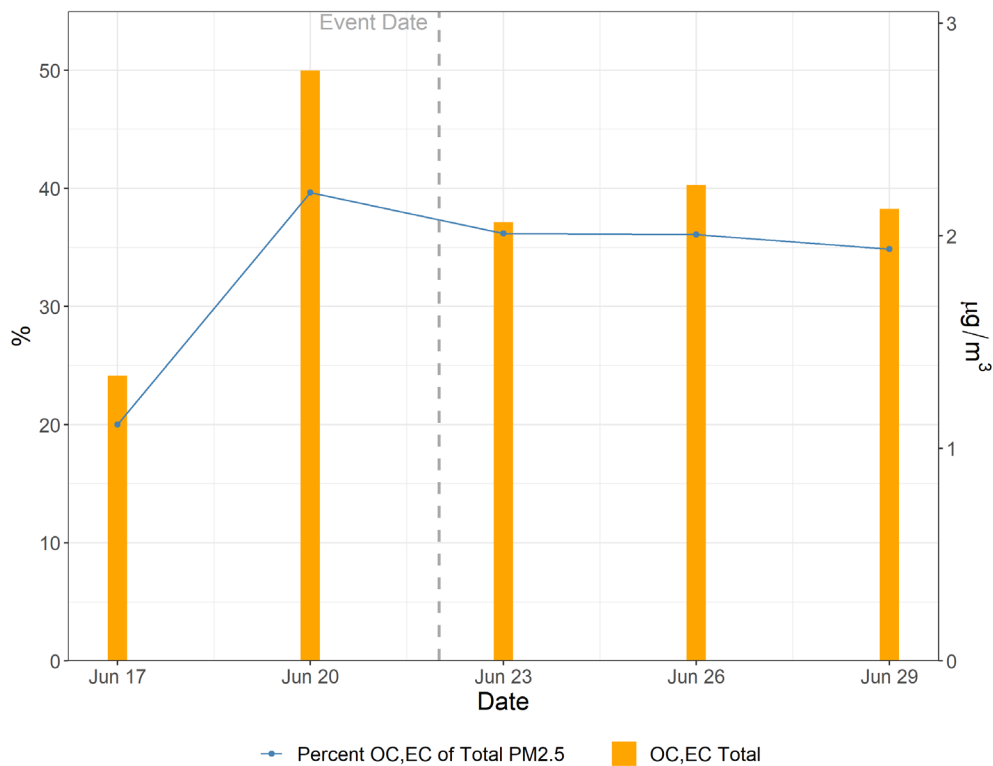
Figure 3-30. Percent of total PM$_{2.5}$ concentrations constituted by OC plus EC (blue line) in the period surrounding the June 22, 2020, event. Total EC plus OC concentration (μg/m³) is represented by the yellow bars. 24-hour speciated PM$_{2.5}$ measurements are available from the Jerome Mack site every three days. June 22 is marked by the dashed gray line.
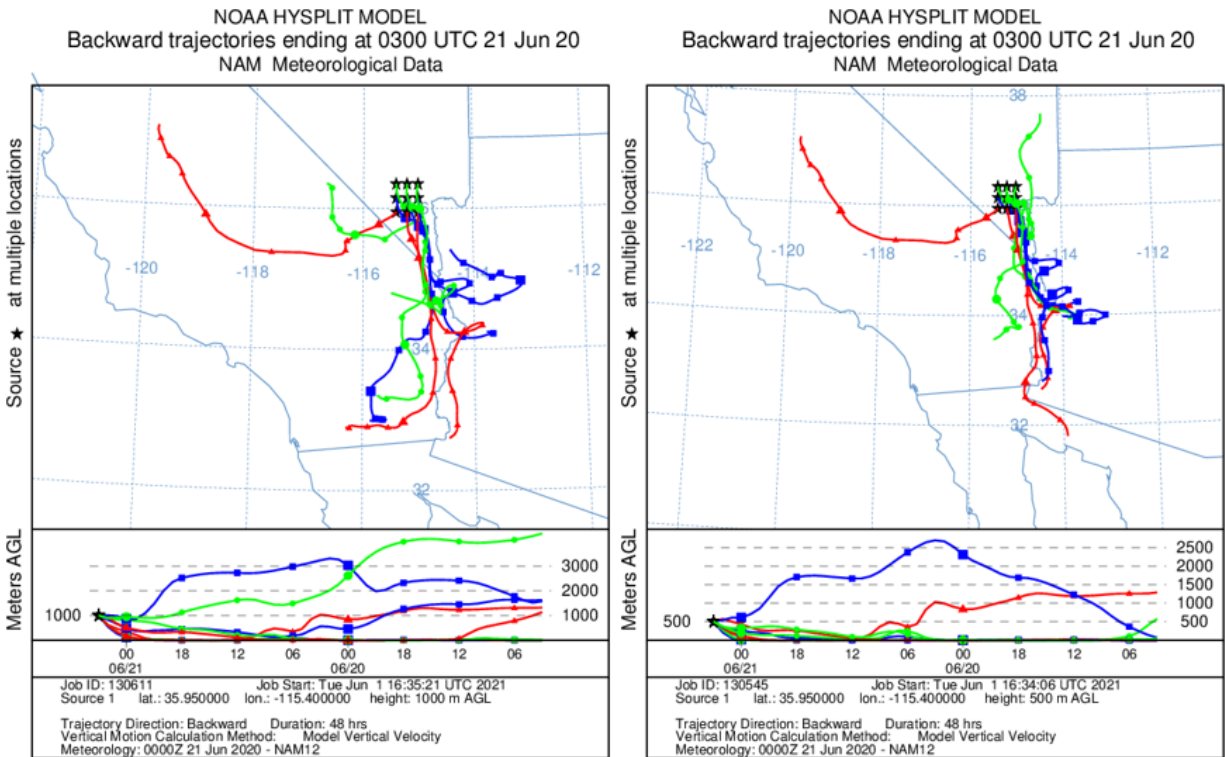
Figure 3-31. 48-hour NAM HYSPLIT back-trajectories at 1,000 m (left) and 500 m (right) above ground level ending in Las Vegas at 8:00 p.m. local time on June 20, 2020.

Diurnal profiles of ozone and CO on June 22 at the Joe Neal site are displayed in **Figure 3-32**. Joe Neal is the only event site for which CO data are available on June 22. This plot also shows the average diurnal profile of CO concentrations and the 5th to 95th percentile range. Two years of CO data are available from Joe Neal. CO levels show a spike above the expected nighttime concentration before midnight on June 21. This spike coincides with a similar peak in $PM_{2.5}$ concentrations at Joe Neal (see Figure 3-27). Though concentrations in this period are all within the 95th percentile, CO levels remained elevated above average between 6:00 a.m. and 12:00 p.m. on June 22, which coincides with the modest deviation from normal shown by $PM_{2.5}$ concentrations during the same period. CO levels show sharp increases throughout the morning, even when the expected diurnal profile indicates that concentrations are expected to decline.
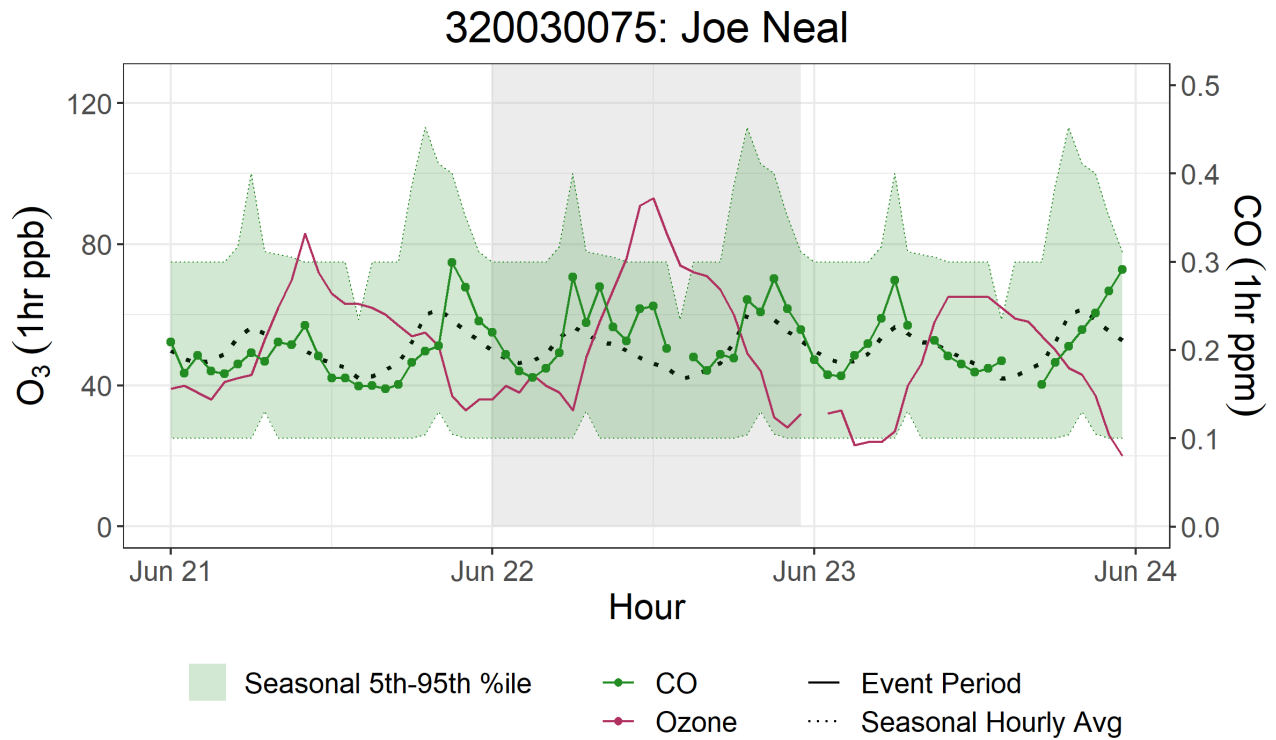
Figure 3-32. Hourly ozone (red) and CO (green) concentrations for the Joe Neal site on June 22. The dashed line shows the seasonal (May to Sept.) average CO concentration diurnal profile. The green shaded area indicates the seasonal 5th to 95th percentile values of CO for statistical reference. The gray area marks the event date. Two years of CO data are available at Joe Neal.

Lastly, concentrations of NO_2 were examined for the June 22 event in Clark County. The only event-affected site with NO_2 data available is Joe Neal, though NO_2 data are also available and displayed for a nearby site, Jerome Mack. Diurnal profiles of ozone and NO_2 on June 22 at Joe Neal and Jerome Mack are displayed in **Figures 3-33 and 3-34**. These plots also show the average diurnal profile of NO_2 concentrations and the 5th to 95th percentile range. Five years of NO_2 data are available from Joe Neal and four years from Jerome Mack. At Joe Neal, a spike in NO_2 concentrations occurs on the night of June 21, aligning with the overnight spikes in $PM_{2.5}$ and CO concentrations shown in Figures 3-25 and 3-29. On the morning of the event date, June 22, there is an increase in NO_2 above the average concentration at this hour of the day at Joe Neal and Jerome Mack. The temporal pattern is consistent with historical morning increases during rush hour. The higher-than-average NO_2 concentrations in the region on the preceding night of the event date lend evidence for wildfire smoke influence in Clark County.
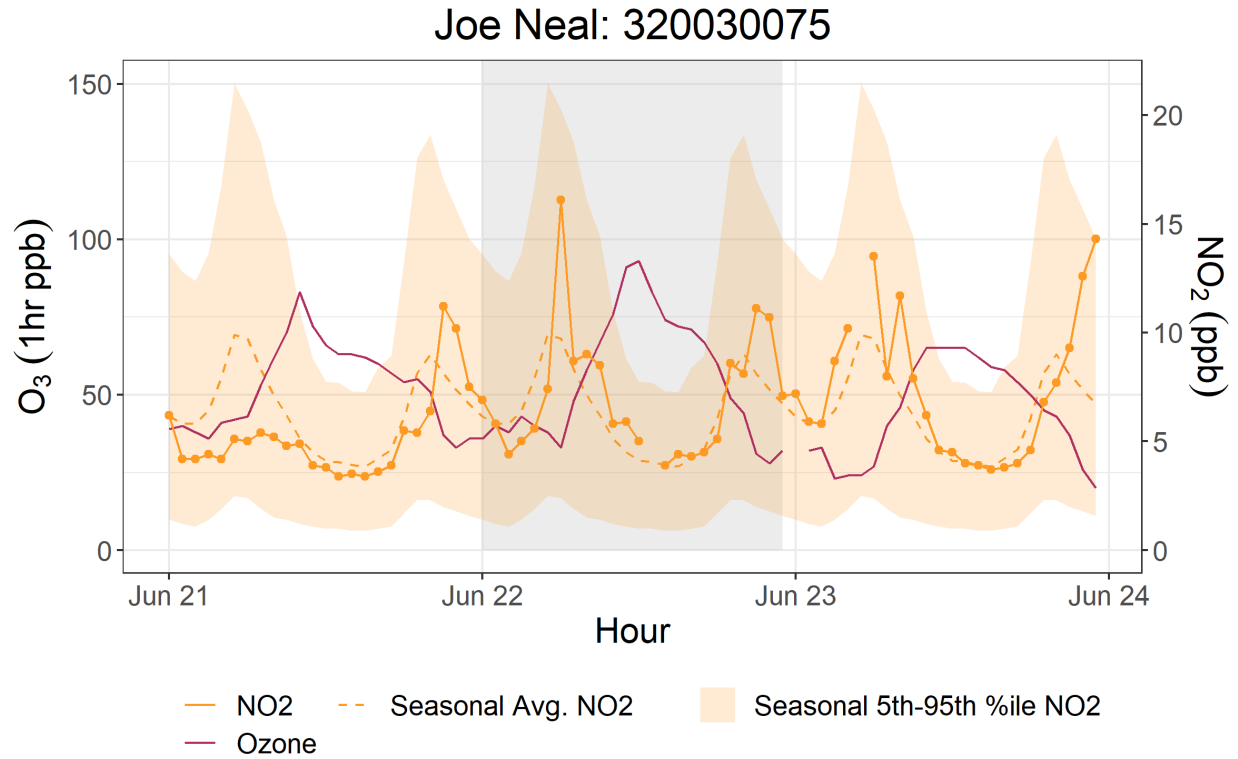
Figure 3-33. Hourly ozone (red) and NO$_2$ (yellow) concentrations for the Joe Neal site on June 22. The dashed line shows the seasonal (May to Sept.) average NO$_2$ diurnal profile. The yellow shaded area indicates the seasonal 5th to 95th percentile values of NO$_2$ for statistical reference. The gray area marks the event date. Five years of NO$_2$ data are available at Joe Neal.
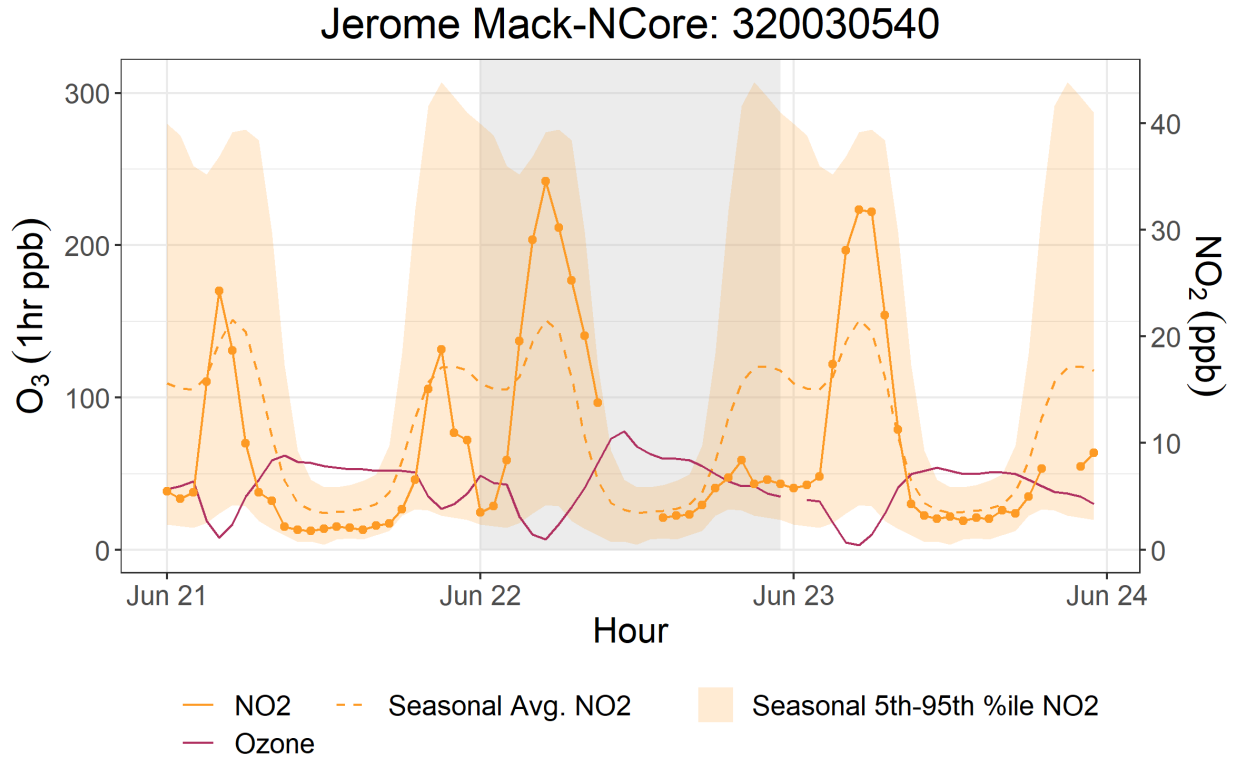
Figure 3-34. Hourly ozone (red) and NO₂ (yellow) concentrations for the supporting Jerome Mack site on June 22. The dashed line shows the seasonal (May to Sept.) average NO₂ diurnal profile. The yellow shaded area indicates the seasonal 5th to 95th percentile values of NO₂ for statistical reference. The gray area marks the event date. Four years of NO₂ data are available at Jerome Mack.

A detailed TNMOC analysis is not available in this discussion due to lack of data. Less than one season's worth of TNMOC data is available from a single Clark County site, the supporting NCore site, Jerome Mack.

Deviations of concentrations of supporting pollutants from diurnal patterns, along with ozone concentrations outside of their normal seasonal or yearly historical averages, provide additional proof of smoke impacts on the Clark County area during June 22, 2020. Wildfires emit ozone precursors including NO_x, and VOCs. While ozone concentrations can be suppressed very near a fire due to NO_x titration, downwind areas are likely to see an increase in ozone concentrations due to the presence of both precursor gases and sufficient UV radiation (i.e., when an air mass leaves an area of very thick smoke that inhibits solar radiation) (Finlayson-Pitts and Pitts Jr, 1997; Jaffe et al., 2008; Bytnerowicz et al., 2010). While the Ivanpah Fire was likely not large enough to cause titration, the Arizona fires were likely large enough to cause titration very near the fires. Ozone precursors from wildfire smoke can be transported a significant distance downwind, and if these compounds are mixed into an urban area (such as Las Vegas), the ozone concentrations produced can be significantly higher than they would be from either the smoke plume or the urban area alone (Jaffe et al., 2013; Wigder et al., 2013; Lu et al., 2016; Brey and Fischer, 2016). Evidence of smoke impacts on

supporting pollutants in Clark County is seen in the elevated contribution of EC and OC to total PM$_{2.5}$, increases in CO and NO$_2$ concentrations during the morning of the event, and a coincident spike in PM$_{2.5}$, CO, and NO$_2$ the night before the event. These findings, along with other analyses in Sections 3.1 and 3.2, suggest that both the direct transport of ozone and the transport of ozone precursor gases likely caused the ozone exceedance on June 22, 2020.

Filter samples were also taken at the Jerome Mack (including a collocated sample) monitoring site in Clark County every three days during 2020. From these filter samples, concentrations of levoglucosan, a wildfire smoke tracer, were analyzed by the Desert Research Institute (DRI) using gas chromatography-mass spectroscopy (GC-MS). Levoglucosan is produced by the combustion of cellulose and is emitted during wildfire events with subsequent transport downwind (Simoneit et al., 1999; Simoneit, 2002; Bhattarai et al., 2019). Levoglucosan has an atmospheric lifetime of one to four days before it is lost due to atmospheric oxidation and can therefore be used as a tracer of biomass burning (wildfires) far downwind from its source (Hoffmann et al., 2009; Hennigan et al., 2010; Bhattarai et al., 2019; Lai et al., 2014). In the Las Vegas region, residential wood combustion has historically not been a significant contributor to levoglucosan concentrations during the late summer timeframe (Kimbrough et al., 2016).

Table 3-11 shows levoglucosan concentration, uncertainty, and positive/negative detection certainty on the day after the June 22 event. Because filter samples are only taken every three days, June 23 data are used in place of June 22 data. Table 3-11 also shows the average levoglucosan concentration from nineteen 2018-2019 background days together with its standard deviation, as well as propagated uncertainty at the Jerome Mack site for comparison. On these background days, no ozone exceedance was observed, and fire/smoke influence was minimal according to HMS. After smoke from the Ivanpah Fire and Arizona wildfires reached Clark County on June 22, a non-zero levoglucosan concentration and a positive detection was seen. The 7 ng/m^3 of levoglucosan on June 23 is likely residual from June 22, and concentrations would have likely been higher during the event. Comparing to the average background concentration of 2±3 ng/m^3 at the Jerome Mack site, the June 23 levoglucosan detection is significant, indicating that wildfire smoke was affecting the area during the time period of the June 22 ozone exceedance.

Table 3-11. Levoglucosan concentrations at monitoring sites around Clark County, Nevada, immediately after the June 22 ozone event. The average levoglucosan concentration, standard deviation, and propagated uncertainty from background days in 2018 and 2019 for the Jerome Mack site are also provided for comparison. Positive or negative detection is also shown.

Sample Date	Sampling Site	Levoglucosan (ng/m^3)	Levoglucosan Uncertainty (ng/m^3)	Levoglucosan Detected?
Background days (2018-2019)	Jerome Mack	2±3	1	N/A
6/23/2020	Jerome Mack	7	1	Positive

3.3   Tier 3 Analyses

3.3.1 Total Column and Meteorological Conditions

The HYSPLIT trajectories shown in Section 3.1 provide evidence that smoke was present over Clark County at the time of the EE on June 22, 2020. However, the visible true color, AOD, and CO satellite data do not provide information about the vertical distribution of visible or measured smoke components. Satellite-retrieved aerosol vertical profiles and ceilometer mixing height measurements were examined to determine whether the smoke plume was present at or near the surface on June 22. Unfortunately, there were no observations from the Cloud-Aerosol Light Detection and Ranging (LIDAR) and Infrared Pathfinder Satellite Observation (CALIPSO) system (which can be used to detect the height of an aerosol layer and aerosol type within the vertical column) for this event.

The local meteorological conditions from June 21 and June 22 provide evidence for the transport of smoke from the Ivanpah and Arizona fires to Clark County, Nevada. Upper-level wind barbs at 500 hPa over southern California and Nevada indicate a very weak westerly and northwesterly wind, however, because transport was predominately at the surface from the Arizona and Ivanpah fires (see HYSPLIT trajectories in Section 3.1.2), upper-level maps do not provide conclusive evidence for smoke transport and are only included for completeness (**Figure 3-35**).
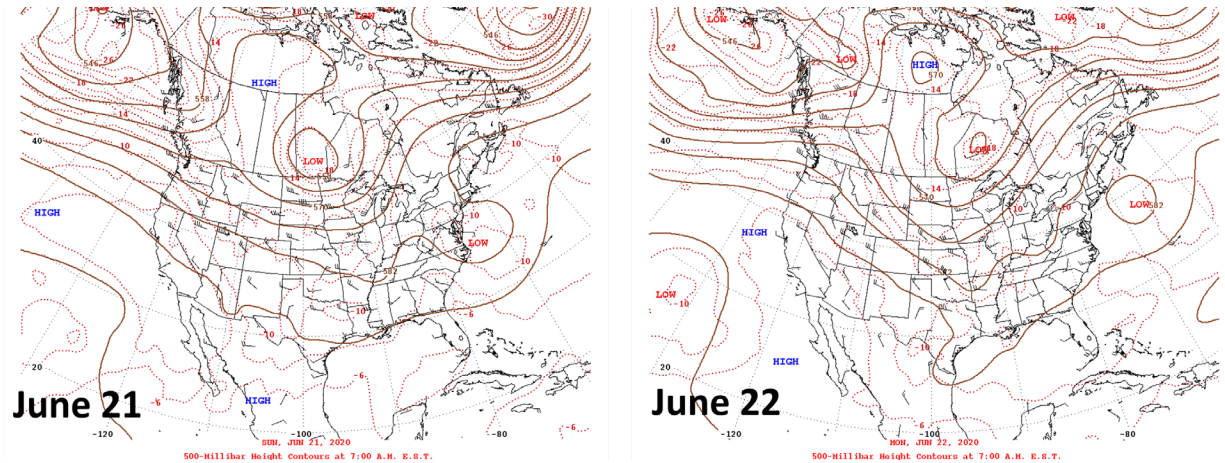
Figure 3-35. Daily upper-level meteorological maps for the one day leading up to the EE and during the June 22 EE.

Local observations of mixing heights in the Las Vegas area on June 22 indicate mixing heights between approximately 2,000–3,750 m for several hours during the day (**Figure 3-36**). However, because the fuel load for the Ivanpah Fire included mostly light, short shrubs, and the distance traveled to Clark County was relatively small, it is likely that smoke did not travel high in the troposphere before it reached Las Vegas to be mixed into the lower boundary layer; rather, smoke likely traveled within the boundary layer to Las Vegas. Further, HYSPLIT trajectories from the fires in western Arizona mostly traveled along the surface, which indicates that vertical mixing into the boundary layer over Las Vegas is not relevant. Therefore, the ceilometer data from the Jerome Mack site does not provide useful evidence connecting the Ivanpah Fire and the fires in western Arizona to smoke impacts at the surface.

A surface low-pressure system was centered over the border of Nevada and California between June 21 and June 22. Low pressure at the surface is associated with enhanced vertical mixing, anti-cyclonic flow, and winds crossing the pressure lines on the map (isobars), which pull air into the low-pressure system (**Figure 3-37**). While vertical mixing is not relevant for the Ivanpah Fire (reasons stated above) or the Arizona fires because they mostly showed transport at the surface (see the HYSPLIT analysis in Section 3.1.3), the surface low would facilitate westward transport from the Arizona fires and eastward transport from the Ivanpah Fire.
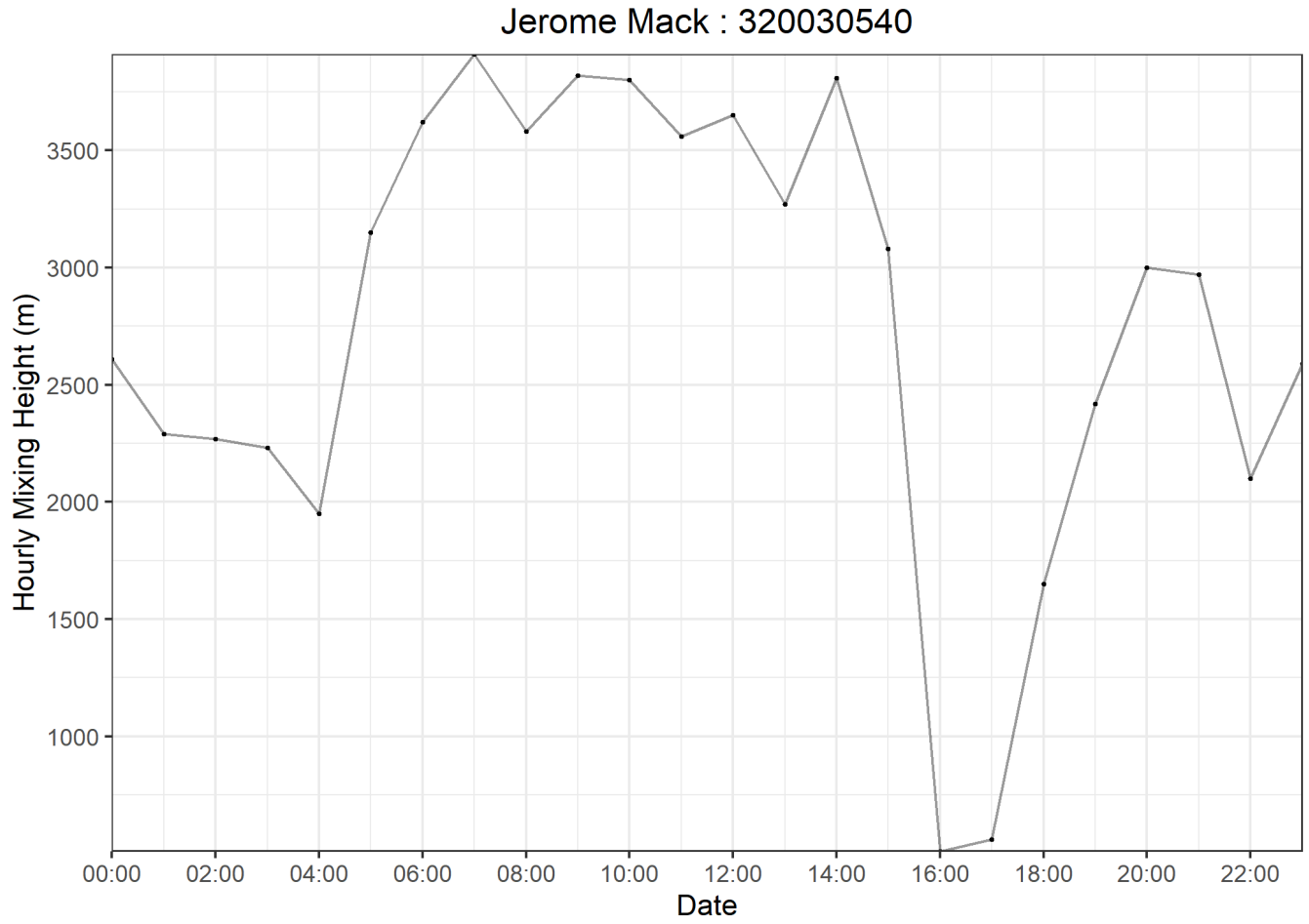
Figure 3-36. Time series of mixing heights taken from the Jerome Mack site (NCore Site) on June 22, 2020.
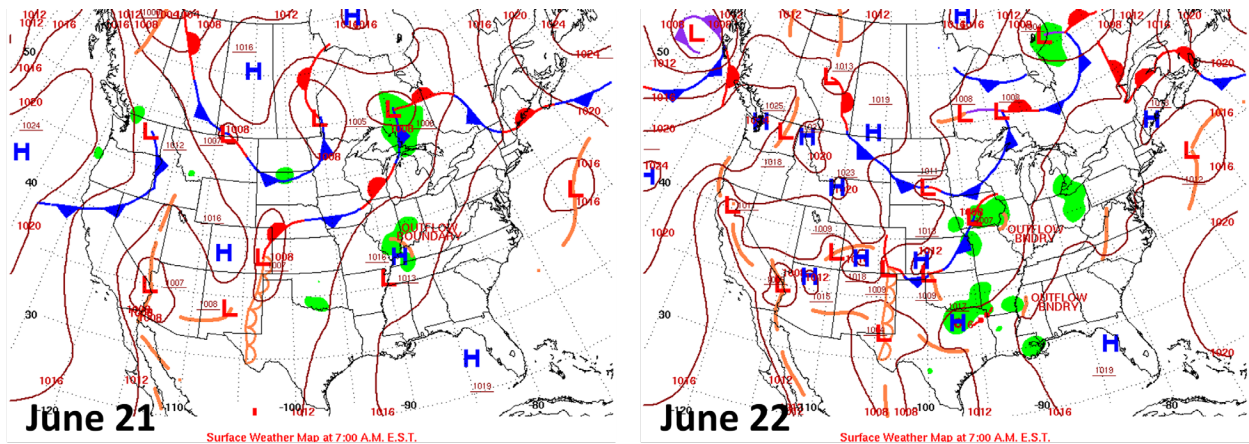
Figure 3-37. Daily surface meteorological maps for the one day leading up to the EE and during the June 22 EE.

In addition to ceilometer-based measurements, vertical temperature profiles (Skew-T diagrams) can also be used to estimate mixing heights. Data collected from the vertical temperature profile at Las Vegas for June 21 and 22 show the vertical atmospheric profile becoming drier in the lower troposphere—as shown by the widening between the temperature profile and the dewpoint profile—with wind directions consistently from the southeast to southwest (**Figure 3-38 and 39**). This indicates smoke transport in the lower levels of the atmosphere from the Ivanpah Fire in the Mojave National Preserve and Arizona wildfires into Clark County. The upper-level weather map and the vertical temperature and wind profile suggest (1) the existence of smoke within the mixed layer, and (2) the transport of smoke from the Ivanpah Fire in the Mojave National Preserve and Arizona wildfires to Clark County.
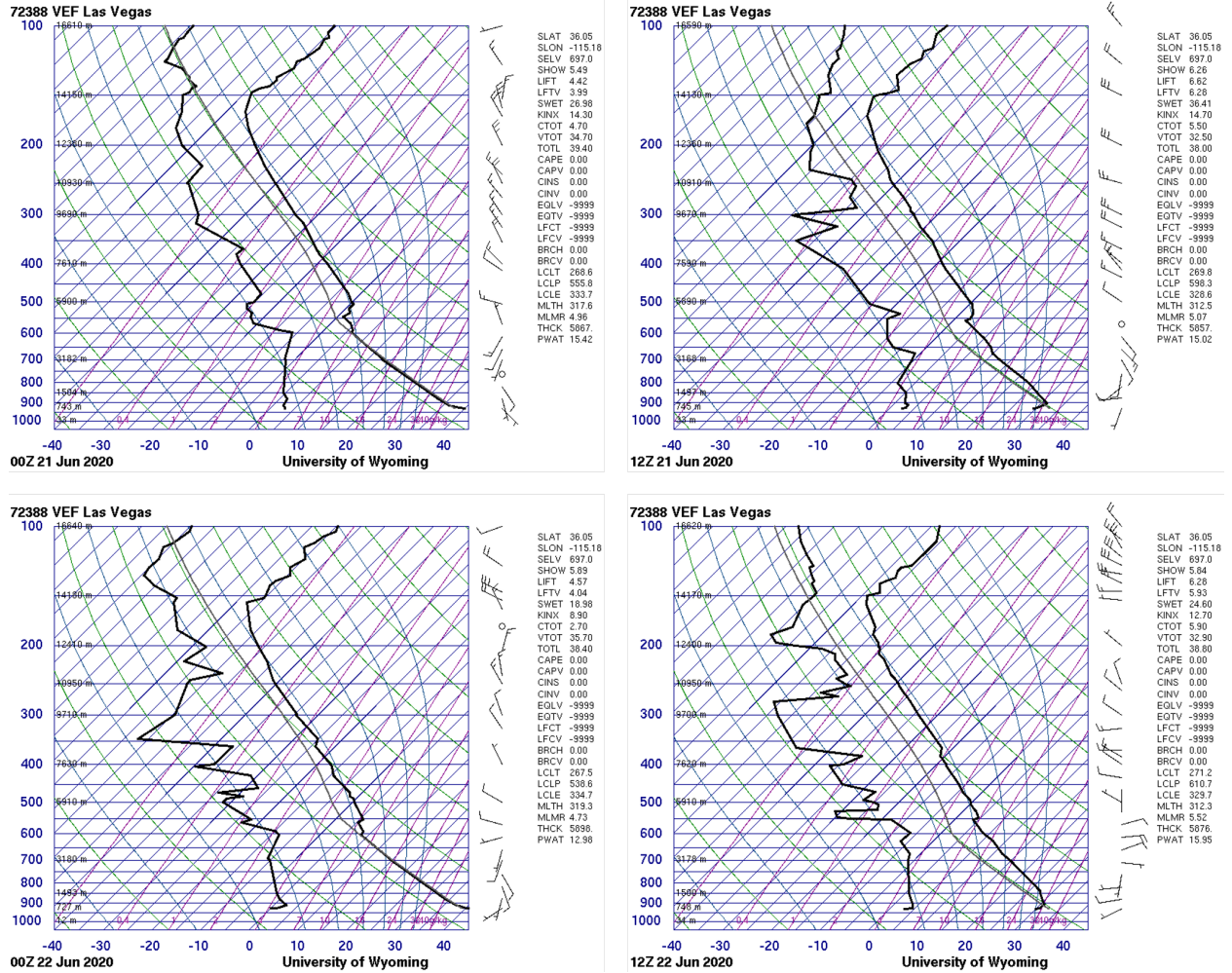
Figure 3-38. Skew-T diagrams from June 21 and 22, 2020 (4:00 p.m. local time on June 20 to 4:00 a.m. on June 22), in Las Vegas, Nevada.
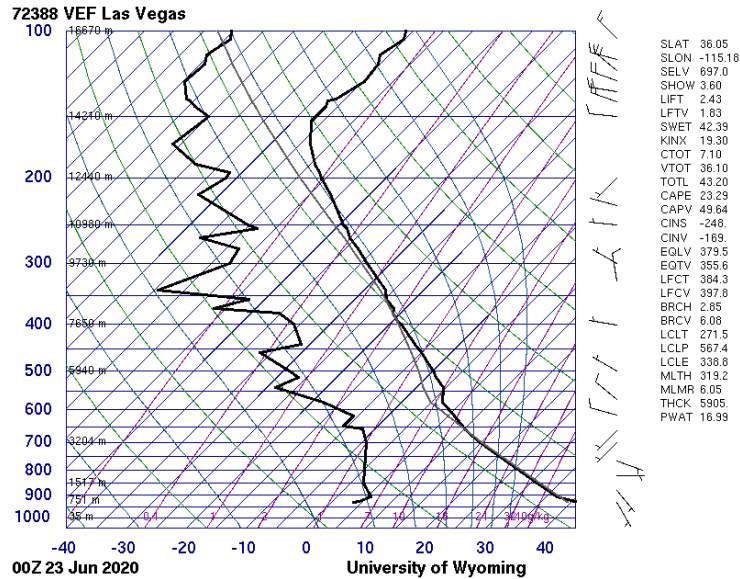
Figure 3-39. Skew-T diagram for June 23, 00:00 UTC (June 22, 4:00 p.m. local time) in Las Vegas, Nevada.

3.3.2 Matching Day Analysis

Ozone production and transport strongly depend on regional and local meteorological conditions. A comparison of ozone concentrations on suspected EE days with non-event days that share similar meteorology can help identify periods when ozone production was affected by an atypical source. Given that similar meteorological days are likely to have similar ozone concentrations, noticeable differences in levels of ozone between the event date and meteorologically similar days can lend evidence to a clear causal relationship between wildfire smoke and elevated ozone concentrations.

Identify Meteorologically Similar Days

In order to identify the best matching meteorology days, both synoptic and local conditions were examined from ozone-season days (April 1 through September 30) between 2014 and 2020. Excluded from this set are days with suspected EEs in the 2018 and 2020 seasons, as well as dates within 5 days of the event date to ensure that lingering effects of smoke transport or stratospheric intrusion did not appear in the data.

To best represent similar air transport, twice daily HYSPLIT trajectories (initiated at 18:00 and 22:00 UTC) from Clark County for 2014-2020 were clustered by total spatial variance. The calculation, based on the difference between each point along a trajectory, provides seven distinct pathways of airflow into Clark County. The cluster that best represents the trajectory on the EE day was chosen, and

ozone-season days within the cluster were then subset for regional meteorological comparison to the EE day.

For the meteorological comparison, a correlation score was assigned to each day from the cluster subset. The National Centers for Environmental Prediction (NCEP) reanalysis data were compiled for the ozone seasons in 2014-2020. Daily average wind speed, geopotential height, relative humidity, and temperature were considered at 1000 mb and 500 mb. At the surface, daily average atmospheric pressure, maximum temperature, and minimum temperature were utilized. Pearson product-moment coefficient of linear correlation (pattern correlation) was calculated between the EE date and each cluster-subset ozone-season day in 2014-2020 for each parameter. The pattern correlation calculates the similarity between two mapped variables at corresponding grid locations within the domain. The statistic was calculated using a regional domain of 30 °N–45 °N latitude and 125° W–105° W longitude. The correlation score for each day was defined as the average pattern correlation of all parameters at each height level. The correlation scores were then ranked by the highest correlation for 1000 mb, surface, and finally 500 mb. The 50 dates with the highest rank correlation scores were then chosen as candidate matching days for further analysis.

Local meteorological conditions for the subset of candidate matching days were then compared to conditions on June 22, and filtered to identify five or more days that best matched the event date. Meteorological maps at the surface and 500 mb, and local meteorological data describing temperature, wind, moisture, instability, mixing layer height, and cloud cover, were examined. The data source for each parameter is summarized in Table 3-12.

Table 3-12. Local meteorological parameters and their data sources.

Meteorological Parameter	Data Source
Maximum daily temperature	Jerome Mack - NCore Monitoring Site
Average daily temperature	Jerome Mack - NCore Monitoring Site
Resultant daily wind direction	Jerome Mack - NCore Monitoring Site (calculated vector average)
Resultant daily wind speed	Jerome Mack - NCore Monitoring Site (calculated vector average)
Average daily wind speed	Jerome Mack - NCore Monitoring Site
Average daily relative humidity (RH)	Jerome Mack - NCore Monitoring Site
Precipitation	Jerome Mack - NCore Monitoring Site
Total daily global horizontal irradiance (GHI)	UNLV Measurement and Instrumentation Data Center (MIDC) in partnership with NREL (**https://midcdmz.nrel.gov/apps/daily.pl?site=UNLV&start =20060318&yr=2021&mo=4&dy=29**)
4:00 p.m. local standard time (LST) mixing layer mixing ratio	Upper air soundings from KVEF (**http://weather.uwyo.edu/upperair/sounding.html**)
4:00 p.m. LST lifted condensation level (LCL)	Upper air soundings from KVEF (**http://weather.uwyo.edu/upperair/sounding.html**)
4:00 p.m. LST convective available potential energy (CAPE)	Upper air soundings from KVEF (**http://weather.uwyo.edu/upperair/sounding.html**)
4:00 p.m. LST 1,000-500 mb thickness	Upper air soundings from KVEF (**http://weather.uwyo.edu/upperair/sounding.html**)
Daily surface meteorological map	NOAA's Weather Prediction Center Daily Weather Maps (**https://www.wpc.ncep.noaa.gov/dailywxmap/index.html**)
Daily 500 mb meteorological map	NOAA's Weather Prediction Center Daily Weather Maps (**https://www.wpc.ncep.noaa.gov/dailywxmap/index.html**)

Results of Matching Day Analysis

The meteorological conditions on June 22, 2020, were typical for the region at this time of year. **Table 3-13** displays that the percentile ranking of each examined meteorological parameter at the Jerome Mack-NCore site falls within the 5th to 95th percentile range among 7 years of observations for the 30-day period surrounding June 22, between June 7 and July 7. The exception is precipitation, for which a measurement of zero is quite common in Clark County. June 22 was fairly warm for this time period. The average daily temperature of 98 degrees is at the 84th percentile, and the maximum temperature of 109 is at the 86th percentile.

Table 3-13. Percentile rank of meteorological parameters on June 22, 2020, compared to the 30-day period surrounding June 22 over seven years (June 7 through July 7, 2014-2020).

Date (Year-Month-Day)	Max Temp (°F)	Avg Temp (°F)	Resultant Wind Direction (°)	Resultant Wind Speed (mph)	Avg Wind Speed (mph)	Avg RH (%)	Precip (in)	Total GHI (kWh/m²)	Mixing Layer Mixing Ratio (g/kg)	LCL (mb)	CAPE (J/kg)	500-1000mb Thickness (m)
2020-06-22	86	84	NA	38	21	21	NA	44	75	61	65	77

The subset of synoptically similar days identified according to the methodology above was further filtered according to parameters listed in Table 3-12 to match local meteorological conditions that existed on the event date. A priority was placed on matching maximum and average temperature, given that June 22, 2020, had higher than average temperatures. **Table 3-14** shows the ten days that best match the meteorological conditions that existed on June 22, 2020, as well as the MDA8 ozone concentration on each of these dates at each exceedance site. Two days from 2020 are included in Table 3-14, May 27 and August 9. These two matching days are especially valuable comparisons because they occurred under similar abnormal anthropogenic emissions due to COVID-19 restrictions. Another meteorologically similar day, June 16, 2017, was excluded from this analysis since there is evidence of smoke influence on this date (see **Appendix E**). The surface maps for June 22, 2020, and each date listed in Table 3-14 all show a surface low pressure system directly over Clark County, with an area of high pressure directly to the east. Though there is more variability in the upper-level pressure maps, there is a consistent area of high pressure south of Clark County and a minimal pressure gradient for all days. These surface and upper-level maps are included in Appendix E.

Maximum and average temperature for the dates listed in Table 3-14 fall within 6 degrees of the event date. Table 3-14 shows the average MDA8 ozone concentration across these eight days with an expected range defined by one standard deviation, a conservative estimate given the small sample size. The average MDA8 ozone concentration across these ten days is well below the 70-ppb ozone

standard at each site, ranging from 59 to 63 ppb. Further, the upper end of the provided range at each site also falls below the ozone NAAQS. This finding lends weight to the assertion that wildfire smoke played a role in the exceptionally high ozone production on June 22, 2020. If meteorology were the sole cause of the ozone exceedance on June 22, 2020, we would expect to see similarly high ozone levels on each of the meteorologically similar days listed in Table 3-14, especially those with even warmer temperatures than experienced on June 22, 2020, lending evidence to the existence of an external source of ozone and precursors on this day.

Table 3-14. Top five matching meteorological days to June 22, 2020. WJ, PM, and JN refer to monitoring sites Walter Johnson, Paul Meyer, and Joe Neal respectively. Average MDA8 ozone concentration (ppb) of meteorologically similar days is shown plus-or-minus one standard deviation rounded to the nearest ppb.[9]

Date (Year-Month-Day)	Max Temp (°F)	Avg Temp (°F)	Resultant Wind Direction (°)	Resultant Wind Speed (kts)	Avg Wind Speed (kts)	Avg RH (%)	Precip (in)	Total GHI (kWh/m²)	Mixing Layer Mixing Ratio (g/kg)	LCL (mb)	CAPE (J/kg)	500-1000 mb Thickness (m)	MDA8 Ozone Concentration (ppb)		
													WJ	PM	JN
2020-06-22	**109**	**98**	**140.81**	**2.01**	**2.81**	**7.96**	**0**	**8.67**	**6.05**	**567**	**23.29**	**5,905**	**74**	**73**	**78**
2014-06-28	106	94.17	195.95	2.23	3.42	17.29	0	8.73	5.42	557	0	5,901	55	54	60
2017-06-15	107	92	178.2	1.1	2.72	10	0	9.04	3.38	512	0	5,871	56	66	68
2017-06-29	108	96.12	147.42	2.85	3.69	7.96	0	8.95	3.5	510	0	5,878	63	67	70
2017-07-01	111	97.54	156.49	3.1	4.2	8.04	0	8.7	4.35	518	162	5,906	64	68	67
2018-06-24	107	95.88	114.12	3.09	3.72	15.83	0	8.64	6.4	582	0	5,890	63	66	63
2019-08-12	105	91.71	113.79	0.96	2.59	13.75	0	7.99	5.17	566	0	5,855	56	57	57
2019-08-14	111	96.62	178.14	0.44	1.43	11.12	0	7.87	5.81	564	78	5,890	59	59	61
2019-08-17	107	96.08	193.57	5.16	5.88	8.71	0	8.11	3.42	511	0	5,889	58	59	59
2020 Dates															
2020-05-27	108	94.38	117.85	0.97	2.6	10.25	0	8.49	4.69	539	40	5,874	63	62	64
2020-08-09	106	94	122.97	1.28	2.11	7.96	0	8.13	3.79	527	0	5,862	62	63	63
Average MDA8 Ozone Concentration of Meteorologically Similar Days													59 ± 4	62 ± 5	63 ± 5

---

[9] June 16, 2017, also identified as a matching day, is omitted from this analysis due to suspected smoke influence (see Appendix E).

This analysis expanded on methods shown in the EPA guidance and a previously concurred EE demonstration submitted by the Arizona Department of Environmental Quality (Arizona Department of Environmental Quality, 2016) in May 2018, to identify ten days that are meteorologically similar to June 22, 2020. In addition to ground measurements of temperature, winds, humidity, boundary layer thickness, and CAPE, regional synoptic patterns, and spatial correlation of meteorology at two atmospheric levels were examined to identify meteorologically similar days. Results show that at each exceedance-affected site, the expected MDA8 ozone concentration is more than 10 ppb below the concentrations measured on June 22, 2020. This validates the existence of an extrinsic ozone source on June 22, 2020.

3.3.3 GAM Statistical Modeling

Generalized additive models (GAM) are a type of statistical model that allows the user to predict a response based on linear and non-linear effects from multiple variables (Wood, 2017). These models tend to provide a more robust prediction than Eulerian photochemical models or simple comparisons of similar events (Simon et al., 2012; Jaffe et al., 2013; U.S. Environmental Protection Agency, 2016). Camalier et al. (2007) successfully used GAM modeling to predict ozone concentrations across the eastern United States using meteorological variables with r^2 values of up to 0.8. Additionally, previous concurred EE demonstrations and associated literature, i.e., Sacramento Metropolitan Air Quality Management District (2011), Alvarado et al. (2015), LDEQ (Louisiana Department of Environmental Quality, 2018), ADEQ (Arizona Department of Environmental Quality, 2016), and Pernak et al. (2019) used GAM modeling to predict ozone events that exceed the NAAQS standards, some in EE cases. By comparing the GAM-predicted ozone values to the actual measured ozone concentrations (i.e., residuals), we can determine the effect of outside influences, such as wildfires or stratospheric intrusions, on ozone concentrations each day (Jaffe et al., 2004). High, positive residuals suggest a non-typical source of ozone in the area but cannot specifically identify a source. Gong et al. (2017) and McClure and Jaffe (2018a) used GAM modeling, in addition to ground and satellite measurements of wildfire pollutants, to estimate the enhancement of ozone during wildfire smoke events. Similar to other concurred EE demonstrations, we used GAM modeling of meteorological and transport variables to estimate the MDA8 ozone concentrations at multiple sites across Clark County for 2014-2020. To estimate the effect of wildfire smoke on ozone concentrations, the GAM residual results (observed MDA8 ozone–GAM-predicted MDA8 ozone) can be coupled with the other analyses to confirm that the non-typical enhancement of ozone is due to wildfires on June 22, 2020.

Using the same GAM methodology as prior concurred EE demonstrations and the studies mentioned above, more than 30 meteorological and transport predictor variables were examined, and through testing, the 16 most important variables were compiled to estimate MDA8 ozone each day at eight monitoring sites across Clark County, Nevada (Paul Meyer, Walter Johnson, Joe Neal, Green Valley, Boulder City, Jean, Indian Springs, and Jerome Mack). As suggested by EPA guidance (U.S. Environmental Protection Agency, 2016), meteorological variables measured at each station

(previous day's MDA8 ozone, daily min/max temperature, average temperature, temperature range, wind speed, wind direction, or pressure) were used if available (see Table 2-1). If meteorological variables were not available at a specific site, the data were supplemented with NCEP reanalysis meteorological data to fill any data gaps. A test of filling data gaps with Jerome Mack meteorological data was made and results had no statistical difference. Sounding data from KVEF (Las Vegas Airport) was used to provide vertical meteorological components; soundings are released at 00:00 and 12:00 UTC daily. Variables such as temperature, relative humidity, wind speed, and wind direction were averaged over the first 1000 m above the surface to provide near-surface, vertical meteorological parameters. Other sounding variables, such as CAPE, lifting condensation level (LCL) pressure, mixing layer potential temperature, mixed layer mixing ratio, and 500-1000 hPa thickness provided additional meteorological information about the vertical column above Clark County. HYSPLIT GDAS 1°x1° 24-hour back trajectories were initiated from downtown Las Vegas (36.173° N, -115.155° W, 500 m agl) at 18:00 and 22:00 UTC (10:00 a.m. and 2:00 p.m. local standard time) each day to provide information on morning and afternoon transport during critical ozone production hours. The twice per day back trajectories from 2014 to 2020 were grouped into seven clusters. **Figure 3-40** shows the clusters, percentage of trajectories per cluster, and heights of each trajectory cluster. Each cluster was associated with a general source region: (1) Northwest U.S., (2) Stagnant Las Vegas, (3) Central California, (4) Long-Range Transport, (5) Northern California, (6) Southern California, and (7) Baja Mexico. Within the GAM the cluster value is used to provide a factor for the distance traveled by each back trajectory. Additionally, day of year (DOY) was used in the GAM to provide information on season and weekly processes. The year (2014, 2015, etc.) was used as a factor for the DOY parameter to distinguish interannual variability.
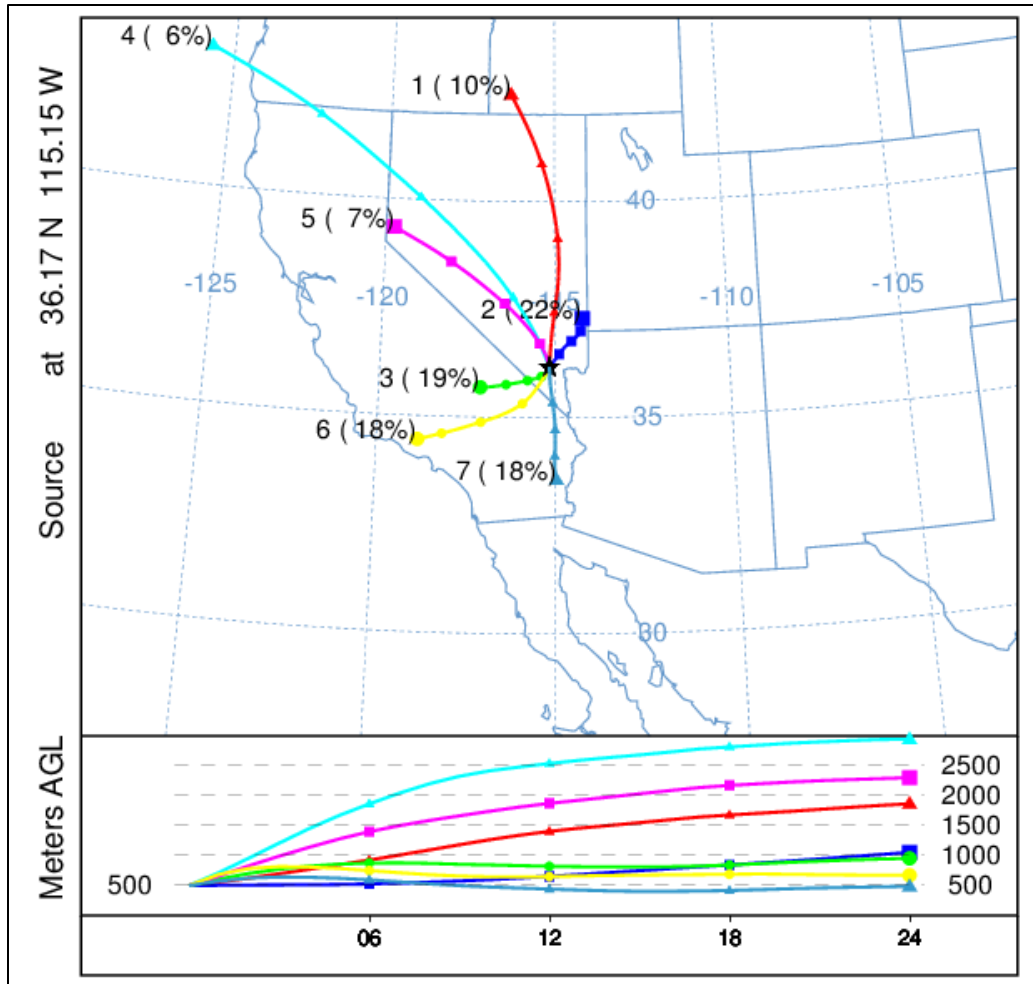
Figure 3-40. Clusters for 2014-2020 back trajectories. Seven unique clusters were identified for the twice daily (18:00 and 22:00 UTC) back-trajectories for 2014 to 2020 initiated in the middle of the Las Vegas Valley. The percentage of trajectories per cluster is shown next to the cluster number. The height of each cluster is shown below the map.

Once all the meteorological and transport variables were compiled, they were inserted into the GAM equation to predict MDA8 ozone:

$$g\left(MDA8\ O_{3,i}\right) = f_1(V1_i) + \ f_2(V2_i) + \ f_3(V3_i) + \cdots + residual_i$$

where f_i are fit functions calculated from penalized cubic regression splines of observations (allowing non-linearity in the fit), Vi are the variables, and i is the daily observation. All variables were given a cubic spline basis except for wind direction, which used a cyclic cubic regression spline basis (Wood, 2017). For DOY and back trajectory distances, we used year factors (i.e., 2014 to 2020) and cluster factors (i.e., 1 to 7) to distinguish interannual variability and source region differences. The factors

provide a different smooth function for each category. For example, the GAM smooth of DOY for 2014 can be different than 2015, 2016, etc. In order to optimize the GAM, knots must be adjusted or any variables removed that are over-fitting or under-performing. The "mgcv" R package was used to summarize and check each variable for each monitoring site (Wood, 2020). A single GAM equation (using the same variables) was used for each monitoring site for consistency. During the initial optimization process, the proposed 2018 and 2020 EE days were removed from the dataset. Ten cross-validation tests were also run by randomly splitting data 80/20 between training/testing for each monitoring site to ensure consistent results. All cross-validation tests showed statistically similar results with no large deviations for different data splits. Data were used for each site from April 2014 through September 2020. The ozone season (April-September) data were used for each year, which is consistent with other papers modeling urban ozone (e.g., Pernak et al., 2019; McClure and Jaffe, 2018a) and ozone concentrations during the periods with EEs are within the representative range of ozone.

Table 3-15 shows the variables used in the GAM and their F-value. The F-value suggests how important each variable is (higher value=more important) when predicting MDA8 ozone. Any bolded F-values had a statistically significant correlation ($p < 0.05$). R^2, the positive 95th quantile of residuals, and normalized mean square residual values for each monitoring site are listed at the bottom of the table.

Table 3-15. GAM variable results. F-values per parameter used in the GAM model are shown for each site. Units and data source for each parameter in the GAM model are shown on the right of the table. 95th quantile, R^2, and normalized mean square residual information is shown at the bottom of the table.

Parameters	Paul Meyer	Walter Johnson	Joe Neal	Green Valley	Jerome Mack	Boulder City	Jean	Indian Springs	Unit	Source
Day of Year (DOY) factored by Year (2014-2020)	**8.11**	**7.09**	**7.65**	**11.8**	**7.94**	**7.11**	**8.68**	**7.53**	--	--
Previous Day MDA8 Ozone	**37.9**	**22.7**	**41.5**	**18.1**	**27.9**	**31.3**	**105.5**	**123.8**	ppb	Monitor Data
Average Daily Temperature	1.92	**2.90**	**4.80**	0.05	1.83	2.13	0.12	1.83	K	
Maximum Daily Temperature	1.37	**2.74**	**2.48**	0.16	0.38	0.02	1.30	1.52	K	
Temperature Range (TMax - TMin)	**4.12**	2.13	1.38	1.74	1.77	1.51	0.50	0.54	K	Monitor Data/NCEP Reanalysis
Average Daily Pressure	**5.54**	**6.42**	**6.74**	**4.64**	**2.94**	0.22	2.17	0.24	hPa	
Average Daily Wind Speed	**11.1**	**5.03**	**7.49**	**5.02**	**15.3**	0.07	0.49	2.19	knots	
Average Daily Wind Direction	0.47	**1.04**	0.24	**1.35**	**2.43**	0.69	0.11	**2.48**	deg	
18 UTC HYSPLIT Distance factored by Cluster	1.70	1.82	1.69	0.92	2.52	2.97	1.66	1.03	km	HYSPLIT Back-Trajectories
22 UTC HYSPLIT Distance factored by Cluster	1.03	0.74	1.47	1.47	1.20	1.26	1.19	0.50	km	
00 UTC Convective Available Potential Energy	3.50	0.13	0.37	1.17	1.16	0.57	**5.71**	**6.49**	J/kg	
00 UTC Lifting Condensation Level Pressure	1.36	**2.78**	2.29	2.41	**3.76**	0.38	1.43	0.38	hPa	
00 UTC Mixing Layer Potential Temperature	0.65	0.79	1.72	0.10	1.23	0.97	1.09	2.53	K	Sounding Data
00 UTC Mixed Layer Mixing Ratio	**2.10**	**2.76**	**2.85**	**3.09**	**3.07**	**2.42**	0.69	1.04	g/kg	
00 UTC 500-1000 hPa Thickness	**2.91**	0.43	1.70	1.60	1.69	**4.11**	**2.18**	1.83	m	
12 UTC 1km Average Relative Humidity	**12.4**	**14.6**	**17.8**	**21.3**	**37.5**	**26.0**	**11.1**	2.18	%	
95th Quantile of Positive Residuals (ppb)	10	10	10	10	9	9	9	10		
R^2	0.55	0.58	0.60	0.58	0.61	0.58	0.57	0.55		
Normalized Mean Square Residual	3.6E-06	7.3E-04	6.1E-05	1.3E-04	3.1E-05	1.3E-04	1.2E-04	1.5E-04		

Table 3-16 provides GAM residual and fit results for all sites for the ozone seasons of 2014 through 2020. Overall, the residuals are low for all data points and similarly low for all non-EE days. However, the 2018 and 2020 EE day residuals are significantly higher than the non-EE day results, meaning there are large, atypical influences on these days. **Figure 3-41** shows non-EE versus EE median residuals with the 95th confidence intervals denoted as notches in the boxplots. The data are shown both ways to provide specific values as well as to illustrate the difference in non-EE versus EE residuals. Since the 95th confidence intervals for median EE residuals are above and do not overlap with those for non-EE residuals at any site in Clark County, the median residuals are higher and statistically different ($p<0.025$). The R^2 for each site ranged between 0.55 and 0.61, suggesting a good fit for each monitoring site and were similar to the results in prior studies and EE demonstrations mentioned previously (R^2 range 0.4-0.8). The positive 95th quantile MDA8 ozone concentration is provided, which is used to estimate a "No Fire" MDA8 ozone value based on the EPA guidance (U.S. Environmental Protection Agency, 2016). The median residuals (and confidence interval) are provided for all non-EE days with observed MDA8 at or above 60 ppb (this threshold was needed for a sufficient sample size to build a representative distribution and derive the median and 95% confidence interval). It should be noted that four out of the seven years modeled by the GAM were high wildfire years, and these values likely include a significant amount of wildfire days. It was not possible to systematically remove wildfire influence by subsetting the Clark County ozone data based on HMS smoke, HMS smoke and $PM_{2.5}$ concentrations, and low wildfire years. These methods produced a significant number of false positives and negatives and yielded datasets that remained affected by wildfire smoke. Therefore, these values should be considered an upper estimate of residuals for high ozone concentration days. The median residuals for 2018 and 2020 EE days are significantly higher than those on non-EE high observed ozone days since their confidence intervals do not overlap (or are comparable for the Jerome Mack station). The non-EE day residuals on days where observed MDA8 was at or above 60 ppb were determined to be normally distributed with a slight positive skew (median skewness = 0.39).

Table 3-16. Overall 2014-2020 GAM median residuals and 95% confidence interval range in square brackets for each site modeled. Sample size is shown in parentheses below the residual statistics. For sample sizes less than ten, a range of residuals is included in square brackets instead of the 95% confidence interval. Residual results are split by non-EE days and the 2018 and 2020 EE days. R^2 for each site is also shown along with the positive 95th quantile result.

Site Name	All Residuals (ppb)	Non-EE Day Residuals (ppb)	2018 & 2020 EE Day Residuals (ppb)	R^2	Positive 95th Quantile (ppb)	Non-EE Day Residuals when MDA8 ≥ 60 ppb (ppb)
Boulder City	0.22 [-0.04, 0.48] (1,132)	0.22 [-0.04, 0.48] (1,130)	12.05 [10.38-13.72] (2)	0.58	9	4.05 [3.55, 4.55] (200)
Green Valley	0.17 [-0.15, 0.48] (948)	0.10 [-0.21, 0.41] (934)	7.38 [5.40, 9.36] (14)	0.58	10	3.76 [3.28, 4.23] (271)
Indian Springs	0.13 [-0.18, 0.44] (1,014)	0.08 [-0.22, 0.38] (1,010)	12.30 [9.37-17.19] (4)	0.55	10	4.79 [4.26, 5.32] (201)
Jean	0.21 [-0.06, 0.48] (1,149)	0.20 [-0.07, 0.47] (1,146)	12.57 [9.59-13.90] (3)	0.57	9	3.40 [2.94, 3.85] (290)
Jerome Mack	0.09 [-0.19, 0.36] (1,152)	0.05 [-0.22, 0.32] (1,141)	6.83 [4.21, 9.45] (11)	0.61	9	3.83 [3.32, 4.33] (242)
Joe Neal	0.23 [-0.08, 0.54] (1,113)	0.17 [-0.13, 0.47] (1,097)	7.77 [5.79, 9.75] (16)	0.60	10	3.32 [2.92, 3.71] (377)
Paul Meyer	0.21 [-0.08, 0.50] (1,159)	0.10 [-0.19, 0.39] (1,137)	8.11 [6.34, 9.88] (22)	0.55	10	3.58 [3.19, 3.97] (388)
Walter Johnson	0.27 [-0.03, 0.57] (1,163)	0.19 [-0.10, 0.48] (1,141)	7.16 [5.11, 9.21] (22)	0.58	10	3.53 [3.13, 3.93] (379)
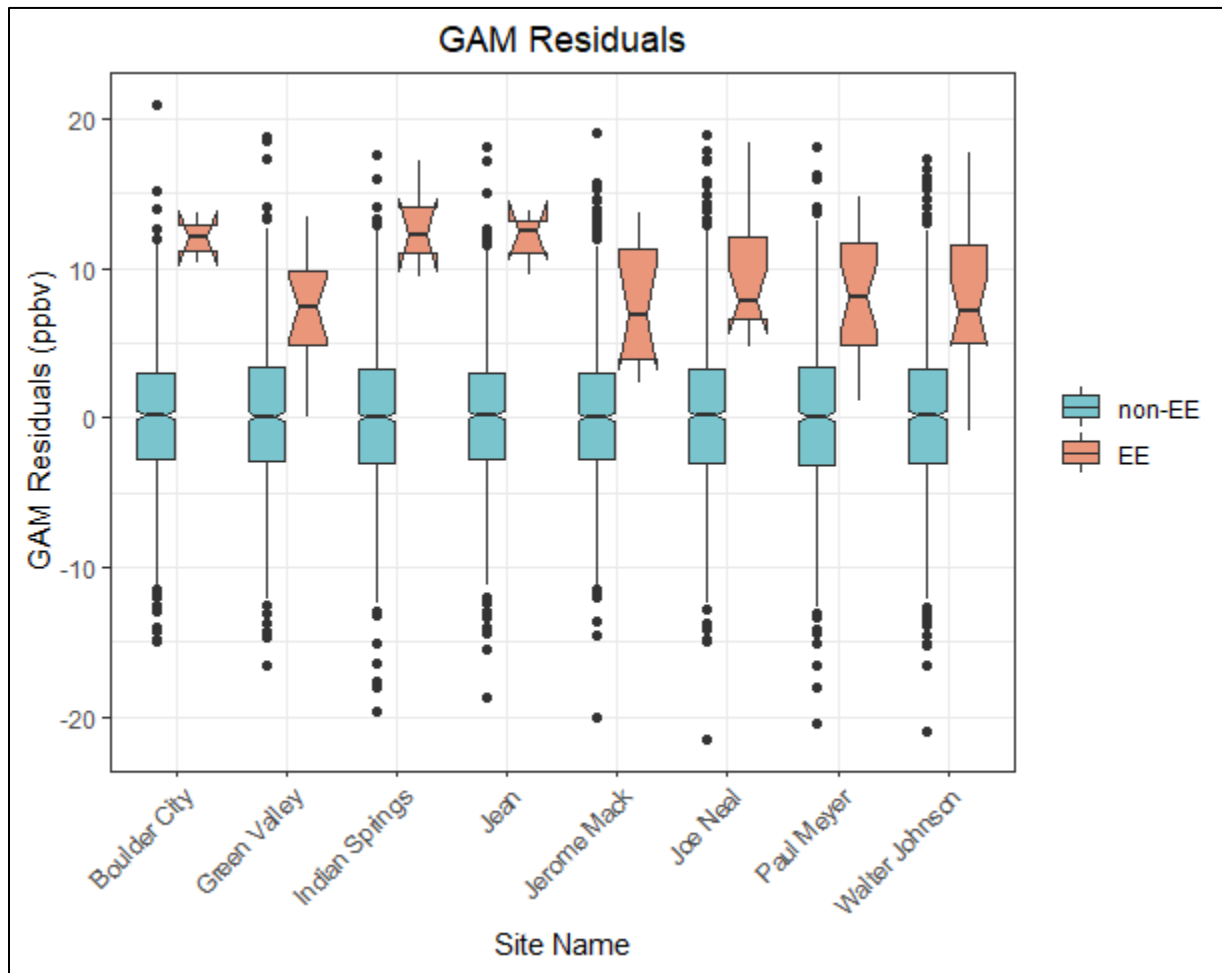
Figure 3-41. EE versus non-EE residuals. Non-EE (blue) and EE (orange) residuals are shown for each site modeled in Clark County. The notches for each box represent the 95th confidence interval around the median. This figure illustrates the information in Table 3-16.

Overall, the GAM results show low bias and consistently significantly higher residuals on EE days compared with non-EE days. The GAM performance was also evaluated on verified high ozone, non-smoke days by looking at specific case studies in order to assess whether high-ozone days, such as the EE days, have a consistent bias that is not evident in the overall or high ozone day GAM performance. Out of the seven years used in the GAM model, four were high wildfire years in California (2015, 2017, 2018, and 2020). Since summer winds in Clark County are typically out of California (44% of trajectories originate in California according to the cluster analysis [not including transport through California in the Baja Mexico cluster]), wildfire smoke is likely to affect a large portion of summer days and influence ozone concentrations. Specific case studies were identified where most monitoring sites in Clark County had an MDA8 ozone concentration greater than or equal to 60 ppb and had no wildfire influence; "no wildfire influence" was determined by inspecting HMS smoke plumes and HYSPLIT back trajectories for each day and confirming no smoke was over,

near, or transported to Clark County. One to two examples were found from each year used in the GAM modeling and required that at least half of the case study days needed to include an exceedance of the ozone NAAQS. Table 3-17 shows the results of these case studies. Most case study days, including NAAQS exceedance days, show positive and negative residuals even when median ozone concentrations are greater than or equal to 65 ppb in Clark County, similar to the results for the entire multi-year dataset. Non-EE day GAM residuals when MDA8 is at or above 60 ppb has a median of 3.69 [95% confidence interval: 3.47, 3.88] (see Table 3-16). The high ozone, non-smoke case study days all show median residuals within or below the confidence interval of the high ozone residuals (from Table 3-16), meaning that the GAM model is able to accurately predict high ozone, non-smoke days within a reasonable range of error. Two additional factors indicate the GAM has good performance on normal, high ozone days: (1) the median residuals for the case studies are mostly lower than the 95% confidence interval of high ozone residuals (i.e., includes non-EE wildfire days) and (2) the case study days were verified as non-smoke days. Thus, residuals above the 95th confidence interval of the median residuals, such as those on the EE days, are statistically higher than days with comparably high ozone concentrations and not biased high because of the high ozone concentrations on these days.

Table 3-17. GAM high ozone concentration, non-smoke case study results. Median GAM residuals for ten days in 2014-2020 are shown where most monitoring sites had MDA8 ozone concentrations of 60 ppb or greater. Sites used to calculate the MDA8 and GAM residual median/range are listed in the Clark County AQS site number column by site number.

Date	Clark County AQS Site Number	Median (Range) of Observed MDA8 Ozone (ppb)	Median (Range) GAM Residual (ppb)
5/17/2014	0601, 0075, 1019, 0540, 0043, 0071	66 (64-71)	1.66 (-0.53-4.28)
6/4/2014	0601, 0075, 0540, 1019, 0043, 0071	69 (66-72)	3.46 (1.70-4.80)
6/3/2015	1019, 0043, 0075, 0540, 7772, 0601, 0071	71 (65-72)	3.01 (-0.34-5.77)
6/20/2015	0601, 0298, 7772, 1019, 0540, 0075, 0043, 0071	65 (63-70)	1.40 (-6.20-5.28)
6/3/2016	0298, 1019, 0075, 0540, 0043, 0071	65 (63-71)	3.89 (1.89-5.26)
7/28/2016	0075, 0071, 0298, 0540, 0043	70 (63-72)	0.24 (-5.95-3.67)
6/17/2017	0601, 0075, 0071, 1019, 0540, 0298, 0043	66 (63-72)	1.85 (-1.94-7.01)
6/4/2018	0601, 0298, 7772, 1019, 0540, 0075, 0043, 0071	65 (60-67)	3.06 (-0.91-3.60)
5/5/2019	0601, 0298, 7772, 1019, 0540, 0075, 0043, 0071	65 (62-67)	1.28 (-2.00-3.42)
5/15/2020	0298, 0043, 0075, 0071	63 (63-65)	1.52 (1.09-3.49)

The bias of GAM residuals versus predicted MDA8 ozone concentrations was evaluated as shown in **Figure 3-42**. Residuals (i.e., observed ozone minus GAM-predicted MDA8 ozone) should be independent of the GAM-predicted ozone value, meaning that the difference between the actual ozone concentration on a given day and the GAM output should be due to outside influences and not well described by meteorological or seasonal values (i.e., variables used in the GAM prediction). Therefore, in a well-fit model, positive and negative residuals should be evenly distributed across all

GAM-predicted ozone concentrations and on average zero. In Figure 3-42, we see that for 2014-2020 at all eight monitoring sites in Clark County, the residuals are evenly distributed across all GAM-predicted ozone concentrations, with no pattern or bias at high or low MDA8 fit concentrations. This evaluation of bias in the model is consistent with established literature and other EE demonstrations ((Gong et al., 2017; McVey et al., 2018; Pernak et al., 2019; Texas Commission on Environmental Quality, 2021), and indicate a well-fit model. In **Figure 3-43**, we also provide a histogram of the residuals at each monitoring site modeled in Clark County. This analysis shows that residuals at each site are distributed normally around a median near zero and none of the distributions show significant tails at high or low residuals (median skew = 0.05 with 95% confidence interval [-0.03, 0.12]). This analysis of error in the model and the results are consistent with previously concurred EE demonstrations (ADEQ, 2016) and previous literature ((Jaffe et al., 2013; Alvarado et al., 2015; Gong et al., 2017; McClure and Jaffe, 2018b; Pernak et al., 2019). **Appendix F** provides GAM residual analysis from the concurred ADEQ and submitted TCEQ demonstrations that compare well with our GAM residual results. Based on these analysis methods, bias in the model is low throughout the range of MDA8 prediction values and confirms that the GAM can be used to predict MDA8 ozone concentrations in Clark County.
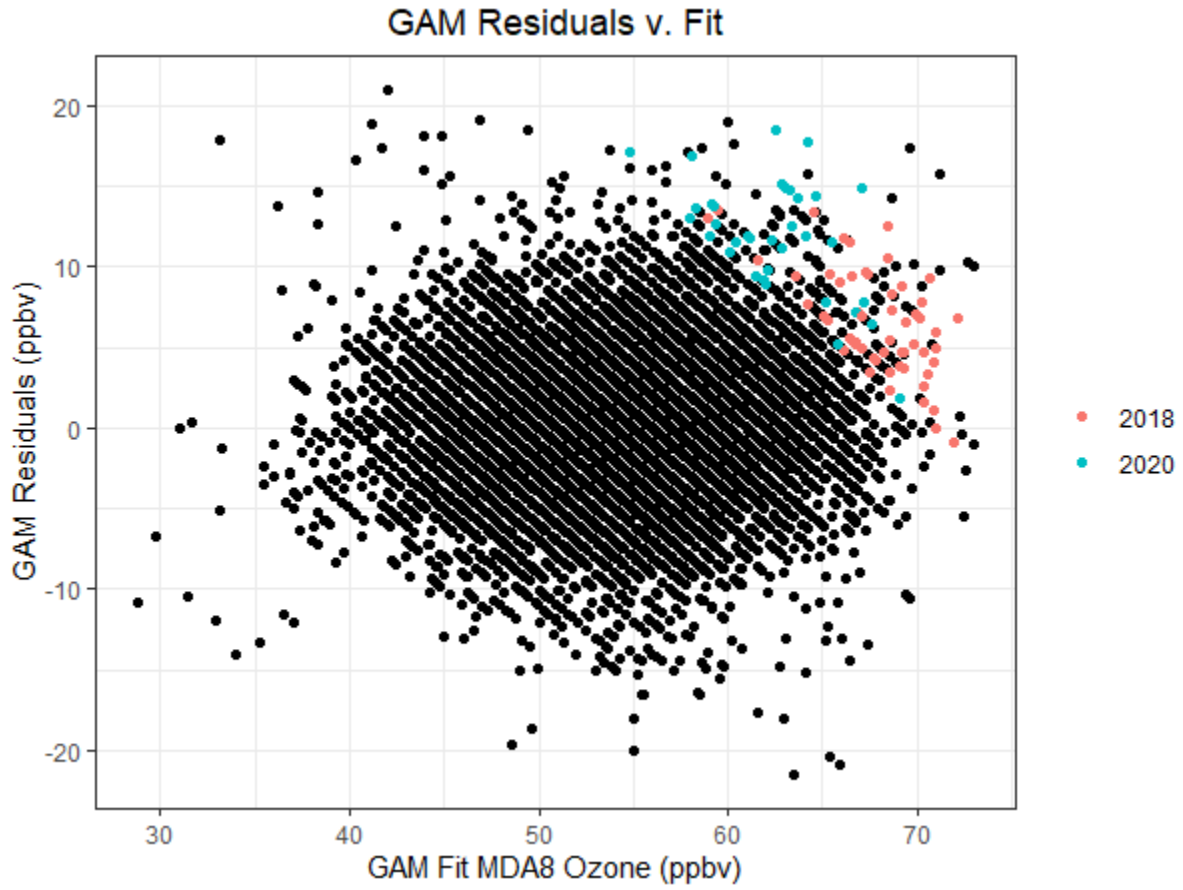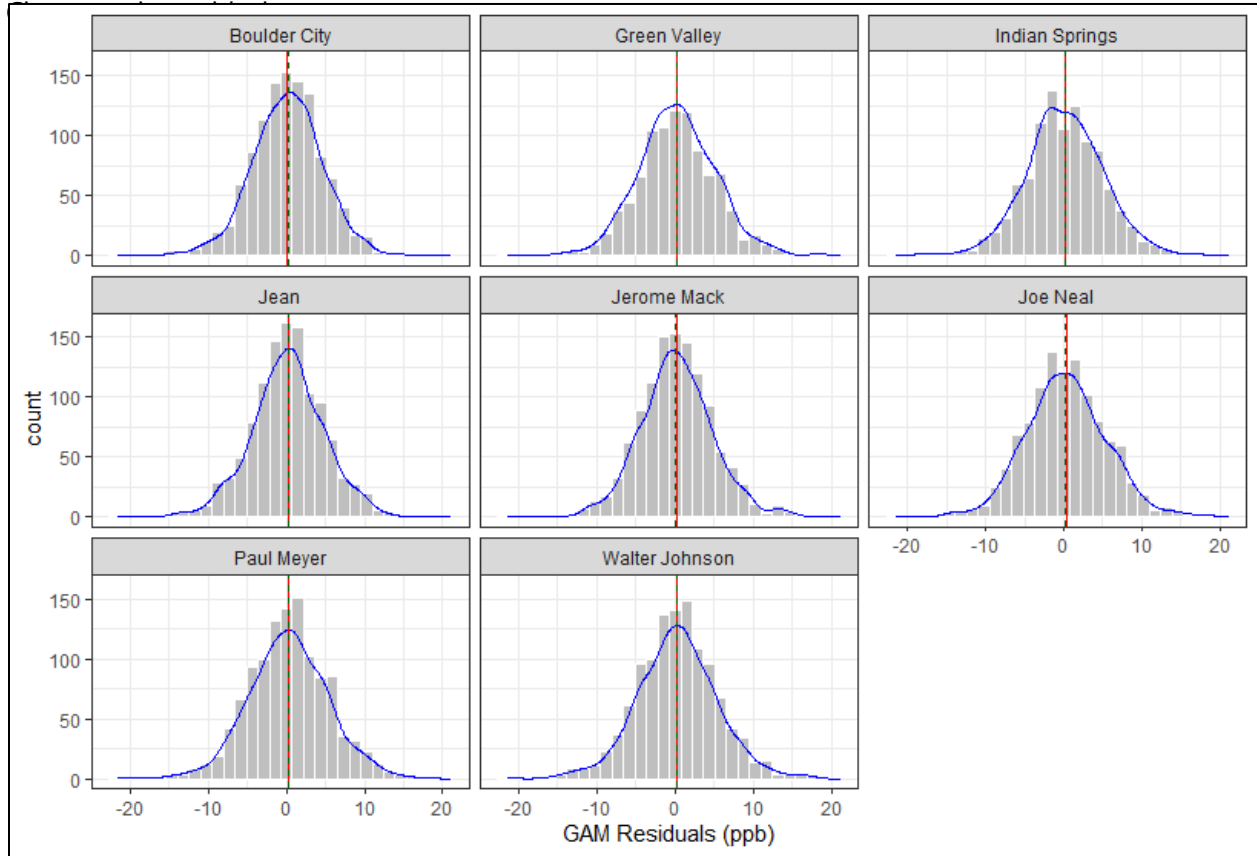
Figure 3-42. Daily GAM residuals for 2014-2020 vs GAM Fit (Predicted) MDA8 Ozone values. 2018 and 2020 EEs residuals are shown in red and blue.

Figure 3-43. Histogram of GAM residuals at all modeled Clark County monitoring sites. The red line indicates the mean, and the green dashed line indicates the median. The blue line provides the density distribution.

Within the GAM model, HYSPLIT 24-hour distance values were included, factored by cluster, to provide source region and stagnation information into the algorithm. A major upwind pollution source for Las Vegas is the Los Angeles Basin (see the Southern California cluster), which is about 400 km away. Since the GAM model uses source region and distance traveled information to help predict daily MDA8 ozone concentrations, contributions from LA should be accounted for in the algorithm. Based on the use of source region and distance, GAM residuals on LA-source region days can be assessed to see if they were significantly different from other source regions. In **Figures 3-44 and 3-45**, GAM results are subset by removing any potential EE days. Results indicate that both morning (18:00 UTC) and afternoon (22:00 UTC) trajectory data have similar distributions for all clusters. The notches in the box plots (representing the 95th confidence interval) provide an estimate of statistical difference and show that for all clusters, the median of residuals is near zero. The Northwest U.S. cluster at 18:00 UTC shows slightly negative residuals, while the Long-Range Transport cluster shows slightly positive residuals for both 18:00 and 22:00 UTC. The Southern California cluster shows a median residual of around zero for both 18:00 and 22:00 UTC trajectories with significant overlap between the 95th confidence intervals of most other clusters (i.e., not statistically different).

Additionally, the number of data points per cluster (bottom of each figure) corresponds well with transport from California being dominant for the April through September time frame. Overall, this analysis provides evidence that even when the Los Angeles Basin (Southern California cluster) is upwind of Las Vegas, the GAM model performs well (low median residuals), and the results are statistically similar to most of the other clusters. This implies that when residuals are large, the Los Angeles Basin influence is unlikely to be the only contributor to enhancements in MDA8 ozone.
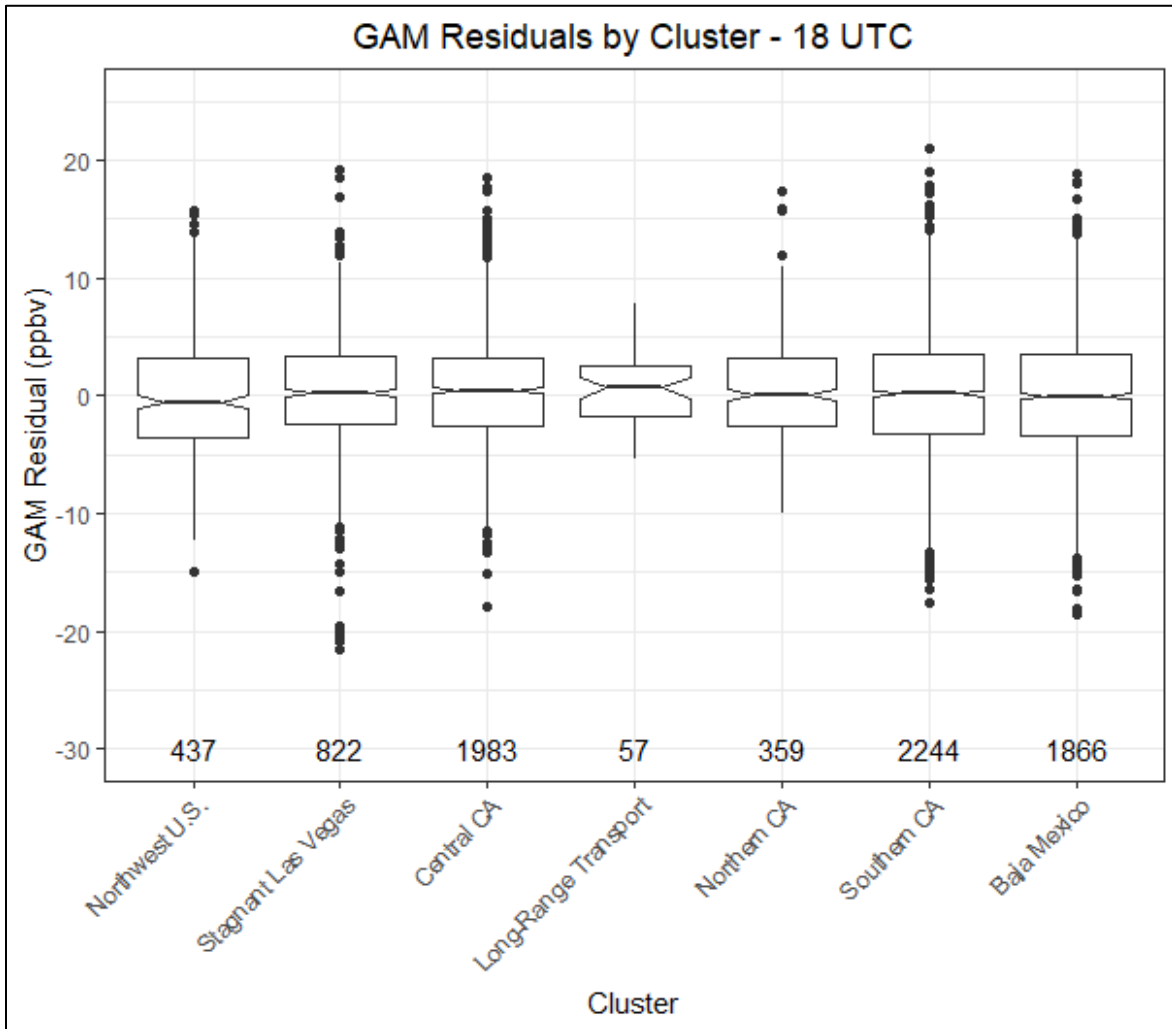
Figure 3-44. GAM cluster residual results for 18:00 UTC. The cluster is determined by grouping 24-hour back trajectories from Las Vegas based on their path. Clusters were created by using back trajectory results from Clark County between 2014 and 2020 (with EE days removed).
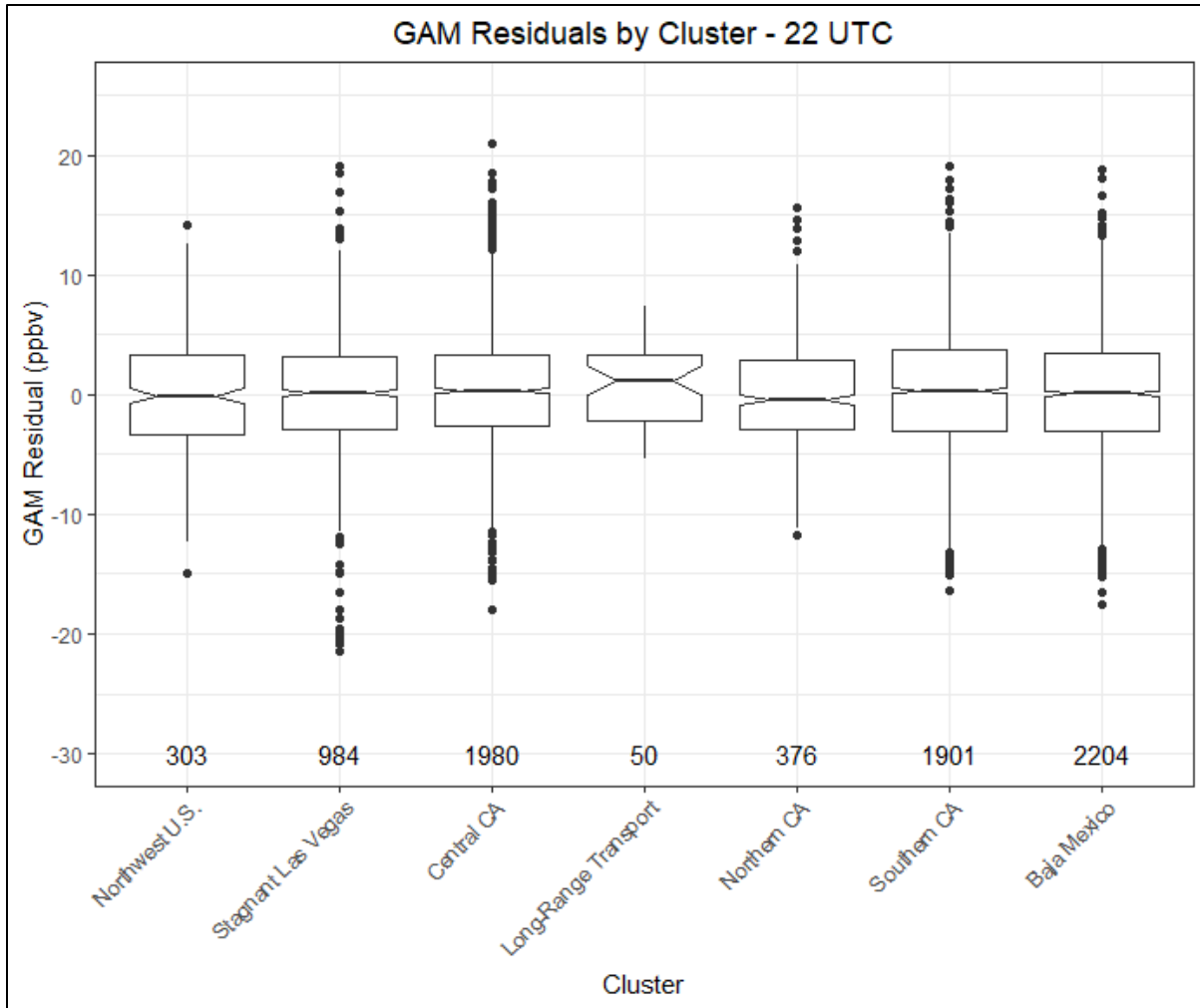
Figure 3-45. GAM cluster residual results for 22:00 UTC. The cluster is determined by grouping 24-hour back trajectories from Las Vegas based on their path. Clusters were created by using back trajectory results from Clark County between 2014 and 2020 (with EE days removed).

Mobile emissions sources decreased throughout the U.S. after COVID restrictions went into place in March 2020. Based on emission inventories from Las Vegas, on-road emissions make up a significant portion of the NO_x emissions inventory (see Section 2.3 for more details). Based on traffic data from the Nevada Department of Transportation, on-road traffic in Clark County in 2020 was significantly different than 2019 through early to mid-June (depending on the area where traffic volume was measured [see **Appendix G** for more details]). **Figure 3-46** provides a scatter plot of MDA8 ozone observed versus GAM fit for all eight monitoring sites, separated by year. The linear regression fit, slope, and intercept do not show a large difference between 2020 and other modeled years. **Figure 3-47** provides a more in-depth look at the most heavily affected months due to COVID restrictions and traffic changes (April to May 2020). The 95th confidence interval (shown as a notch in the box plots) shows overlap between 2020 and most other years (except 2015 and 2016). The May 6, 9, and

28 EE days are included in the 2020 box. This analysis shows that there was not a statistically different GAM response in 2020 compared with other years; this is confirmed in the COVID analysis section (Appendix G) April – May MDA8 ozone during 2020 in Las Vegas showed no statistical difference from previous years. While the reduction in traffic emissions due to COVID restrictions did not affect the June 22 event, it was important to address the potential effects of COVID restrictions in the 2020 GAM results. Overall, ozone concentrations in Clark County did not change significantly and, similarly, GAM results were not significantly affected.
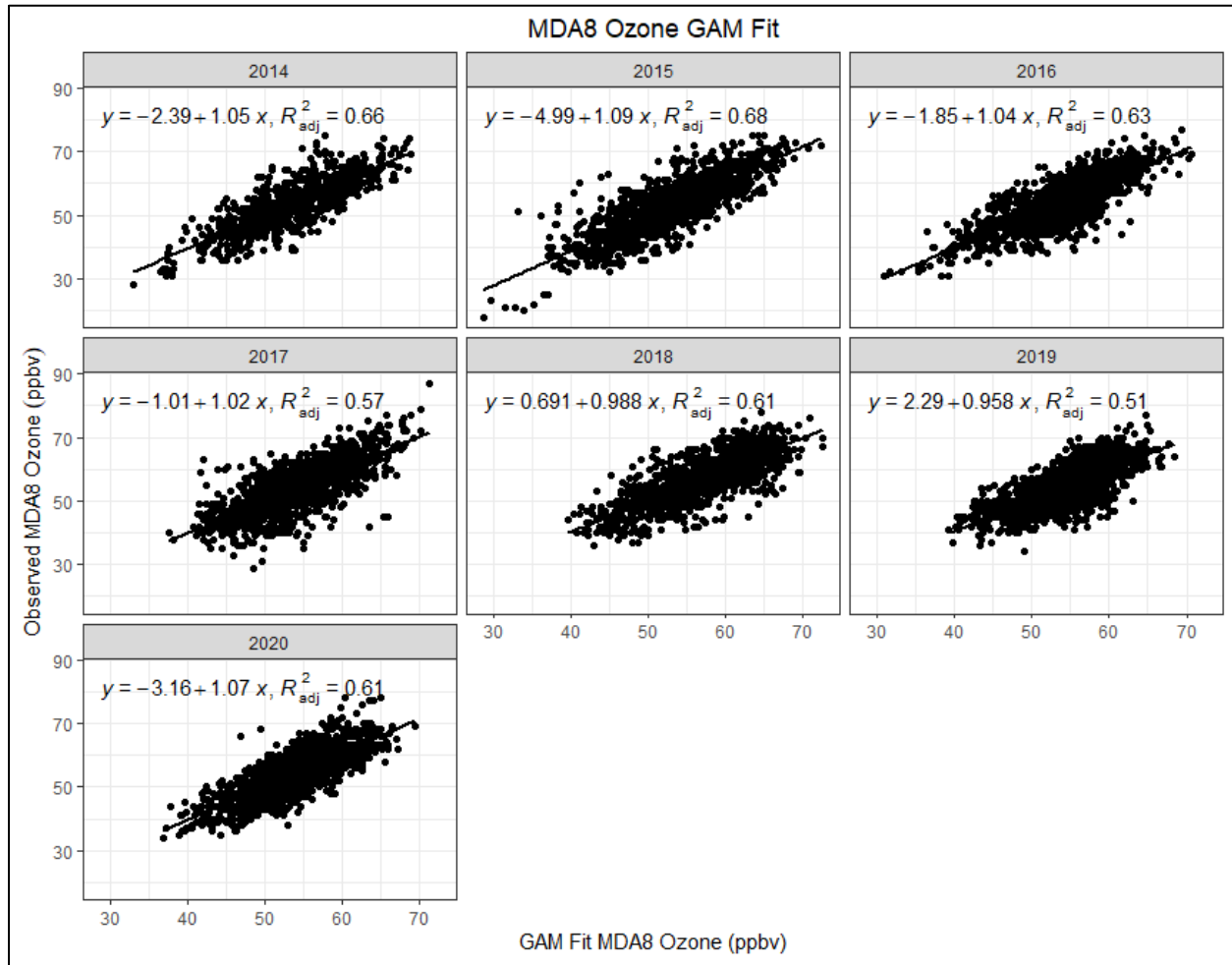
Figure 3-46. Observed MDA8 ozone versus GAM fit ozone by year. The relationship between observed MDA8 ozone and GAM fit ozone at all eight modeled monitoring sites in Clark County is broken out by year with linear regression and fit statistics shown (slope, intercept, and r²). EE days are not included in the regression equations.

Change color to black
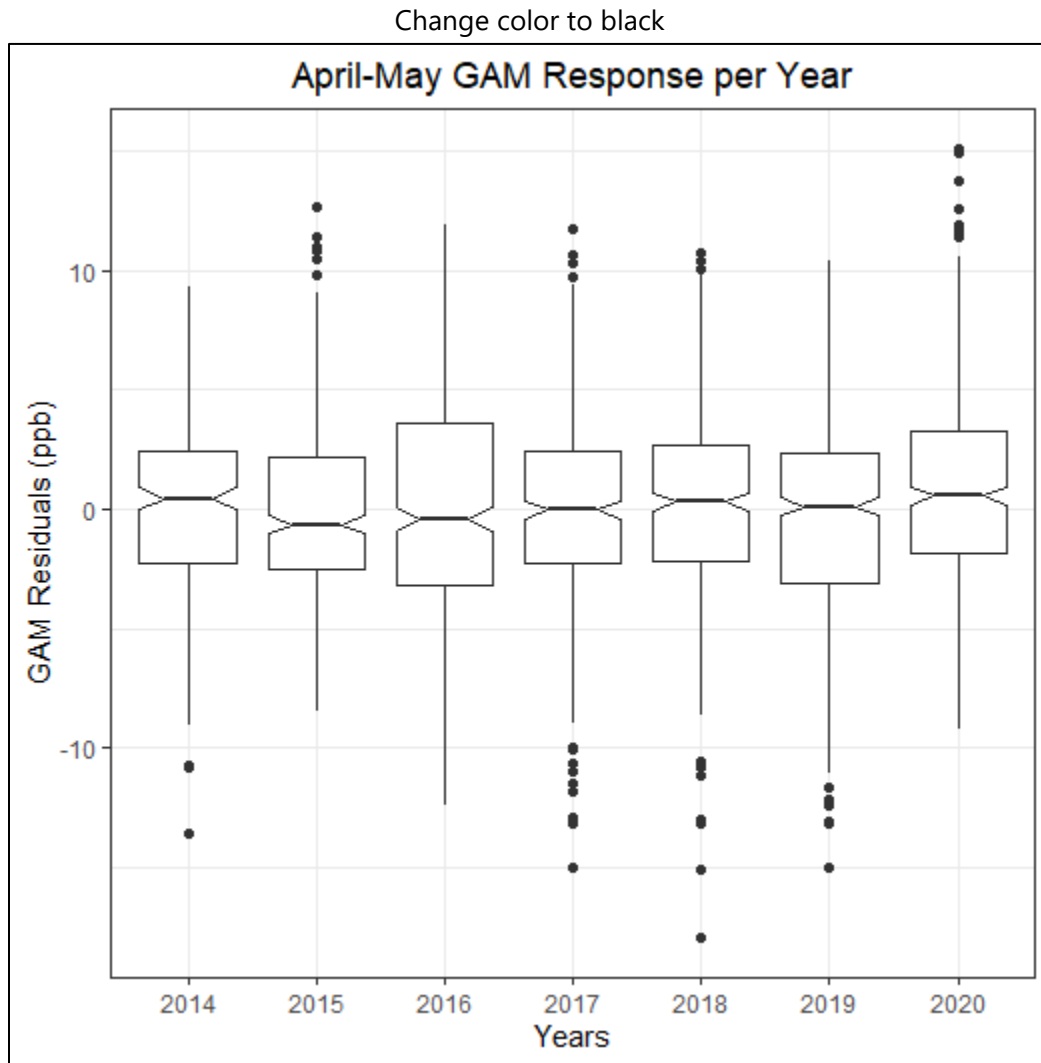
Figure 3-47. April-May Interannual GAM Response. April-May residuals per year (2014-2020) are plotted for all eight modeled monitoring sites in Clark County. May 6, 9, and 28, 2020 potential EE days are included.

Figure 3-48 provides the observed MDA8 ozone versus GAM Fit MDA8 from 2014 through 2020 for the sites affected on June 22 (Joe Neal, Paul Meyer, and Walter Johnson). We marked the possible 2020 (red), 2018 (blue), and other (purple) EE days to show that observed MDA8 ozone on these days is higher than those predicted by the GAM. The other (purple) points are from 2014 to 2016 suspected wildfire events, as indicated in EPA AQS record. We also highlight the June 22, 2020, EE day as a large red triangle in each figure. Linear regression statistics (slope, intercept, and r^2) are also provided for context. Both linear regressions show a slope near unity and a low intercept value (around 4 ppb) with a good fit r^2 value.
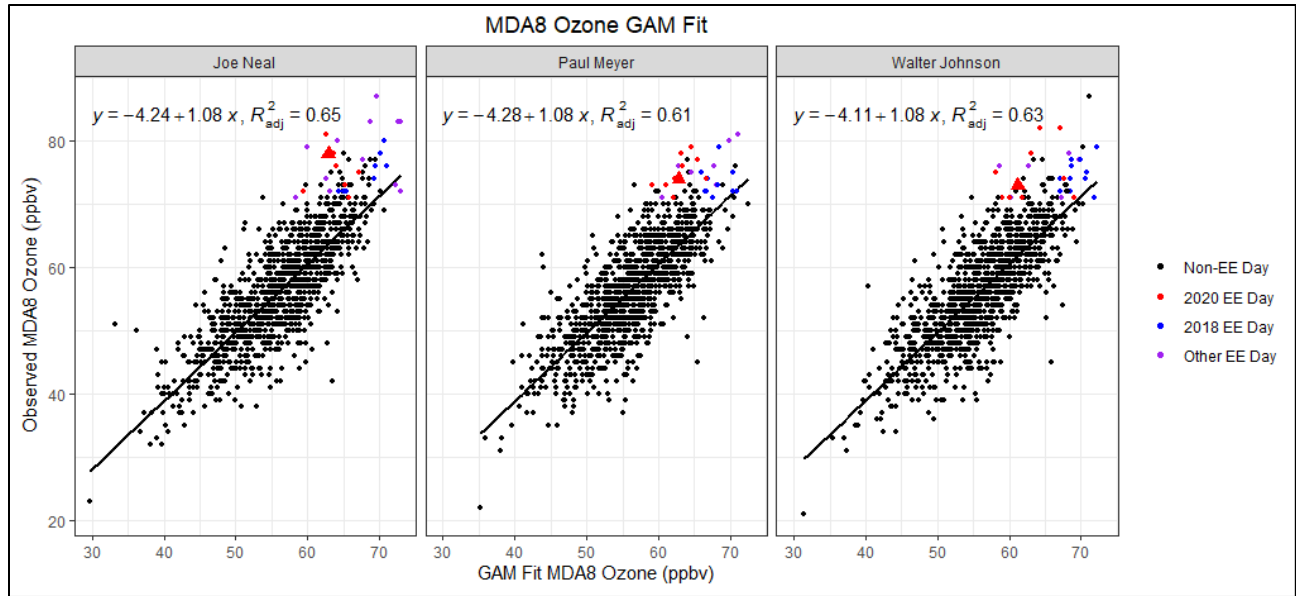
Figure 3-48. GAM MDA8 Fit versus Observed MDA8 ozone for EE affected sites on June 22, 2020. Black circles indicate data not associated with the 2018 or 2020 EE days, red circles indicate 2020 EE days, blue circles indicate 2018 EE days, and purple circles indicate 2014 to 2016 EE days. June 22 is shown as a red triangle. The black line is linear regression of the data and statistics (equation and r² value) are shown in the top of each sub-figure.

Table 3-18 provides the GAM results for June 22, 2020, at each monitoring site affected by the EE. GAM residuals show a modeled wildfire impact between 12 and 15 ppb for all monitoring sites, with MDA8 GAM prediction values well below the 0.070 ppm standard. EPA guidance requires a further level of investigation; by adding the GAM MDA8 Prediction value and the Positive 95th quantile of residuals, the "No Fire" MDA8 ozone value was calculated. The difference between observed and "No Fire" MDA8 ozone value is a conservative estimate of the influence of wildfire smoke at each site (2 to 6 ppb). Due to the large number of wildfires affecting Clark County during the seven-year modeling period, the "No Fire" and minimum predicted fire influence given the 75th percentile was calculated (7 to 10 ppb). This parameter provides a range of minimum smoke enhancement (2 to 10 ppb). The actual enhancement due to wildfire smoke likely lies between the minimum smoke enhancement estimate and the GAM residual. Previous studies and concurred EE demonstrations show and discuss the limitations of the 95th positive percentile evaluation (Miller et al., 2014; Arizona Department of Environmental Quality, 2016). Additionally, production of ozone is an extremely complex process that can only be predicted by meteorological variables in a GAM model with a 50-80% correlation based on previously cited papers (GAM model for this demonstration shows a 55-61% correlation). Therefore, EEs, wildfire influence during high wildfire years, stratospheric intrusions, non-normal emissions, non-normal meteorology, etc., make up the other 39-45% of variance. Due to the large number of high wildfire years used in the GAM model, we assert that the minimum predicted fire influence value (as determined by the positive 95th quantile) should not be used as strict guideline for actual fire influence. Based on the values from the GAM model, there is a

significant, non-typical enhancement in MDA8 ozone concentrations at the affected Clark County monitoring sites on June 22, 2020.

Table 3-18. June 22 GAM results and residuals for each site. The GAM residual is the difference between observed MDA8 ozone and the GAM Prediction. The minimum predicted fire influence based on the positive 95th quantile and GAM prediction value is estimated.

Site Name	MDA8 O$_3$ Concentration[a] (ppm)	MDA8 GAM Prediction[b] (ppm)	GAM Residual (ppm)	Positive 75th to 95th Quantile[c] (ppm)	"No Fire" MDA8[b+c] (ppm)	Minimum Predicted Fire Influence[a-(b+c)] (ppm)
Paul Meyer	0.074	0.062	0.012	0.005-0.010	0.067-0.072	0.002-0.007
Walter Johnson	0.073	0.061	0.012	0.005-0.010	0.066-0.071	0.002-0.007
Joe Neal	0.078	0.062	0.015	0.006-0.010	0.068-0.072	0.006-0.010

Finally, **Figure 3-49** shows a two-week time series of observed MDA8 ozone values across Clark County and GAM prediction values at those sites. June 22, 2020 (and June 26, which is another EE day), shows a large gap between observed MDA8 ozone and GAM-predicted values. Outside of the possible EE day, the GAM prediction values are very close to the observed values, suggesting that immediately before and after the event, typical fluctuations in ozone on non-event days can be accurately predicted.
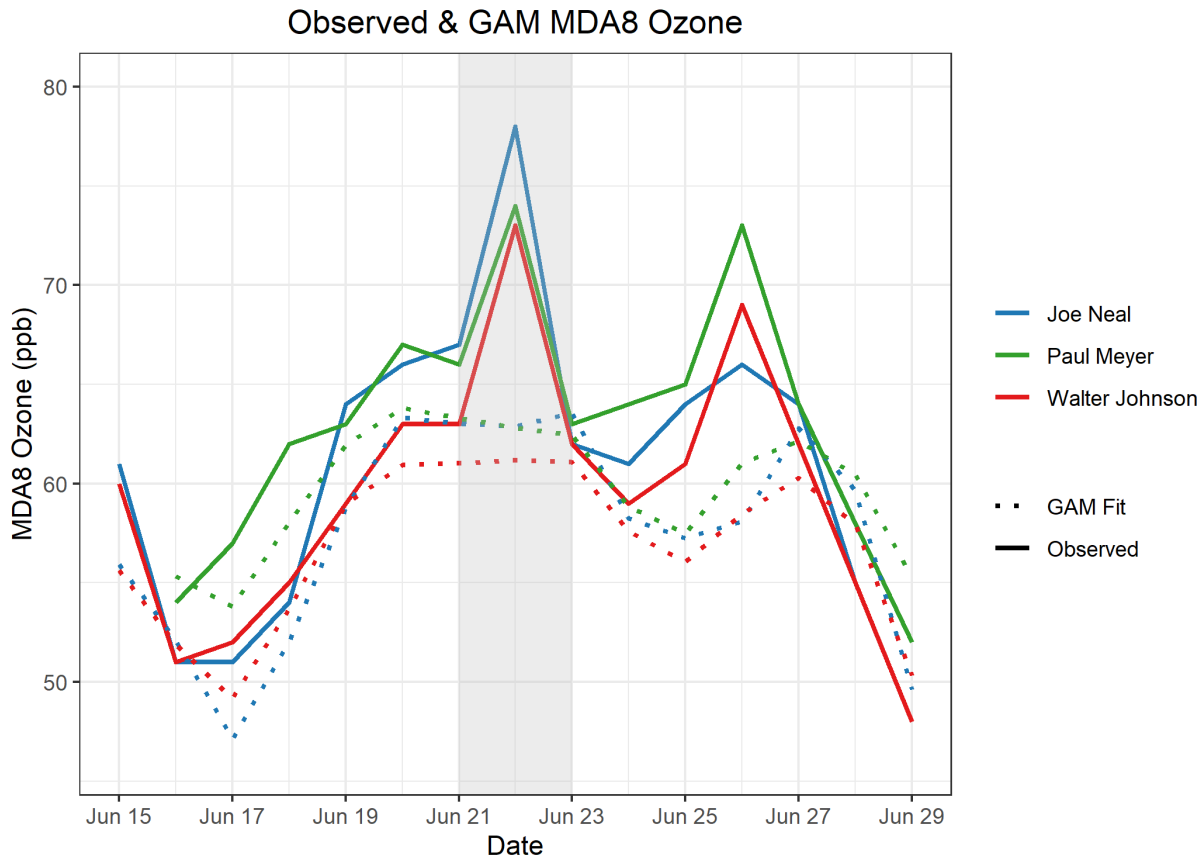
Figure 3-49. GAM time series showing observed MDA8 ozone for two weeks before and after the June 22 EE (solid lines). The GAM MDA8 ozone fit value is also shown for two weeks before and after June 22 (dotted line).

Overall, the GAM evidence clearly demonstrates that a non-typical source of ozone significantly impacted concentrations on June 22, 2020, at both EE-affected Clark County sites. Coupled with wildfire smoke evidence from all other tiers of analyses, the data show by weight of evidence that the enhancement in ozone is due to smoke from the wildfires in Arizona and the Ivanpah Fire.

3.4   Clear Causal Relationship Conclusions

The analyses conducted in this report support the impact of smoke from the Ivanpah Fire in California and large wildfires in Arizona on ozone concentrations in Clark County, Nevada, on June 22, 2020. Analyses showed:

1. HMS smoke imagery, news articles, and back trajectories support the conclusion of smoke transport from wildfires in Arizona, and to a smaller extent the Ivanpah Fire, to Clark County.

2. Meteorological analyses, back trajectories starting near the fire and ending at the surface in Clark County, and surface enhancements of wildfire-related pollutants (CO, NO_x, and levoglucosan) in Clark County support the conclusion that smoke was mixed down to the surface in Clark County.

3. Comparisons with non-event concentrations, meteorologically similar matching day analysis, and GAM statistical modeling support the conclusion that the ozone concentrations seen in Clark County were well above typical summer concentrations.

The analyses presented in this report fulfill the requirements for a Tier 3 EE demonstration, and all conclusions for each type of analysis are summarized in Table 3-19. The effect of the Arizona wildfires and the Ivanpah Fire on Clark County caused ozone exceedances at the Paul Meyer, Walter Johnson, and Joe Neal monitoring stations. Based on the evidence shown that the Arizona wildfires and the Ivanpah Fire were natural events and unlikely to recur, as well as the clear causal relationship between the wildfire events and the monitored exceedances, the ozone exceedance event on June 22, 2020, in Clark County was not reasonably controllable or preventable.

Table 3-19. Results for each tier analysis for the June 22 EE.

Tier	Requirements	Finding

1	• Comparison of fire-influenced exceedance with historical concentrations
	• Key factor: Evidence that fire and monitor meet one of the following criteria:
	  – Seasonality differs from typical season, or
	  – Ozone concentrations are 5-10 ppb higher than non-event related concentrations
	• Evidence of transport of fire emissions to monitor:
	  – Trajectories of fire emissions (reaching ground level), or
	  – Satellite images and supporting evidence from surface measurements
	  – Media coverage and photographic evidence of smoke
		• The June 22, 2020, ozone exceedance occurred during a typical ozone season, but event concentrations were significantly higher than typical non-event concentrations.
		• Trajectories, satellite images, media coverage, and ground images support smoke transport from the Ivanpah Fire and Arizona wildfires into and near Clark County.

2	• All Tier 1 requirements
	• Key Factor #1: Fire emissions and distance of fires
	• Key Factor #2: Comparison of the event-related ozone concentration with non-event-related high ozone concentrations (high percentile rank over five years/seasons)
	  – Annual and seasonal comparison
	• Evidence that fire emissions affected the monitor (at least one of the following):
	  – Visibility impacts
	  – Changes in supporting measurements
	  – Satellite enhancements of fire-related species (i.e., NOx, CO, AOD, etc.)
	  – Fire-related enhancement ratios and/or tracer species
	  – Differences in spatial/temporal patterns
		• Q/d values for the Ivanpah and Arizona wildfires were well below 100.
		• Ozone concentrations at all sites showed high percentile rank over the past six years and ozone seasons.
		• Surface concentrations of supporting pollutants (CO and NO_x) show enhanced concentrations and changes in typical diurnal profiles, consistent with smoke and a late night peak in co-pollutants from the Arizona fires.
		• Levoglucosan, a wildfire tracer, showed a positive detection immediately following this event.

3	• All Tier 2 requirements
	• Evidence of fire emissions effects on monitor:
	  – Multiple analyses from those listed for Tier 2
	• Evidence of fire emissions transport to the monitor:
	  – Trajectory or satellite plume analysis, and
	  – Additional discussion of meteorological conditions
	• Additional evidence such as:
	  – Comparison to ozone concentrations on matching (meteorologically similar) days
	  – Statistical regression modeling
	  – Photochemical modeling of smoke contributions to ozone concentrations
		• Meteorology patterns during this event show transport from the Arizona fires and the Ivanpah Fire to Clark County.
		• Vertical profiles transport along the surface as well as increased aerosol in the column.
		• Meteorologically similar day analysis shows that average MDA8 ozone across similar days was well below the ozone NAAQS and 10 ppb lower than the June 22 exceedance at all affected sites.
		• GAM statistical modeling predicts ozone concentrations lower than observed, suggesting an impact from non-typical sources on ozone concentrations in Clark County during this event.

4. Natural Event

A wildfire is defined in 40 CFR 50.1(n) as "any fire started by an unplanned ignition caused by lightning; volcanoes; other acts of nature; unauthorized activity; or accidental, human-caused actions, or a prescribed fire that has developed into a wildfire. A wildfire that predominantly occurs on wildland is a natural event." Furthermore, a "wildland" is "an area in which human activity and development are essentially non-existent, except for roads, railroads, power lines, and similar transportation facilities. Structures, if any, are widely scattered." 40 CFR 50.1(o). As shown in Table 3-3, each fire that contributed to this event was cause by either lightning, or accidental, human-caused actions, and therefore meets the definition of wildfire. Based on the documentation provided in Section 3.2.1 of this submittal, the collection of fires in Arizona and California that contributed to wildfire smoke in Clark County predominately took place on wildlands designated as National Forests, as seen in Figure 3-17. Therefore, under 40 CFR §50.1, each wildfire listed in Table 3-3 can be classified as natural event that is unlikely to recur. Accordingly, the Clark County Department of Environment and Sustainability has shown in this submittal that smoke from Arizona and California wildfires, which led to an ozone exceedance in Clark County of June 22, 2020, may be considered for treatment as an EE.

5. Not Reasonably Controllable or Preventable

As shown by the documentation provided in Section 3.2.1 of this submittal, each wildfire listed in Table 3-3 burned predominantly on wildland. The Exceptional Events rule stated in 40 CFR 50.1(j) indicates that a wildfire that occurs on wildland is not reasonably controllable or preventable. Previous sections of this report have shown that each fire referenced in this report was a wildfire that occurred on wildland. The National Wildfire Coordinating Group specified that the Bush Fire occurred on "steep and rugged terrain," and that high winds exacerbated the spread of the Bush Fire reducing the possibility and effectiveness of any firefighting efforts.[10] Additionally, the Ivanpah Fire burned quickly across over 1,000 acres in one day in the Mojave National Preserve. Therefore, emissions from these wildfires that caused ozone exceedances in Clark County were not reasonably controllable or preventable.

---

[10] https://inciweb.nwcg.gov/incident/article/6773/52285/, https://inciweb.nwcg.gov/incident/6741/

6. Public Comment

This EE demonstration will undergo a 30-day public comment period concurrent with EPA's review beginning July 1, 2021. A copy of the public notice, along with any comments received and responses to those comments, will be submitted to EPA after the comment period has closed, consistent with the requirements of 40 CFR 50.14(c)(3)(v). **Appendix H** contains documentation of the public comment process.

7. Conclusions and Recommendations

The analyses conducted in this report support the conclusion that smoke from the Bighorn, Bush, and Mangum fires in Arizona and the Ivanpah Fire in Mojave National Preserve impacted ozone concentrations in Clark County, Nevada, on June 22, 2020. This EE demonstration has provided the following elements required by the EPA guidance for wildfire EEs (U.S. Environmental Protection Agency, 2016):

1. A narrative conceptual model that describes the Arizona wildfires and Ivanpah Fire and how the emissions from these wildfires led to ozone exceedances downwind in Clark County (Sections 1 and 2).

2. A clear causal relationship between the Arizona wildfires and the Ivanpah Fire and the June 22 exceedance through ground measurements, satellite-based analyses, trajectories, emission modeling, comparisons with non-event concentrations, meteorologically similar day analyses, and statistical modeling (Section 3).

3. Event ozone concentrations at or above the 99th percentile when compared with the last six years of observations at each site and among the four highest ozone days at each site (excluding other 2018 and 2020 EE events – Section 3).

4. The Ivanpah Fire and wildfires in Arizona were started by ether human-caused accidents, lightning, or an unknown cause; these fires began in wildland areas and grew rapidly and quickly beyond firefighting controls, which classifies this event as unlikely to recur (Section 4).

5. Demonstration that the emissions from the Ivanpah Fire and Arizona wildfires being transported to Clark County was neither reasonably controllable or preventable (Section 5).

6. This demonstration went through the public comment process via Clark County's Department of Environment and Sustainability (Section 6).

The major conclusions and supporting analyses found in this report are:

1. HMS smoke imagery, news articles, and back trajectories support the conclusion of smoke transport from wildfires in Arizona, and to a smaller extent the Ivanpah Fire, to Clark County.

2. Meteorological analyses, back trajectories starting near the fire and ending at the surface in Clark County, and surface enhancements of wildfire-related pollutants (CO, NO_x, and levoglucosan) in Clark County support the conclusion that smoke was mixed down to the surface in Clark County.

3. Comparisons with non-event concentrations, meteorologically similar matching day analysis, and GAM statistical modeling support the conclusion that the ozone concentrations seen in Clark County were well above typical summer concentrations.

The analyses presented in this report fulfill the requirements for a Tier 3 EE demonstration, and all conclusions for each type of analysis are summarized in Table 3-15. The effect of the Bighorn, Bush, and Mangum fires in Arizona and the Ivanpah Fire in Mojave National Preserve in Clark County caused ozone exceedances at the Paul Meyer, Walter Johnson, and Joe Neal monitoring stations. Based on the evidence shown that the Arizona wildfires and the Ivanpah Fire were natural events and unlikely to recur, as well as the clear causal relationship between the wildfire events and the monitored exceedances, we conclude that the ozone exceedance event on June 22, 2020, in Clark County was not reasonably controllable or preventable.

8. References

Alvarado M., Lonsdale C., Mountain M., and Hegarty J. (2015) Investigating the impact of meteorology on O_3 and $PM_{2.5}$ trends, background levels, and NAAQS exceedances. Final report prepared for the Texas Commission on Environmental Quality, Austin, TX, by Atmospheric and Environmental Research, Inc., Lexington, MA, August 31.

Aragon J.P., First responder (2021), 5/14.

Arizona Department of Environmental Quality (2016) State of Arizona exceptional event documentation for wildfire-caused ozone exceedances on June 20, 2015 in the Maricopa nonattainment area. Final report, September. Available at https://static.azdeq.gov/pn/1609_ee_report.pdf.

Bhattarai H., Saikawa E., Wan X., Zhu H., Ram K., Gao S., Kang S., Zhang Q., Zhang Y., Wu G., Wang X., Kawamura K., Fu P., and Cong Z. (2019) Levoglucosan as a tracer of biomass burning: recent progress and perspectives. *Atmospheric Research*, 220, 20-33, doi: 10.1016/j.atmosres.2019.01.004. Available at http://www.sciencedirect.com/science/article/pii/S0169809518311098.

Brey S.J. and Fischer E.V. (2016) Smoke in the city: how often and where does smoke impact summertime ozone in the United States? *Environ. Sci. Technol.*, 50(3), 1288-1294, doi: 10.1021/acs.est.5b05218, 2016/02/02.

Bytnerowicz A., Cayan D., Riggan P., Schilling S., Dawson P., Tyree M., Wolden L., Tissell R., and Preisler H. (2010) Analysis of the effects of combustion emissions and Santa Ana winds on ambient ozone during the October 2007 southern California wildfires. *Atmospheric Environment*, 44, 678-687, doi: 10.1016/j.atmosenv.2009.11.014.

Camalier L., Cox W., and Dolwick P. (2007) The effects of meteorology on ozone in urban areas and their use in assessing ozone trends. *Atmospheric Environment*, 41, 7127-7137, doi: 10.1016/j.atmosenv.2007.04.061.

Clark County Department of Air Quality (2019) Ozone Advance program progress report update. August.

Clark County Department of Environment and Sustainability (2020) Revision to the Nevada state implementation plan for the 2015 Ozone NAAQS: emissions inventory and emissions statement requirements. September. Available at https://files.clarkcountynv.gov/clarknv/Environmental%20Sustainability/SIP%20Related%20Documents/O3/20200901_2015_O3%20EI-ES_SIP_FINAL.pdf?t=1617690564073&t=1617690564073.

Draxler R.R. (1991) The accuracy of rrajectories during ANATEX calculated using dynamic model analyses versus rawinsonde observations. *Journal of Applied Meteorology*, 30, 1446-1467, doi: 10.1175/1520-0450(1991)030<1446:TAOTDA>2.0.CO;2, February 25. Available at https://journals.ametsoc.org/doi/abs/10.1175/1520-0450%281991%29030%3C1446%3ATAOTDA%3E2.0.CO%3B2.

Finlayson-Pitts B.J. and Pitts Jr J.N. (1997) Tropospheric air pollution: Ozone, airborne toxics, polycyclic aromatic hydrocarbons, and particles. *Science*, 276, 1045-1051, (5315).

Gong X., Kaulfus A., Nair U., and Jaffe D.A. (2017) Quantifying O_3 impacts in urban areas due to wildfires using a generalized additive model. *Environ. Sci. Technol.*, 51(22), 13216-13223, doi: 10.1021/acs.est.7b03130.

Hennigan C.J., Sullivan A.P., Collett J.L., Jr., and Robinson A.L. (2010) Levoglucosan stability in biomass burning particles exposed to hydroxyl radicals. *Geophysical Research Letters*, 37(L09806), doi: 10.1029/2010GL043088. Available at https://www.firescience.gov/projects/09-1-03-1/project/09-1-03-1_hennigan_etal_grl_2010.pdf.

Hoffmann D., Tilgner A., Iinuma Y., and Herrmann H. (2009) Atmospheric stability of levoglucosan: a detailed laboratory and modeling study. *Environ. Sci. Technol.*, 44, 694–699.

Jaffe D., Chand D., Hafner W., Westerling A., and Spracklen D. (2008) Influence of fires on O₃ concentrations in the western U.S. *Environ. Sci. Technol.*, 42(16), 5885-5891, doi: 10.1021/es800084k.

Jaffe D.A., Bertschi I., Jaegle L., Novelli P., Reid J.S., Tanimoto H., Vingarzan R., and Westphal D.L. (2004) Long-range transport of Siberian biomass burning emissions and impact on surface ozone in western North America. *Geophys. Res. Let.*, 31(L16106).

Jaffe D.A. and Wigder N.L. (2012) Ozone production from wildfires: a critical review. *Atmospheric Environment*, 51, 1-10, May. Available at https://www.sciencedirect.com/science/article/pii/S1352231011012507.

Jaffe D.A., Wigder N., Downey N., Pfister G., Boynard A., and Reid S.B. (2013) Impact of wildfires on ozone exceptional events in the western U.S. *Environ. Sci. Technol.*, 47(19), 11065-11072, doi: 10.1021/es402164f, October 1. Available at http://pubs.acs.org/doi/abs/10.1021/es402164f.

Lai C., Liu Y., Ma J., Ma Q., and He H. (2014) Degradation kinetics of levoglucosan initiated by hydroxyl radical under different environmental conditions. *Atmospheric Environment*, 91, 32-39, doi: 10.1016/j.atmosenv.2014.03.054, 2014/07/01/. Available at http://www.sciencedirect.com/science/article/pii/S1352231014002398.

Langford A.O., Senff C.J., Alvarez R.J., Brioude J., Cooper O.R., Holloway J.S., Lin M.Y., Marchbanks R.D., Pierce R.B., Sandberg S.P., Weickmann A.M., and Williams E.J. (2015) An overview of the 2013 Las Vegas Ozone Study (LVOS): impact of stratospheric intrusions and long-range transport on surface air quality. *Atmospheric Environment*, 109, 305-322, doi: 10.1016/j.atmosenv.2014.08.040, 2015/05/01/. Available at http://www.sciencedirect.com/science/article/pii/S1352231014006426.

Louisiana Department of Environmental Quality (2018) Louisiana exceptional event of September 14, 2017: analysis of atmospheric processes associated with the ozone exceedance and supporting data. Report submitted to the U.S. EPA Region 6, Dallas, TX, March. Available at https://www.epa.gov/sites/production/files/2018-08/documents/ldeq_ee_demonstration_final_w_appendices.pdf.

Lu X., Zhang L., Yue X., Zhang J., Jaffe D., Stohl A., Zhao Y., and Shao J. (2016) Wildfire influences on the variability and trend of summer surface ozone in the mountainous western United States. *Atmospheric Chemistry & Physics*, 16, 14687-14702, doi: 10.5194/acp-16-14687-2016.

McClure C.D. and Jaffe D.A. (2018a) Investigation of high ozone events due to wildfire smoke in an urban area. *Atmospheric Environment*, 194, 146-157, doi: 10.1016/j.atmosenv.2018.09.021, 2018/12/01/. Available at http://www.sciencedirect.com/science/article/pii/S1352231018306137.

McClure C.D. and Jaffe D.A. (2018b) US particulate matter air quality improves except in wildfire-prone areas. *Proceedings of the National Academy of Sciences*, 115(31), 7901-7906, doi: 10.1073/pnas.1804353115. Available at https://www.pnas.org/content/pnas/115/31/7901.full.pdf.

McVey A., Pernak R., Hegarty J., and Alvarado M. (2018) El Paso ozone and PM₂.₅ background and totals trend analysis. Final report prepared for the Texas Commission on Environmental Quality, Austin, Texas, by Atmospheric and Environmental Research, Inc., Lexington, MA, June. Available at https://www.tceq.texas.gov/assets/public/implementation/air/am/contracts/reports/da/582188176307-20180629-aer-ElPasoOzonePMBackgroundTotalsTrends.pdf.

Miller D., DeWinter J., and Reid S. (2014) Documentation of data portal and case study to support analysis of fire impacts on ground-level ozone concentrations. Technical memorandum prepared for the U.S. Environmental Protection Agency, Research Triangle Park, NC by Sonoma Technology, Inc., Petaluma, CA, STI-910507-6062, September 5.

National Weather Service Forecast Office (2020) Las Vegas, NV: general climatic summary. Available at https://www.wrh.noaa.gov/vef/lassum.php.

Pernak R., Alvarado M., Lonsdale C., Mountain M., Hegarty J., and Nehrkorn T. (2019) Forecasting surface O₃ in Texas urban areas using random forest and generalized additive models. *Aerosol and Air Quality Research*, 19, 2815-2826, doi: 10.4209/aaqr.2018.12.0464.

Sacramento Metropolitan Air Quality Management District (2011) Exceptional events demonstration for 1-hour ozone exceedances in the Sacramento regional nonattainment area due to 2008 wildfires. Report to the U.S. Environmental Protection Agency, March 30.

Simon H., Baker K.R., and Phillips S. (2012) Compilation and interpretation of photochemical model performance statistics published between 2006 and 2012. *Atmospheric Environment*, 61, 124-139, doi: 10.1016/j.atmosenv.2012.07.012.

Simoneit B.R.T., Schauer J.J., Nolte C.G., Oros D.R., Elias V.O., Fraser M.P., Rogge W.F., and Cass G.R. (1999) Levoglucosan, a tracer for cellulose in biomass burning and atmospheric particles. *Atmospheric Environment*, 33, 173-182.

Simoneit B.R.T. (2002) Biomass burning - a review of organic tracers for smoke from incomplete combustion. *Applied Geochemistry*, 17, 129-162.

Texas Commission on Environmental Quality (2021) Dallas-Fort Worth area exceptional event demonstration for ozone on August 16, 17, and 21, 2020. April. Available at https://www.tceq.texas.gov/assets/public/airquality/airmod/docs/ozoneExceptionalEvent/2020-DFW-EE-Ozone.pdf.

U.S. Census Bureau (2010) State & County QuickFacts. Available at http://quickfacts.census.gov/qfd/states/.html.

U.S. Environmental Protection Agency (2016) Guidance on the preparation of exceptional events demonstrations for wildfire events that may influence ozone concentrations. Final report, September. Available at www.epa.gov/sites/production/files/2016-09/documents/exceptional_events_guidance_9-16-16_final.pdf.

U.S. Environmental Protection Agency (2020) Green Book: 8-hour ozone (2015) area information. Available at https://www.epa.gov/green-book/green-book-8-hour-ozone-2015-area-information.

Wigder N.L., Jaffe D.A., and Saketa F.A. (2013) Ozone and particulate matter enhancements from regional wildfires observed at Mount Bachelor during 2004–2011. *Atmospheric Environment*, 75, 24-31, doi: 10.1016/j.atmosenv.2013.04.026, August. Available at http://www.sciencedirect.com/science/article/pii/S1352231013002719.

Wood S. (2020) Mixed GAM computation vehicle with automatic smoothness estimation. Available at https://cran.r-project.org/web/packages/mgcv/mgcv.pdf.

Wood S.N. (2017) *Generalized additive models: an introduction with R*, 2nd edition, CRC Press, Boca Raton, FL.

Zhang L., Lin M., Langford A.O., Horowitz L.W., Senff C.J., Klovenski E., Wang Y., Alvarez R.J., II, Petropavlovskikh I., Cullis P., Sterling C.W., Peischl J., Ryerson T.B., Brown S.S., Decker Z.C.J., Kirgis G., and Conley S. (2020) Characterizing sources of high surface ozone events in the southwestern US with intensive field measurements and two global models. *Atmospheric Chemistry & Physics*, 20, 10379-10400, doi: 10.5194/acp-20-10379-2020. Available at https://acp.copernicus.org/articles/20/10379/2020/acp-20-10379-2020.pdf.